“An expert is a person who has made all the mistakes that can be made in a very narrow field.”

-- *Niels Bohr*

University of Alberta

Biological patterns and processes of glass sponge reefs

by

Jackson Wing Four Chu

A thesis submitted to the Faculty of Graduate Studies and Research
in partial fulfillment of the requirements for the degree of

Master of Science

Biological Sciences

Fall 2010
Edmonton, Alberta

Examining Committee

Sally Leys, Biological Sciences

Jens Roland, Biological Sciences

Rolf Vinebrooke, Biological Sciences

Lindsey Leighton, Earth & Atmospheric Sciences

Abstract

The glass sponge reefs of western Canada are modern analogues to ancient reefs and are unique habitats requiring conservation. However, the patterns and processes of the glass sponges have not been empirically studied. Here, I characterized the biology of the glass sponges in their reefs.

I examined the community structure of the sponges at 3 reefs in the Strait of Georgia (SOG), their role in silica cycling, and the stable isotopes ($\delta^{13}C$ and $\delta^{15}N$) of the reef forming sponge *Aphrocallistes vastus*. Sponges are spatially structured in patches which localize the abundance of other animals. Long term dissolution of spicules is negligible and thus a reef can be considered a silica sink. Lastly, isotope compositions can differentiate populations of *A. vastus* and depleted carbon signatures at 2 reefs suggest a terrestrial component in their diet.

My work represents the biological baseline of 3 glass sponge reefs in the SOG.

Acknowledgements

The network of mentors, colleagues, students, and friends I established during my thesis created an amazing learning experience. My supervisor, Dr. Sally Leys, took a chance on me as a graduate student. Her infinite energy and enthusiasm is unequalled and her feedback into every chapter and aspect of this thesis pushed me to excel beyond my limits. My committee members, Dr. Jens Roland and Dr. Rolf Vinebrooke, helped me understand the ecological details specific to my degree.

I am extremely fortunate to have participated in multiple research cruises. I thank the entire ROPOS team and the Captains and crew of the CCGS Vector, CCGS Neocaligus and CCGS JP Tully for their technical expertise, support, and efficiency during the surveys and sampling. They directly attributed to the success of my degree. I would also like to thank the large team of colleagues that helped me during my cruises. Dr. Henry Reiswig, with every spoken word, taught me something new about glass sponges. Kim Conway provided valuable insight into the glass sponge reefs and I am forever thankful for his part in discovering this wonderful system. Dr. Gitai Yahel taught me how to be efficient during cruises. Also, Andia Chaves-Fonnegra, Emily Adams, Dr. Ana Riesgo, Danielle Ludeman, Jeannette Bedard, Nathalie Forget and Dr. Marjolaine Matabos helped with shipboard activities during the cruises.

My time was spent in both Edmonton and Bamfield and the support network at both locations helped shape my degree. I thank my lab mates in Edmonton, Dr. Glen Elliott, Gabrielle Tompkins-MacDonald, Pam Windsor, Emily Adams, Emilio Lanna, and Dr. Ana Riesgo, all who understood the inner workings of sponge world. The Bamfield Marine Sciences Centre, the director Dr. Brad Anholt, and Beth Rogers allowed me to establish a wonderful home base of operations at Bamfield for the majority of my degree and allowed me to carve out a teaching niche with the multiple teaching assistantship positions I was awarded from the marine station.

At the BMSC, I was fortunate to have mentored students in the very same courses that inspired me as an undergraduate student. I am forever grateful to Dr. Marjorie Wonham for letting me be her trusted sidekick as her teaching assistant during the 3 courses I taught at the BMSC. By shadowing her teachings I became a better communicator, researcher and teacher. I thank the Marine Invertebrate Zoology class of 2009 and especially the fall program classes of 2008 and 2009. My own work was reinforced by sharing the experience and enthusiasm of scientific discovery with each and every student.

Finally, I would like to acknowledge my family for letting me explore my passion. Without this gift, I would not have begun nor finished this degree.

Specific people collaborated with me in each of my thesis chapters and I wish to address their contributions:

Chapter 2 benefited from the early 2005 pilot work at Fraser reef done by Dr. Sally Leys, Dr. Gitai Yahel and Alison Page. Dr. Leys and Dr. Yahel helped design the sampling methodology during 2007 dives. Jim Boutillier, Wolfgang Carolsfeld, James Pegg and the Pacific Biological Station (DFO, Department of Fisheries and Oceans Canada) provided a substantial gift of ship time with the CCGS Neocaligulus and use of their Phantom HD2+2 ROV. Kim Conway provided bathymetric data and knowledge of the reefs. Dr. Richard Thomson helped immensely by providing his detailed knowledge and data on the benthic flow patterns in the Strait of Georgia. Dr. Yahel helped with the multivariate analysis. Dr. Jens Roland helped greatly with theoretically knowledge and guidance on the semivariogram analyses. Charlene Nielsen provided GIS instruction. Danielle Ludemann helped with image analysis. Dr. Henry Reiswig provided valuable insight into hexactinellid natural history and taxonomy. Sandra Millen confirmed identification of the nudibranch *Peltodoris lentiginosa*. Dr. Leys, Dr. Yahel, Dr. Ana Riesgo and Dr. Marjorie Wonham provided feedback on early drafts of this chapter.

Chapter 3 benefited from early experimental input from Dr. Leys, Dr. Yahel, Dr. Manuel Maldonado, Dr. Frank Whitney and Bill Austin. During the 2007 cruise, water sampling, filtering and processing was done by Dr. Yahel and

Dr. Maldonado. Dr. Maite Maldonado provided invaluable information on diatom culturing. Dr. Bruce Cameron and Tao Eastham provided the spectrophotometer, glass cuvettes, and research space at the BMSC for my dissolution experiments. George Braybook and De-Ann Rollings assisted with scanning electron microscopy. Dr. Roland and Dr. Wonham provided early feedback and advice on the experimental design of the dissolution experiments. Dr. Leys, Dr. Manuel Maldonado, Dr. Riesgo and Dr. Yahel provided feedback on early drafts of this chapter.

Chapter 4 benefited from input by Dr. Tom Reimchen who supervised and provided the space and resources for preparing my samples used in the stable isotope analyses. Jeannette Bedard and Danielle Ludemann filtered water for the POM samples during the 2009 cruise. Dr. Rolf Vinebrooke and Dr. Kim Juniper provided background knowledge on stable isotope analyses during the initial stages of this study.

Chapter 5 benefited from discussions with Dr. Richard Emlet and, in particular, Dr. Mark Denny who provided theoretical background, feedback and advice on my pilot work on the biomechanics of glass sponge spicules. My ideas on future research directions stemmed from taking the course: Biomechanics, Ecological Physiology and Genetics of Intertidal Communities at the Hopkins Marine Station in Pacific Grove, California. I thank the David and Lucile Packard Foundation and the Gordon and Betty Moore Foundation for funding my participation in this course. Monetary support for the work at Learmonth Bank was provided by the Department of Fisheries and Oceans and the Canadian Healthy Oceans Network (CHONe).

Monetary support for this thesis came from graduate student teaching assistantships at the Bamfield Marine Sciences Centre and University of Alberta, a Queen Elizabeth II scholarship. NSERC Ship Time and Discovery Program grants to Dr. Leys allowed me to experience an extensive amount of cruise and ROV time during my degree.

Table of Contents

Chapter 1

Chapter 2

Chapter 3

Chapter 4

Chapter 5

Appendices

List of Tables

List of Figures

Chapter 1

A General Introduction

1.0 Deep sea communities – defining the patterns of a system

The deep ocean, considered the depths just beyond the continental shelf (> 200 m), begins at the lower limits of primary productivity and is 90% of the marine environment (Koslow 2007). At the margins of the continental shelf, the bathymetry is marked by steep depth gradients where the sinking of detritus from primary production (Billet et al. 1983), fecal pellets (Shrader 1971), and the bodies of dead animals (Smith 1985) are the main sources of energy to the seafloor. Despite early predictions that the deep sea harboured "living fossils" (Darwin 1868) and the discovery of several hundred new species during the voyage of the H.M.S. Challenger in the 1870's (Koslow 2007), the idea that the deep sea was impoverished of species persisted until the 1960's when semi-quantitative sampling revealed the deep sea benthos to be diverse with worms, molluscs, and crustaceans (Sanders & Hessler 1969).

In the last 40 years, advances in submersible technology allowed for *in situ* exploration of the deep ocean where scientific expeditions with the manned submersible *Alvin* led to the serendipitous discoveries of several unique ecosystems. Compared to the characteristic groups of invertebrates found in the deep (Gage & Tyler 1991), these new systems were different because a select few charismatic macroinvertebrates dominated the community assemblage in areas previously unknown to harbour life. For example, in the late 1970's, clusters of the large vestimentiferan tubeworm, *Riftia pachyptila*, were discovered at hydrothermal vent communities in the eastern Pacific Ocean (for a review, see Van Dover 2000). In the mid 1980's, beds of the bathymodiolid mussel *Bathymodioulus childressi* were found in cold seeps (hydrocarbon and brine) communities in the Gulf of Mexico (Paull et al. 1984; Hecker et al. 1985). In

these newly discovered systems, how did these dense populations of animals establish and maintain themselves?

The abiotic attributes of the system are the initial drivers of exploration. Each system was first characterized by its geological history, chemical and physical properties of the sea water, and the oceanic variables such as flow to determine the range of conditions in which the macroinvertebrates were found. After the abiotic factors were defined, focused research on the iconic fauna established a foundation of natural history and eventually allowed these deep sea ecosystems to be defined by their symbiotic associations with chemoautotrophic bacteria (Van Dover 2000). Thus, these unique ecosystems were characterized by the biological patterns of their dominant megafauna.

Glass sponge reefs (Porifera, Hexactinellida) can be considered the most recent system to be discovered when in 1989 immense populations of hexactinellid sponges were found to form reefs on the north-eastern continental shelf of the Pacific Ocean (Conway et al. 1991). Similar to the hydrothermal vent and cold seep communities, the geological and oceanographic settings of these modern reefs were the first to be studied (Conway et al. 1991; Barrie & Conway 1999; Krautter et al. 2001; Whitney et al. 2005), however, the biological patterns and processes of the glass sponges have not yet been addressed and thus are the focus of my thesis.

1.1 Overview of the System

1.1.1 Jurassic glass sponge reefs and modern reefs as analogues

Glass sponge reefs represent a modern analogue to ancient reefs that once dominated the northern portions of the Tethys Sea during the Jurassic (~150 Mya). Ancient reefs occurred in depths of at least 30-150 m and fossil evidence of their existence is presently found in areas throughout Europe (Ghiold 1991; Leinfelder 1993; Brunton & Dixon 1994; Leinfelder et al. 1994; Schmid et al. 2001). The proliferation and success of glass sponges during this period is attributed to low tectonic activity, low sedimentation and climatic stability

(Leinfelder et al. 1993; Leinfelder et al. 1994). Reef formation was most strongly linked to reduced (but not absent) input of allochthonous mud that enabled cementing of the lower, oldest portions of a reef (Schmid et al. 2001). After the Cretaceous, the fossil record shows a complete disappearance of hexactinellid reefs in the Tethys Sea (~65 mya, Brunton & Dixon 1994). Changes in ocean chemistry during the mid-Cretaceous reflect the radiation of diatoms and their subsequent dominance in the silica cycle (Maliva et al. 1989) and may have reduced the amount of silicic acid available for sponges with heavily silicified skeletons (Maldonado 1999). However, significant changes in any of the abiotic or biotic factors responsible for successful reef formation could also explain their disappearance.

In 1989, the first four extant reefs were discovered in Hecate Strait, Queen Charlotte Sound (Fig. 1-1A) where 3 species of hexactinellids, *Aphrocallistes vastus, Heterochone calyx,* and *Farrea occa* formed large sponge mounds (Conway et al. 1991). More recently, several smaller reefs, built by only *A. vastus* and *H. calyx*, were discovered in the Strait of Georgia (Fig. 1-1B; Conway et al. 2005; 2007). During the late Pleistocene (13,000 to 10,000 ya) glaciation, isostatic rebound, and sediment remobilization exposed several troughs in the Queen Charlotte Basin (Barrie & Bornhold 1989). During this period glass sponges recruited to the now exposed hard substrate and slowly built massive reefs covering a benthic area of >700 km^2 in the Queen Charlotte Sound alone (Conway et al. 2001).

The reefs in the Strait of Georgia (Fig. 1-1B) cover a fraction of the area covered by the 4 reefs in Hecate Strait but are similarly found on elevated bedrock features caused by tectonic folding and glacial scouring (Conway et al. 2004; 2005). The long term persistence of sponge skeletons after death creates a platform for larval recruitment (Leys et al. 2004; Krautter et al. 2006). Multiple generations of recruitment and gradual burial by sediment of the oldest generations results in the vertical growth of a glass sponge reef. The ecology of modern reef formation may mirror the conditions leading to the establishment of

the ancient reefs and thus provides us with a living system to expand our knowledge beyond correlations in the fossil record.

1.1.2 Glass sponges and their ecology

The 500-600 species of known glass sponges (Reiswig 2006) are mostly found in the deep ocean (common between 300-600 m, down to 6300 m depths, Tabachnick 1994; Leys et al. 2007) where slow growth (Dayton et al. 1979) and long life spans (Leys & Lauzon 1998; Fallon et al. 2010) reflect the stable conditions of the deep sea environment (Tabachnick 1991). Hexactinellids are perhaps the most unusual class within the Porifera (Fig. 1-2) and represent one of the oldest known lineages with extant representatives first appearing ~560 Mya during the Neoproterozoic (Gehling & Rigby 1996). As the the only syncytial metazoans, glass sponges coordinate the arrest of water pumping with action potentials (Leys & Mackie 1997) in response to environmental stimuli such as high sedimentation (Tompkins-Macdonald & Leys 2008). Glass sponges are also especially sensitive to environmental change. For example, in the boot sponge *Rhabdocalyptus dawoni*, temperatures outside of the range of 7-12°C disrupts the action potential (Leys & Mackie 1997; Leys & Meech 2006) where <7°C, pumping can not resume after an arrest, and >12°C , arrests can not occur.

The majority of our knowledge of their ecology comes from studies on dense populations of glass sponges known from only a handful of locations (Table 1-1, Fig. 1-3). Although they only form reefs in Hecate Strait and the Strait of Georgia, glass sponges are particularly abundant in Antarctica and fjords of British Columbia in waters with high levels of silicic acid (Austin 1983; 1999). In areas of high glass sponge abundance, they increase the local abundance of other invertebrates by adding topographic complexity to an otherwise flat, featureless benthos (Dayton et al. 1974; Barthel 1992a, b; Bett & Rice 1992). Animals use glass sponge spicules as a hard substrate for recruitment (Bett & Rice 1992, Beaulieu 2001), a limiting resource in the vast mud floor of the ocean. Although the ecological importance of glass sponge communities is established, we know little about what controls and constrains their biology compared to their

demosponge counterparts from shallower waters because of the relatively few experimental studies on glass sponges.

The narrow ecological niche filled by glass sponges determines where dense populations can establish and ultimately, where glass sponge reefs are formed. To determine the ecological importance of glass sponge reefs and the controls on their formation first requires us to know where the live sponges occur at a reef and in what abundance.

1.1.3 Study organism: the cloud sponge, Aphrocallistes vastus

All species of glass sponges are unified by having spicules made out of amorphous hydrated silica. Hexactine spicules have three axes of symmetry (triaxonal) with 6 branching rays or less originating from a square axial proteinaceous filament (Leys et al. 2007). The species, *A. vastus* (Fig. 1-4A), *H. calyx* (Fig. 1-4B), and *F. occa* (Fig. 1-4C) are the only extant glass sponges known to form reefs. Reef-forming glass sponges have secondary silica deposition that fuses individual megasclere spicules into a 'dictyonine' skeleton which builds the underlying framework of a reef (Fig. 1-4D). Glass sponges that lack this secondary fusion have a 'lyssacine' (loose) skeleton. The absence of *F. occa* in the reefs in the Strait of Georgia differentiates them from the reefs in Hectate Strait and also indicates a potential ecological control that is different between the two regions. In the Strait of Georgia, *A. vastus* and *H. calyx* are morphologically very similar, difficult to tell apart in the field, and have similar suites of spicules. However, a trained individual can taxonomically differentiate between the two based on spicule morphology and arrangement (Reiswig 2002). Both *A. vastus* and *H. calyx* have a dictyonine (fused) framework (Fig. 1-5A, B) but only *A. vastus* have oxyhexaster spicules (Fig. 1-5C) and diactines lining on the atrial side of the body wall. Both have pinnular hexactins, but the ornamental ray of these spicuels on *A. vastus* can be identified as spikey (Fig. 1-5D) whereas the rays of *H. calyx* are identified as scaley (Fig. 1-5E). The heavily silicified skeletons of *A. vastus* and the dense populations of sponges at reefs suggest a large amount of silica is currently locked into sponge biomass.

A. vastus appears to be the dominant reef-forming sponge in the Strait of Georgia and thus is the ideal study organism to elucidate the biological patterns of entire sponge reefs. Like all other glass sponges, *A. vastus'* syncytial tissue is a unique single multinucleate cytoplasm with cellular components connected via distinct plugged cytoplasmic junctions (Leys 2003). Extensive water canals and flagellated chambers line the body wall with incurrent flow occurring through the ostia and excurrent flow exiting through the osculum (Leys 1999). This optimized pumping mechanism is used for selective suspension feeding of bacteria in the water column (Yahel et al. 2006) as well as waste removal. The dense populations of *A. vastus* in reefs may, therefore, be significantly coupled with the microbial loop as large consumers of particulate organic matter (POM) on the west coast of Canada.

1.2 Thesis objectives

The objectives of my thesis were to survey biological patterns expressed by the main reef forming glass sponge, *A. vastus*, at three reefs (Fig 1-1B; Howe, Fraser and Galiano reefs) in the Strait of Georgia. Specific goals were to: (1) determine the spatial structure and distribution patterns of the glass sponges, (2) determine the how the glass sponges structure the community of other animals found in reefs, (3) determine the amount of silica biomass in a reef, (4) determine if dissolution occurs in glass sponge skeletons, (5) establish a silica balance for a glass sponge reef and, (6) determine the variability in feeding patterns of *A. vastus*. The results of my work would expand our knowledge on glass sponge ecology and also provide insight into why these unique glass sponge reefs are found only on the west coast of Canada.

1.3 Overview and structure of chapters

My thesis is composed of 5 chapters. Chapter 1 is this introductory chapter. Chapter 2 reports the spatial structure, distribution, and abundance of the glass sponges and their associated community of animals. Chapter 3 reports on biomass measurements of the glass sponges and dissolution experiments on

sponge skeletons. Chapter 4 reports on the spatial variability of stable isotopes ($\delta^{13}C$ and $\delta^{15}N$) in reef and non-reef populations of *A. vastus.* Chapter 5 is a general conclusions chapter.

Chapter 2. To understand the mechanisms and controls involved with reef formation and patterning, I set out to map the distribution and abundances of the live sponge populations at 3 reefs in the Strait of Georgia. In this chapter, my results show that each reef is different in live sponge cover, abundance and oscula density. Also, sponge populations are very patchy and confined within a narrow range of depths, suggesting (1) a reef is structured at multiple scales and (2) reef locations like determined by flow enhancement over the underlying topography. The community composition between reefs is strongly structured by the abundance of certain taxa with the most animals found in the reef with the densest sponge populations (Galiano reef).

Chapter 3. *A. vastus* and its dead skeletons create the structural foundation for reef growth and are used as habitat for a diverse community of animals. The potential long term persistence of the heavily silicified sponge skeletons reflects the stability of the system but also represents a large amount of silica locked into sponge biomass. Using quantified Ekman grab sampling at each reef and biomass measurements, I show *A. vastus* is propotionally 80% silica and determine the reservoir of silica locked into each of the 3 reefs. I also report on experiments on the dissolution of glass sponge skeletons, and use past empirical data on growth rates to show that a glass sponge reef represents a large silica sink in the coastal waters of British Columbia, Canada.

Chapter 4. To understand the flow of energy and the feeding patterns that support the high abundances of sponge biomass in a reef, I explore the spatial variation in stable isotopes ($\delta^{13}C$ and $\delta^{15}N$) in *A. vastus* between reefs in the SOG and offshore non-reef populations. Within a reef, *A. vastus* has a highly selective, homogenous diet, but $\delta^{13}C$ and $\delta^{15}N$ are distinctly different between reefs and compared to non-reef populations. My results suggest spatially differentiated diets between populations of *A. vastus* and that potential anthropogenic input from terrestrial organic matter is expressed in the $\delta^{13}C$ and $\delta^{15}N$ of sponges in the SOG.

In Chapter 5, I suggest directions of future research to further characterize the glass sponge reef system based on the patterns I reveal in my thesis.

1.4 Literature Cited

Austin WC (1983) Underwater birdwatching. Can Tech Rep Hydrog Ocean Sci 38:83-89

Austin WC (1999) The relationship of silicate levels to the shallow water distribution of hexactinellids in British Columbia. Mem Qld Mus 44:44

Barrie JV, Bornhold BD (1989) Surficial geology of Hecate Strait, British Columbia continental shelf. Can J Earth Sci 26:1241-1254

Barrie JV, Conway KW (1999) Late Quaternary Glaciation and postglacial stratigraphy of the northern Pacific margin of Canada. Quat Res 51: 113-123

Barthel D (1992a) Do hexactinellids structure Antarctic sponge associations? Ophelia 36:111-118

Barthel D (1992b) Antarctic hexactinellids: a taxonomically difficult, but ecologically important benthic component. Verh Dtsch Zool Ges 85:271-276

Beaulieu SE (2001) Life on glass houses: sponge stalk communities in the deep sea. Mar Biol 138:803-817

Bett BJ, Rice AL (1992) The influence of hexactinellid sponge (*Pheronema carpenteri*) spicules on the patchy distribution of macrobenthos in the Porcupine Seabight (bathyal NE Atlantic). Ophelia 36:217-226

Billet DSM, Lampitt RS, Rice AL, Montoura RFC (1983) Seasonal sedimentation of phytoplankton to the deep-sea benthos. Nature 302:520-522

Brunton FR, Dixon OA (1994) Siliceous sponge-microbe biotic associations and their recurrence through the Phanerozoic as reef mound constructors. Palaios 9:370-387

Conway KW, Barrie JV, Austin WC, Luternauer JL (1991) Holocene sponge bioherms on the western Canadian continental shelf. Cont Shelf Res 11:771-790

Conway KW, Krautter M, Barrie JV, Neuweiler M (2001) Hexactinellid sponge reefs on the Canadian continental shelf: a unique “living fossil” Geosci Can 28:71-78

Conway KW, Barrie JV, Krautter M (2004) Modern siliceous sponge reefs in a turbid, siliciclastic setting: Fraser River delta, British Columbia, Canada. N Jb Geol Palaont Mh 6:335-350

Conway KW, Barrie JV, Krautter M (2005) Geomorphology of unique reefs on the western Canadian shelf: sponge reefs mapped by multibeam bathymetry. Geo-Mar Lett 25: 205-213

Conway KW, Barrie JV, Hill, PR, Austin WC, Picard K (2007) Mapping sensitive benthic habitats in the Strait of Georgia, coastal British Columbia: deep-water sponge and coral reefs. Geol Surv Can, 2007-A2:1-6

Darwin C (1859) The origin of species by means of natural selection or the preservation of favoured faces in the struggle for life. John Murray, London

Dayton PK, Robilliard, GA, Paine, RT, Dayton LB (1974) Biological accommodation in the benthic community at Mcmurdo Sound, Antarctica. Ecol Monogr 44:105-128

Dayton PK (1979) Observations of growth, dispersal and population dynamics of some sponges in McMurdo Sound, Antarctica. Colloques internationaux du CNRS 291:271-282

Dohrman M, Janussen D, Reitner J, Collins AG, Wörheide G (2008) Phylogeny and evolution of glass sponges (Porifera, Hexactinellida). Syst Biol 57:388-405

Fallon SJ, James K, Norman R, Kelly M, Ellwood MJ (2010) A simple radiocarbon dating method for determining the age and growth rate of deep-sea sponges. Nucl Instrum Methods in Phys Res B 268:1241-1243

Gage JD, Tyler PA (1991) Deep-sea biology: A natural history of organisms at the deep-sea floor. Cambridge University Press, Cambridge

Gehling JG, Rigby JK (1996) Long expected sponges from neoproterozoic Ediacara fauna of South Australia. J Paleontol 70:185-195

Ghiold J (1991) The sponges that spanned Europe. New Sci 2:58-62

Hecker B (1985) Fauna from a cold sulphur-seep in the Gulf of Mexico: Comparison with hydrothermal vent communities and evolutionary implications. Biol Soc Wash Bull 6:465-473

Koslow T (2007) The Silent Deep. University of Chicago Press, Chicago

Krautter M, Conway KW, Vaughn Barrie J, Neuweiler M (2001) discovery of a "living dinosaur": globally unique modern hexactinellid sponge reefs off British Columbia, Canada. Facies 44: 265-282

Krautter M, Conway KW, Vaughn Barrie J (2006) Recent Hexactinosidan sponge reefs (silicate mounds) off British Columbia, Canada: frame-building processes. J Paleont 80:38-48

Leinfelder RR (1993) Upper Jurassic reef types and controlling factors. Profil 5:1-45

Leinfelder RR, Krautter M, Laternser R, Nose M, Schmid DU, Schweigert G, Werner W, Keupp H, Herrmann R, rehfeld-Kiefer, U, Schröder JH, Reinhold C, Koch R, Zeiss A, Schweizer V, Christmann H, Menges G, Luterbacher H(1994) The origin of Jurassic reefs: current research developments and results. Facies 31:1-56

Leys SP, Mackie GO (1997) Electrical recording from a glass sponge. Nature 387:29-30

Leys SP, Lauzon NRJ (1998) Hexactinellid sponge ecology: growth rates and seasonality in deep water sponges. J Exp Mar Biol Ecol 230:111-129

Leys SP (1999) The choanosome of hexactinellid sponges. Invertebr Biol 118, 221-235

Leys SP (2003) The significance of syncytial tissues for the position of the Hexactinellida in the Metazoa. Int Comp Biol 43:19-27

Leys SP, Wilson K, Holeton C, Reiswig HM, Austin WC, Tunnicliffe V (2004) Patterns of glass sponge (Porifera, Hexactinellida) distribution in coastal waters of British Columbia Canada. Mar Ecol Prog Ser 283:133-149

Leys SP, Meech RW (2006) Physiology of coordination in sponges. Can J Zool 84:288-306

Leys SP, Mackie GO, Reiswig HM (2007) The biology of glass sponges. Adv Mar Biol 52:1-145

Maldonado MM, Carmona MC, Uriz MJ, Cruzado A (1999) Decline in Mesozoic reef-building sponges explained by silicon limitation. Nature 401:785-788

Maliva RG, Knoll AH, Siever R (1989) Secular change in chert distribution: A reflection of evolving biological participation in the silica cycle. Palaios 4:519-532

Pick KS, Philippe H, Schreiber F, Erpenbeck D, Jackson DJ, Wrede P, Wiens M, Alié A, Morgenstern B, Manuel M, Wörheide G (2010) Improved phylogenomic taxon sampling noticeably affects non-bilaterian relationships. Mol Biol Evol *in press*

Pile AJ, Young CM (2006) The natural diet of a hexactinellid sponge: benthic-pelagic coupling in a deep-sea microbial food web. Deep-Sea Res Part I 53:1148-1156

Rice AL, Thurston MH, New AL (1990) Dense aggregations of a hexactinellid sponge, *Pheronema carpenteri*, in the Porcupine Seabight (northeast Atlantic Ocean), and possible causes. Prog Oceanogr 24:179-196

Paull CK, Hecker B, Comeau R, Freeman-Lynde RP, Neumann C, Corso WP, Golubic S, Hook JE, Sikes E, Curray J (1984) Biological communities at the Florida Escarpment resemble hydrothermal vent taxa. Science 226:965-967

Reiswig HM (2002) Family Aphrocallistidae Gray, 1867. In: Hooper JNA, van Soest RWM (eds) Systema Porifera: A guide to the classification of sponges, Vol 2, Plenum, New York

Reiswig HM (2006) Classification and phylogeny of Hexactinellida (Porifera). Can J Zool 84:195-204

Sanders HL, Hessler RR (1969) Ecology of the deep-sea benthos. Science 163:1419-1424

Schmid DU, Leinfelder RR, Nose M (2001) Growth dynamics and ecology of Upper Jurassic mounds, with comparisons to Mid-Palaeozoic mounds. Sediment Geol 145:343-376

Schrader HJ (1971) Fecal pellets: role in sedimentation of pelagic diatoms. Science 174: 55-57

Smith CR (1985) Food for the deep sea: Utilization, dispersal and flux of nekton falls at the Santa Catalina Basin floor. Deep-Sea Res Part A 32:417-442

Tabachnick KR (1991) Adaptation of the hexactinellid sponges to deep-sea life. In Fossil and Recent Sponges (J. Reitner and H. Keupp, eds) pp. 378-386

Tabachnick, KR (1994) Distribution of recent Hexactinellida. In: van Soest R, van Kempen B, Braekman G (Eds) Sponges in Time and Space. Balkema, Rotterdam, pp 225–232

Tompkins-MacDonald GJ, Leys, SP (2008) Glass sponges arrest pumping in response to sediment: implications for the physiology of the hexactinellid conduction system. Mar Biol 154: 973-984

Vacelet J, Boury-Esnault N, Harmelin JG (1994) Hexactinellid cave, a unique deep-sea habitat in the scuba zone. Deep-Sea Res Part I 41:965-973

Van Dover, CL (2000) The ecology of deep-sea hydrothermal vents. Princeton University Press, Princeton

Whitney FA, Conway K, Thomson R, Barrie JV, Krautter M, Mungov G (2005) Oceanographic Habitat of sponge reefs on the Western Canadian Continental Shelf. Cont Shelf Res 25:211-226

Yahel G, Eerkes-Medrano DI, Leys SP (2006) Size independent selective filtration of ultraplankton by hexactinellid glass sponges. Aquat Microb Ecol 45:181-194

Table 1-1. Worldwide locations of dense populations of glass sponges. The locations, densities, depths, and species from each known glass sponge populations are listed next to their source.

Location	Density	Depth range (m)	Main Species	Source
(1) California bathyal basin	2-3 per 10 m^2	4100	*Hyalonema* sp.	Beaulieu (2001)
(2) Porcupine Seabight	15 per 10 m^2	1000 - 3000	*Pheronema carpenteri*	Rice et al. (1990)
(3) Hawaii	47 per 10 m^2	360 - 460	*Sericolophus hawaiicus*	Pile & Young (2006)
(4) Mediterranean submarine cave	1000 per 10m^2	18-24	*Oopsacus minuta*	Vacelet et al. (1994)
(5) Antarctica	80% of benthos (of 31 m^2)	33-600	*Rossella nuda* *R. racovitzae* *Scolymastra joubini*	Dayton (1979)
(6) New Zealand fjords	unknown	25–1200 common at ~100 m	*Symplectella rowi*	[a]H. Reiswig & [b]M. Kelly pers. comm.
(7) British Columbia (BC) fjords (non-reef)	40-240 per 10 m^2	20 - 200	Populations of dictyonine & lyssacine	Leys et al. (2004)
(8) BC – Learmonth Bank, Dixon Entrance	Up to 36 per 10 m^2	160 - 482	Populations of dictyonine & lyssacine	This thesis (Chapter 5)
(9) BC – sponge reefs	Up to 85% of benthos	59 - 175	*A. vastus* *H. calyx*	This thesis (Chapter 1)

[a] Dr. Henry M. Reiswig of the University of Victoria and the Royal British Columbia Museum, Victoria, Canada
[b] Dr. Michelle Kelly of the National Centre for Aquatic Biodiversity & Biosecurity, Aukland, New Zealand.

Figure 1-1. Geographic locations of all known glass sponge reefs. (a) Four are known in Hecate Strait. (b) Thirteen are known in the Strait of Georgia. Howe reef, Fraser reef and Galiano reef (yellow circles) are the primary study reefs of this thesis (adapted from Conway et al. 2007).

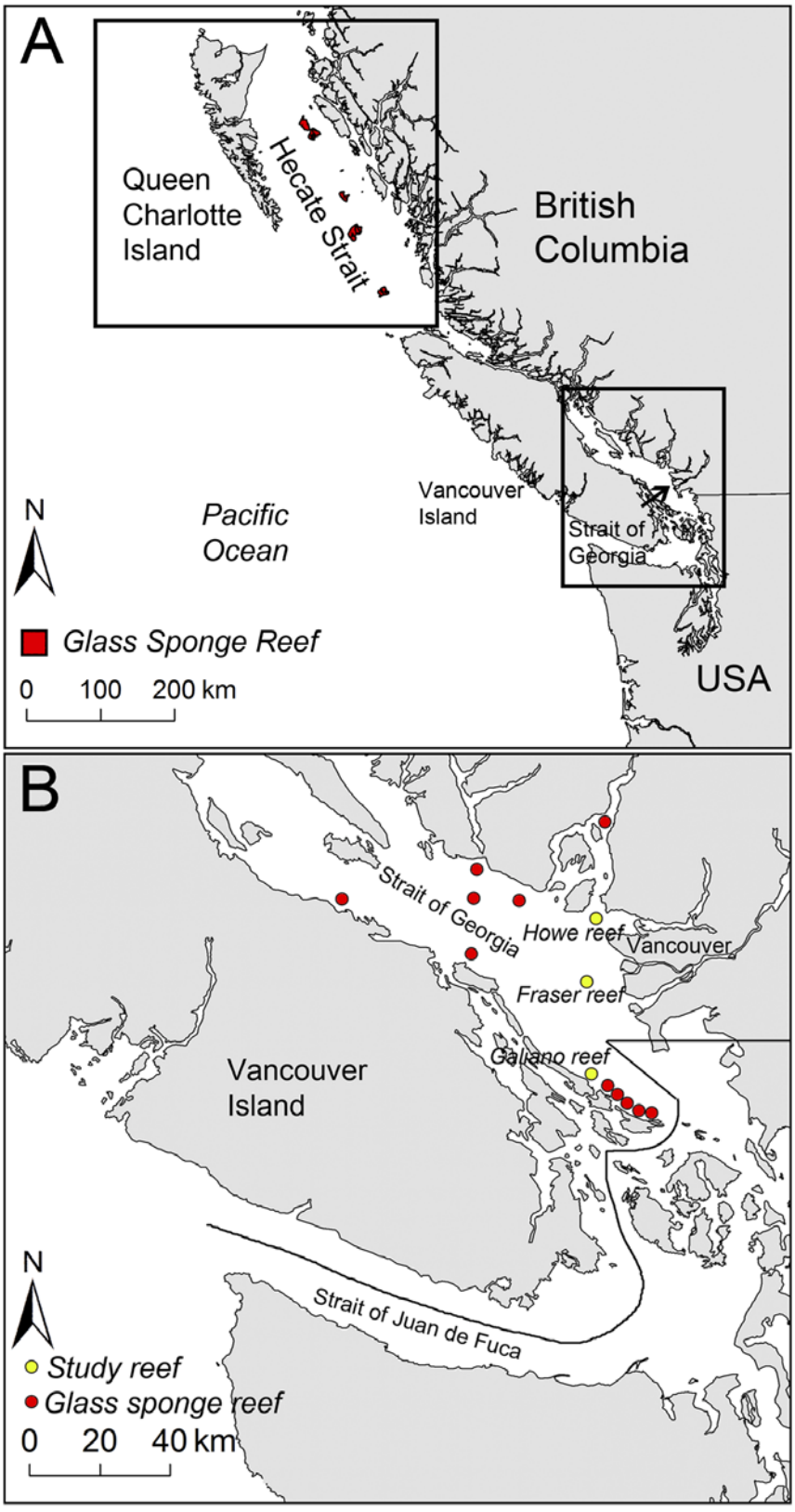
A
Queen
Charlotte
Island
Hecate Strait
British
Columbia
Vancouver
Island
Strait of
Georgia
N
Pacific
Ocean
Glass Sponge Reef
0 100 200 km
USA
B
Strait of Georgia
Howe reef
Vancouver
Fraser reef
Galiano reef
Vancouver
Island
N
Strait of Juan de Fuca
Study reef
Glass sponge reef
0 20 40 km

Figure 1-1

Figure 1-2. Current phylogeny of basal metozoan relationships based on morphological and molecular data by Dohrmann et al. (2008) and Pick et al. (2010). Hexactinellida is one of 3 classes within the phylum Porifera and is the only metazoan clade with syncytial tissue.

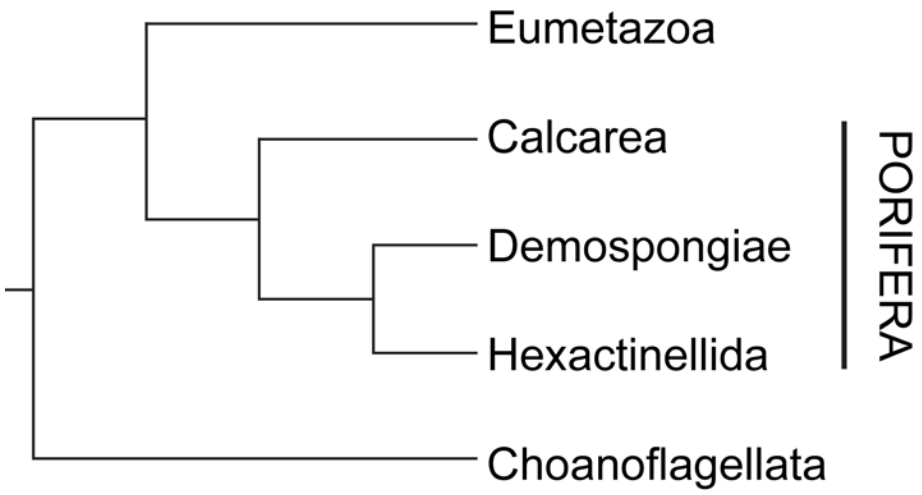
Eumetazoa
Calcarea
Demospongiae
Hexactinellida
PORIFERA
Choanoflagellata

Figure 1-2

Figure 1-3. Worldwide locations of known dense glass sponge populations. Although glass sponges are common fauna in deeper waters, dense populations are only known and have been studied in a few regions. Numbers correspond to the locations summarized in Table 1-1.

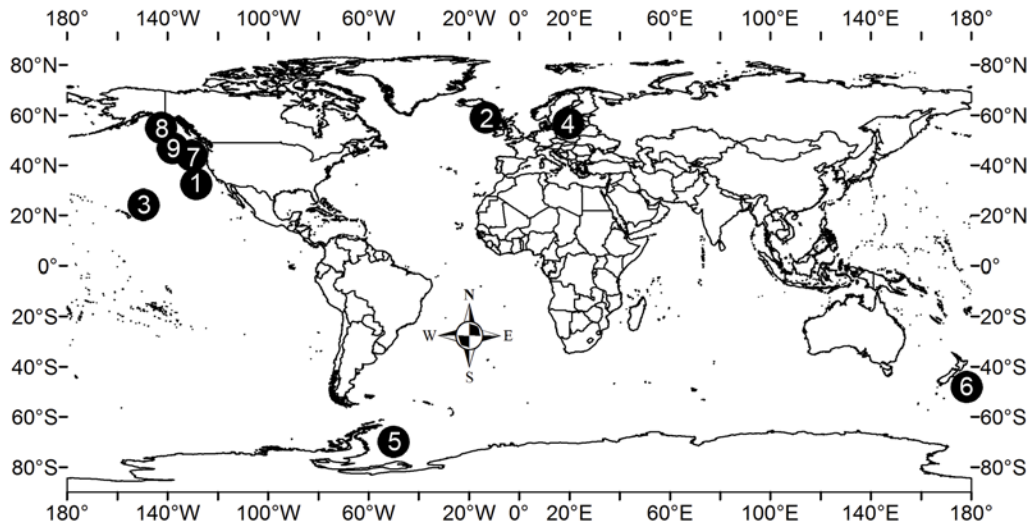
180°
140°W
100°W
60°W
20°W
0°
20°E
60°E
100°E
140°E
180°
80°N
60°N
40°N
20°N
0°
20°S
40°S
60°S
80°S
N
W
E
S
1
2
3
4
5
6
7
8
9
Figure 1-3

Figure 1-4. The 3 glass sponge species known to form reefs on the Pacific coast of Canada. (A) *Aphrocallistes vastus* (B) *Heterochone calyx* (C) *Farrea occa* (not in SOG). (D) Only *A. vastus* and *H. calyx* form glass sponge reefs in the SOG.

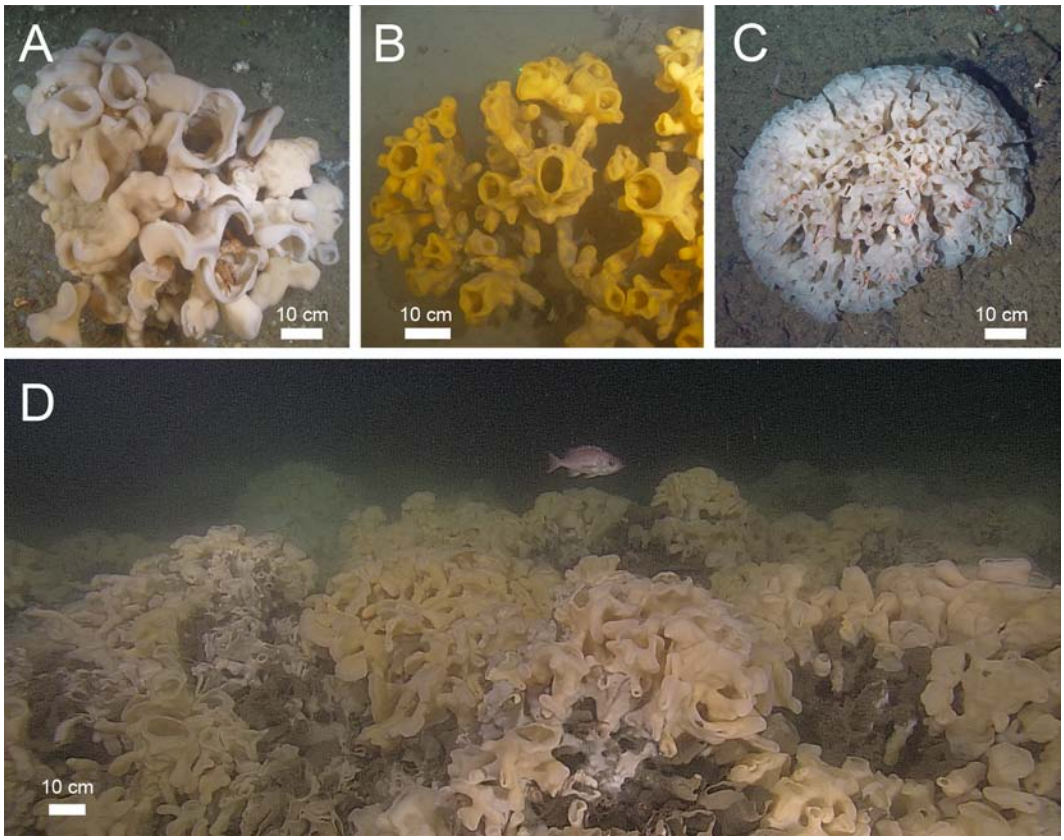

Figure 1-4

Figure 1-5. Spicules of the two reef forming speices in the Strait of Georgia, *Aphrocallistes vastus* and *Heterochone calyx*. (A,B) Dictyonine skeletons. Both (A) *A. vastus* and (B) *H. calyx* have a dictyonine framework made from fusion of megasclere spicules from secondary silica deposition. (C) Only *A. vastus* has oxyhexaster spicules. Both *A. vastus* and *H. calyx* have pinnular hexactins, but the ornamental ray, distal to the dermal surface of the sponge, is characteristically spikey in (D) *A. vastus* compared to a scaly form in (E) *H. calyx*.

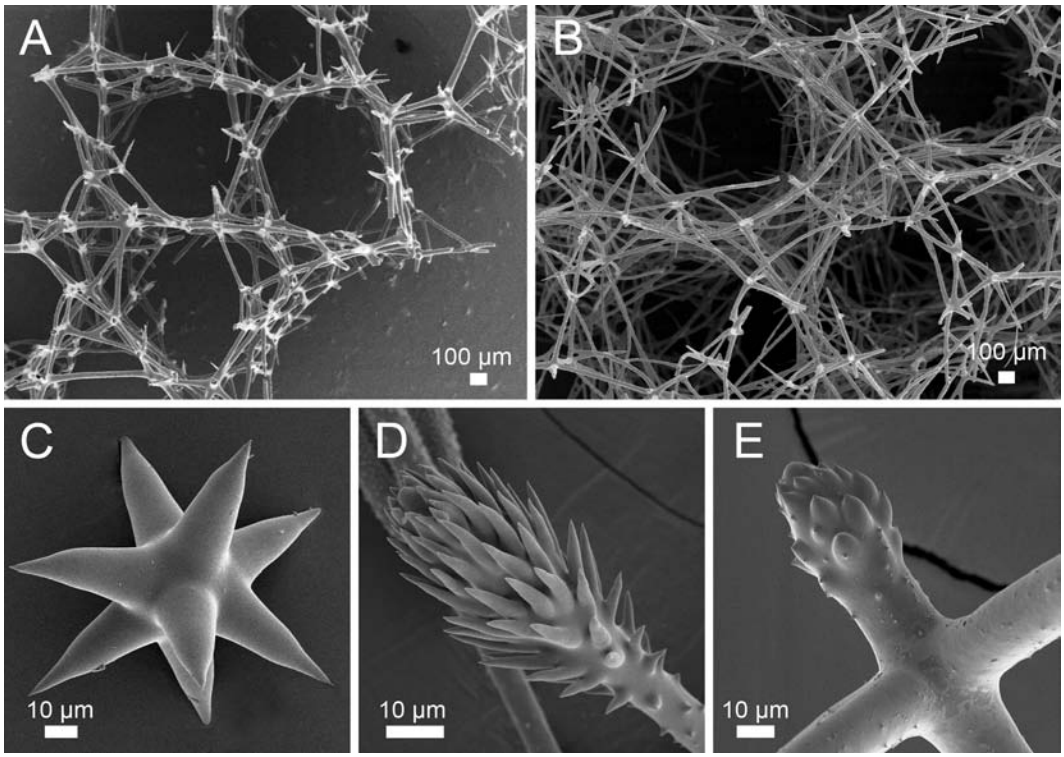

Figure 1-5

Chapter 2

High resolution mapping of community structure in three glass sponge reefs (Porifera, Hexactinellida)

2.0 Introduction

Glass sponge reefs (Porifera, Hexactinellida) are unique habitats found on the Pacific coast of Canada where they discontinuously cover over 700 km^2 of the sea floor (Conway et al. 2001; 2004). Pacific coast reefs represent a modern analogue to extinct reefs that once formed a 7000 km belt of glass sponges in the northern Tethys Sea a region that now covers large parts of Europe (Ghiold 1991; Leinfelder et al. 1994). Today, glass sponges are generally found in deep water (>30m), and often at depths greater than 300 m (Tabachnick 1994; Leys et al. 2007). Some 500-600 species of glass sponges have been described (Reiswig 2006) and these fall into two categories based on their spicule skeleton: those with a skeleton of loose spicules termed lyssacine, and those in which spicules are fused together by secondary silica deposition to form a rigid skeleton, termed dictyonine (Leys et al. 2007). In Hecate Strait, three species of dictyonine sponges form reefs: *Aphrocallistes vastus*, *Heterochone calyx*, and *Farrea occa* (Conway et al. 2001; Krauuter et al. 2001; Whitney et al. 2005) but in the Strait of Georgia, *A. vastus* and *H. calyx* are the only reef builders; *F. occa* does not occur inside of Vancouver Island (Leys et al. 2004).

The first modern glass sponge reefs were found at depths of 165-240 m on the continental shelf (Conway et al. 2001; Krautter et al. 2001; Whitney et al. 2005) but some have recently been documented as shallow as 30 m in fjords (e.g. Howe Sound, see Marliave et al. 2009). It should be noted that dense populations of glass sponges ('sponge gardens') are found throughout B.C. fjords as described by Leys and colleagues (2004), but these do not generally form characteristic reef mounds in which skeletons of successive generations of sponges settle and grow on each other. Typical reefs like this gradually accumulate to reach heights of up

A version of this chapter has been accepted for publication in the journal Marine Ecology Progress Series (2010.08.13) under "Chu, JWF and Leys, SP. High resolution mapping of three glass sponge reefs (Porifera, Hexactinellida)".

to 21 m, where the bulk of the mounds consist of dead sponges buried by sediments with only the most recent generation growing 1-2 m above the surface (Conway et al. 2001; 2005).

Glass sponges have a major ecological role in deep water habitats. In other regions of the world, dennse populations of lyssacine sponges have been documented to create benthic complexity and support whole communities of other organisms (Dayton et al. 1974; Barthel 1992a,b; Bett & Rice 1992). Also, as highly efficient feeders on ultraplankton (<10 μm), the sponges assimilate large amounts of carbon and are an important link between the pelagic and benthic environments (Pile & Young 2006; Yahel et al. 2007). Much is known about non-reef forming glass sponge communities in Antarctica, the Atlantic and mid-Pacific, but very little about glass sponge reefs, such that even the basic patterns of distribution, abundance, and growth of the sponge populations at the reefs have not yet been quantified. Glass sponge reefs, due to their three dimensional structure, are expected to create habitat like other glass sponge assemblages, but due to the immense area they cover, the scale of their impact may be much greater.

Until now, the location of reefs has been determined using multibeam echo sounders which provide a landscape scale (kilometres) interpretation of distribution (Conway et al. 1991; 2001; 2005; 2007). Despite the value of multibeam, this technique cannot differentiate between live, dead, and buried portions of glass sponges within a reef. Furthermore, past linear transects and box core sampling highlighted the ecology of the reefs (Cook 2005; Cook et al. 2008; Marliave et al. 2009) but quantified the community patterns of associated invertebrates and fish without first empirically establishing the extent of the live sponges and thus may be biased in interpretation. Because the living portions of a reef have not been measured we have been unable to properly address questions pertaining to the biology of the reefs, their community ecology and the role glass sponge reefs have in nutrient cycling.

Therefore, the goal of my study was to use high resolution mapping techniques to determine the distribution patterns and spatial structure of live

sponges at three reefs in the Strait of Georgia, British Columbia. The logistical challenges of working in deep water makes sampling at a small scale difficult (Grassle 1991). However, as pattern detection is scale dependent (Levin 1992; Legendre et al. 1997), I took a small scale approach by sampling at 25 m and 12.5 m intervals within a stratified grid design using remote operated vehicles (ROV) and high resolution imagery to systematically survey the entire populations of live sponges at each reef. From observations of the patchy nature of the reefs (Conway et al. 2005), I predicted that the sponges would have a high degree of spatial structure and used semivariogram analysis and geographic information systems (GIS) to map their distributions. Dense populations of other suspension feeders have been found in areas where elevated topography amplifies water flow (Sebens 1984; Genin et al. 1986; Barry & Dayton 1988) and thus I predicted the distributions of glass sponges, also found on elevated mounds and ridges in the Strait of Georgia, would be strongly related to their position on the mounds. The high resolution imagery allowed me to determine patterns of association of other invertebrates and fish with the glass sponges. Finally, I used my measurements of the sponges together with previous knowledge of their filtration rates (Yahel et al. 2007) to estimate the impact sponge reefs have on bentho-pelagic coupling of nutrients.

2.1 Materials and Methods

2.1.1 Reef Sites

The Strait of Georgia (SOG, Fig. 2-1 inset) is approximately 28 km wide by 222 km long with an average depth of 155 m and separates the British Columbia mainland from Vancouver Island on the Pacific coast of Canada (Thomson 1981). Glass sponge reefs in the SOG are only found on undifferentiated bedrock features elevated from the fine grained depositional sediments comprising the majority of the seafloor in the SOG basin. The three reefs in this study are referred to by names reflecting their proximity to local geographic features (Fig. 2-1).

Howe Sound reefs: Howe Sound (49°19'57.672"N, 123°17'42.297"W) is a fjord located north of the city of Vancouver. High freshwater discharge carrying fine silts from the nearby Squamish River, Cheakamus River and the Fraser River plume are characteristic of the surface waters flowing over this area (Burd et al. 2008). The glass sponge reefs here exist in several discontinuous patches on sloped bathymetry outside of the mouth of Howe Sound. One reef was surveyed at the mouth of Howe Sound (hereafter referred to as Howe reef). Marliave et al. (2009) described the associated animal community from ROV videotapes of a ~200 m transect running diagonally through this reef.

Fraser Ridge reefs: The Fraser Ridge (49°9'15.673"N, 123°23'3.705"W) is an elevated mound capped by glacial sediments (Conway et al. 2004) that lies slightly offshore in the path of the Fraser River outflow (Conway et al. 2005). The surface waters here experience high sedimentation rates as the Fraser River is the source of 80% of the sediments in the SOG (Hill et al. 2008). The glass sponge reefs (hereafter referred to as Fraser reef) occur in several small patches on the northeast and west sides of the mound (Conway et al. 2004).

Galiano Ridge reefs: The Galiano Ridge (48°54'51.468"N, 123°19'27.654"W) is a continuous submarine crest that runs linearly in a Northwest-Southeast direction for over 40 km parallel to the eastern shoreline of Galiano Island in the Strait of Georgia. The ridge is a crustal fold created at the tectonic forearc from the subduction zone of the Juan de Fuca plate moving under the North American landmass (Hill et al. 2008). The glass sponge reefs here are found in discontinuous patches along an approximate 5-6 km stretch north and south of Active Pass (Conway et al. 2007). A 1.5 km section north of Active Pass was surveyed (hereafter referred to as Galiano reef).

2.1.2 ROV field sampling

Quantified field surveys were carried out during three scientific cruises (ROPOS 2007, Phantom 2008 and ROPOS 2009). To establish a replicable sampling protocol, a pilot survey was carried out at Fraser Ridge in 2005 with the Canadian operated ROV, ROPOS. To maximize the logistical tradeoffs of small

scale sampling relative to the large benthic area covered by a reef, we used a sampling grid of 25 m established during the pilot survey. A perimeter was created around all the sponges during this pilot survey and a georeferenced 25 m stratified grid of points (n = 300) was overlaid within this perimeter for our quantified sampling in 2009 (Fig. 2-2A). For Howe and Galiano reefs a 25 m grid of points (n = 309, n = 238 respectively) was determined by delineating the reef perimeter from multibeam bathymetry mapped by Canadian Hydrographic Service in 2007 (Fig. 2-2B, C), with *a priori* knowledge (K. Conway, NRCan pers. comm.) and was modified during the survey.

During each survey ROPOS flew to each point in the grid, hovered 1-2 m above the benthos and captured an image with a downward looking digital still camera (DSC, Sony Cyber-Shot DSC F707). A Phantom HD2+2 ROV (Deep Ocean Engineering) operated by the Pacific Biological Station (Nanaimo, British Columbia) and equipped with a DSC (Olympus SP350) with slaved strobe (TTL capable Ikelite 200) was also used to survey a different area at Galiano reef. Because of the difference in size, power, and hardware configuration between the two ROV platforms, current induced drag on the ROV-tether prevented the Phantom from remaining stationary at predetermined points. Instead of a stratified grid design, the Phantom flew 25 m spaced transect lines running northwest of the ROPOS waypoints created in 2007 (Fig. 2-2C) and captured one image approximately every 20 seconds (n = 515) while flying approximately 1 m above the benthos. The slaved strobe allowed sharp images to be taken while the Phantom was in motion. Each ROPOS image was 5 megapixels (MP) and covered approximately 3.2 m^2 of substrate. Each Phantom image was 8 MP and covered 1.2 m^2 of substrate. Images from both ROV platforms had 10 cm laser dots for scale.

Fine scale survey. Preliminary analysis of data from the 25 m grid survey at Galiano reef in 2007 suggested spatial patterns occur at a scale less than 25 m. Therefore in 2009, I subdivided the original 25 m grid with additional waypoints to sample an area of high sponge density in a 12.5 m grid (Fig. 2-2D).

2.1.3 Image analysis of glass sponges and reef biota

The area of each image was measured in Adobe Photoshop CS3 with the image analysis tool. Areas of live sponge, dead sponge and bare substrate (mud or exposed bedrock) were delineated and converted into a percentage of cover. Only ROPOS 2009 images were used to compare sponge morphology among reefs. Because the osculum (the excurrent vent of the sponge) determines the volume of water the sponge processes, the number of oscula was used as an indicator of the density live animals and therefore and robustness of a reef. All dictyonine sponge oscula were counted and the area of those facing directly into the camera was measured. The size distributions of oscula at each reef, their mean area, standard deviation (SD), and coefficient of variation (CV) were calculated for each reef. *A. vastus* and *H. calyx* are morphologically very similar in the reefs, and because we could not perform extensive sampling for species confirmation, we were unable to differentiate between the two closely related dictyonine species using only our survey images and therefore refer to them as dictyonine sponges in our interpretations where appropriate.

Individual oscula, as a single pumping (water processing) unit were counted, rather than individual sponges, because it was not possible to identify individuals in the mass of oscula arising from the reef. The number of live oscula in the area surveyed and the number of live oscula in a continuous patch of live sponges were standardized to obtain density per m^2. Only images covering areas >1 m^2 were used to prevent extrapolation of oscula density measurements; 78 images from each reef were analyzed for density over the substrate, and 10 images were chosen at random from each reef and analyzed for density per live sponge cover.

All animals >4 cm in length were identified to the lowest taxonomic level possible from the ROPOS 2009 dives and the Phantom 2008 dives. Abundance data could not be pooled across ROV platforms because of the differences in area sampled and the increased resolution of the Phantom camera.

Multivariate and univariate analyses were used to compare differences in the community composition and abundances of animals in a reef. Using only ROPOS 2009 images, a matrix was created on square root transformed abundance data using the Bray Curtis similarity index, then analysis of similarity (ANOSIM) tests were used to determine differences in the community composition and analysis of variance was used to determine differences in total animal abundance between the 3 reefs. Similarly, using only Phantom 2008 images, the differences in the community composition and the abundance of individual taxa (Porifera, Cnidaria, Annelida, Mollusca, Arthropoda, Echinodermata, and fish) were determined between areas with and without glass sponges. Counts of unidentifiable fish, large blurred schools (>30 individuals) and highly mobile fish species (ratfish) were not included in the analyses in order to avoid counting individuals more than once. All multivariate analyses were done with PRIMER v5.2.2 and all univariate analyses were done with JMP v7.0

2.1.4 Spatial analyses of glass sponge distributions

Patchy distributions are ideally suited for semivariogram analysis which can determine the maximum distance two points are spatially autocorrelated in an area (Robertson et al. 1988; Rossi et al. 1992). If spatial autocorrelation exists, the semivariogram model parameters can then be used to interpolate the unsampled regions between points to create a continuous surface, here the sponge cover across the entire area surveyed. Spatial UTM coordinates (metres) and values of percent live sponge cover were used as the xyz data for creating our semivariogram models. Spherical models best explained the data based on the proportion of variance resolved by the spatial structure [$(C/C_0 + C)$], the coefficient of determination (r^2) and the residual sum of squares (RSS). Estimated parameters were the nugget effect (C_0) which captures variation at distances less than our minimum sampling distance between points, the sill ($C_0 + C$) which indicates where the semivariance asymptotes or the overall variance of the sponge cover, and the range (A_0) which defines the maximum distance at which spatial autocorrelation exists. Points separated at distances greater than the

range were considered spatially independent. All semivariogram analyses were performed in GS+ 3.1.7.

Visual estimates of live sponge cover were made during each dive in 2009 and preliminary isopleths were interpolated directly onboard the ship to create rough maps of sponge distributions. These maps were used to sample live sponges for other research objectives and allowed us to ground truth the semivariogram models. Since spatial autocorrelation existed in all the surveys, percent live sponge cover (from precise area measurements in each image) was interpolated into 5% isopleth intervals by Kriging. In ArcView v9.2 a layer mask polygon was created using the outer grid points as the perimeter to prevent extrapolation outside the surveyed area. The proportional area covered by all isopleth levels was summed to estimate the total area of live and dead sponge cover. All maps are displayed in projection GCS WGS 1984 and all spatial analyses were done in projection WGS 1984 Complex UTM Zone 10N.

For analysis of the relationship between live sponge cover and depth and slope, I only used images that were separated by a distance greater than the range distance revealed from each reef's semivariogram model. A slope (incline in degrees) raster layer was created from the high resolution (5 m cell) multibeam bathymetry data using the spatial analysis tool in ArcView v9.2. Each of our survey points was then intersected with the depth and slope layers with the Hawth's Analysis Tools extension (Beyer 2004). The extent to which percent cover of live sponges was correlated with dead sponges, depth, and slope was analysed with Spearman rank correlation coefficients. Bathymetry data was provided by the Canadian Hydrographic Service in cooperation with the Geological Survey of Canada (Barrie et al. 2005).

2.2 Results

2.2.1 Live sponge distribution at each reef

Relative to the total area surveyed at each reef, Howe reef had the least live sponge cover (11.6% of the benthos covered with sponges); live sponge cover at Fraser reef was also low (14.5%), while Galiano reef had the highest relative

live sponge cover (26%) (Table 2-1). The distribution of sponges was confirmed to be patchy because the distribution of live sponges was spatially autocorrelated at all reefs. Within reefs, our spherical models resolved 75-80% of the structural variance and revealed range distances of 42, 58 and 72 m for Fraser, Howe and Galiano reefs at a 25 m sampling resolution (Table 2-2, Fig. 2-3). At Galiano reef, the semivariogram of our 12.5 m fine scale survey showed that sponge patches were correlated at half that distance, with a range distance of 35 m, even though a similar proportion of the structural variance (78%) was resolved by both surveys. At all reefs, points were uncorrelated beyond these distances based on the clear horizontal sill found in all semivariograms (Fig. 2-3). All semivariograms had a nugget variance (C_0) between 27 and 34% of the structural variance (C) which indicates spatial structure occurs at scales less than our minimum sampling distances of 25 m and 12.5 m (Table 2-1).

Kriging at 5 % sponge cover intervals revealed where the densest concentrations of live sponges were located at each reef. At Howe reef, live sponge cover occurred in sparse patches with most areas showing <20% cover and a few areas showing >50% cover (Fig. 2-4A). The substrate in between the sparse patches consisted of large expanses of fine silt-clay sediments. At Howe reef the area of live sponge cover was smaller than that identified by the multibeam data (Fig. 2-4). At Fraser reef, patches of live sponges occurred in hotspots with 4 nodes of >80% cover (Fig. 2-4B), and large expanses of mud were less common. At Galiano reef, live sponges formed multiple hotspots in concentric patterns along the crest. Seven nodes had >80% live sponge cover and several smaller regions had over 50% coverage of live sponges (Fig. 2-4C); there were few mud patches in the area we surveyed at Galiano reef. Fine scale sampling (12.5 m) at Galiano reef showed that the sponges were on either side of the ridge top as the percent live cover increased with increasing slope down from the pinnacle (Fig. 2-5A, B).

At all 3 reefs, the live glass sponges were confined to a narrow range of depths (<50 m), but were on a wide range of slopes (1-52°). At Howe and Fraser reefs, live sponges were found on one side of the underlying mounds; the majority

of sponges at Galiano reef were found on both sides of the ridge slopes (Table 2-3). At all reefs live sponge cover was positively correlated with dead sponge cover, negatively correlated with depth and despite predominantly being found on sloped topography, at none of the reefs was live sponge cover correlated with slope angle (Table 2-3).

2.2.2 Density and size of sponge oscula at each reef

Most dictyonine sponges in the reefs formed tightly clustered buses of tubes each with an osculum growing up to 1 m above the surface. At Galiano reef, small sponges (<10 cm oscula diameter) had tissue extending from their base to form additional oscula (Fig. 2-6A). We interpret growth to occur by this process because groups of oscula were all fused to a single base (Fig. 2-6B). Larger bushes with oscula facing many directions (Fig. 2-6C) may therefore arise from multiple branching events, as shown by the single basal attachment point on a dead sponge bush in Fig. 2-6D.

The density of sponge oscula (counts of oscula per m^2 surveyed) was significantly different between reefs (Kruskal-Wallis; $p < 0.0001$). Galiano reef had the highest density of oscula, 17.4 oscula m^{-2}, Fraser reef, 9.4 oscula m^{-2} and Howe reef, 5.5 oscula m^{-2} (Fig. 2-7A). Within continuous patches of live sponge, the density of sponge oscula was also significantly greater at Galiano reef (46.3 oscula m^{-2}) than at Howe reef (30.9 oscula m^{-2}) or Fraser reefs (23.0 oscula m^{-2}) (Fig. 2-7B; Kruskal-Wallis; $p < 0.0001$). However, whereas there were fewer oscula at Fraser reef, the average size oscula at Fraser reef was significantly larger (38.3 cm^2) than at either Galiano (23.0 cm^2) or Howe (12.8 cm^2) reefs (Fig. 2-7C; Kruskal-Wallis; $p < 0.0001$).

At all reefs, the size of oscula was highly variable but was nevertheless positively skewed towards smaller class sizes (Fig. 2-8). Log transformed size data normalized distributions of the size classes at Howe reef and Galiano reef, but not at Fraser reef because of the greater number of individuals with large oscula. The proportion of sponges with small oscula (<5 cm^2) was greatest at Howe reef (28%) compared to Galiano reef (19%), and Fraser reef (11%). The

converse was also found: Howe reef had the fewest sponges oscula ≥100 cm^2 (1%) compared to Galiano reef (3%) and Fraser reef (9%).

2.2.3 Animals associated with glass sponges in the reefs

I identified a diverse assemblage of animals living on and among dictyonine sponges representing 7 phyla and 14 classes from our Phantom 2008 and ROPOS 2009 survey images (Table 2-4). The community composition was significantly different between all three reefs (Table 2-5, ANOSIM, R=0.153, p<0.001). The differences between communities were mainly driven by the greater abundance of the squat lobster, *Munida quadraspina*, spot prawn *Pandalus platyceros* rockfish *Sebastes* spp. at Galiano reef; greater abundance of the demosponge *Tetilla* sp. at Fraser reef; and greater abundance of the seawhip *Halipteris willeomoesi* at Howe reef. In general, significantly more animals were found at Galiano reef than either Fraser or Howe reefs (Fig 2-9; Kruskal-Wallis; $p < 0.0001$).

At Galiano reef, the total abundance of animals was significantly greater in the presence of reef sponges than in areas of bare substrate (Fig 2-10; Mann-Whitney U; $p < 0.0001$). The community composition was also significantly different in the presence of glass sponges compared to areas of bare substrate (Table 2-5, ANOSIM, R=0.246, p<0.0001). The main driver of this difference was the greater abundance of *M. quadraspina* in the presence of glass sponges. However, when I looked at the abundance within each phyla, there were significantly more crustaceans and fish found in the presence of reef sponges (Fig 2-10, separate Mann-Whitney U tests; $p < 0.0001$) with significantly fewer other sponges (Fig 2-10, Mann-Whitney U; $p < 0.0001$), and molluscs (Fig 2-10, Mann-Whitney U; $p < 0.05$) in the presence of reef sponges. There was no detectable difference in the abundance of cnidarians and echinoderms and annelids in the presence or absence of reef sponges (Fig 2-10, separate Mann-Whitney U tests; $p > 0.05$).

Lyssacine glass sponges (likely all *Rhabdocalyptus dawsoni*, but only one sample was collected at Galiano reef), were seen growing on and among dead

dictyonine skeletons at Howe reef and Fraser reefs, but at Galiano reef they were only found at the periphery of the population of dictyonine sponges. At Howe reef a dense bed (>2 ind m^{-2}) of the sea whip *Halipteris willeomoesi* was found at the upper northwest perimeter of reef stretching down parallel to the western extent of the reef. There is a clear boundary with no overlap between sea whips and glass sponges for the ~400 m length of the perimeter.

The only soft-bodied animal observed on live dictyonine sponges was the nudibranch *Peltodoris lentiginosa* (Fig. 2-11). Spicules of *A. vastus*, *H. calyx* and the encrusting demosponge *Desmacella austinii* (Lehnert et al. 2005) were found in the gut and in the fecal contents (for up to 1 week after sampling) of 4 sampled individuals of *P. lentiginosa* from Galiano reef (Fig. 2-12, Appendix 1). The gut contents of one nudibranch fixed in formaldehyde had a large intact piece of fused glass sponge skeleton (*H. calyx*) encrusted with *D. austini* along with several loose spicules from *H. calyx* and *D. austini*. The three live nudibranchs collected had relative wet weights and body lengths of 142.27 g (10.51cm), 286.10 g (15.4cm) and 329.39 g (15.81cm). From the analysis of images and video footage *P. lentiginosa* was only observed at Howe and Galiano reefs (Table A1-1 in Appendix 1), and average body length of accurately measureable individuals were 13.85 ± 4.39 (n=17) with the largest individual measuring 24.39 cm at 102 m depth found at the Howe Reef. This is the first confirmed predator of a reef forming glass sponge.

Crustaceans comprised 95% of all the identified megafauna and, other than *P. lentiginosa*, crustaceans were the only animals seen living directly on live reef sponges. The squat lobster *M. quadraspina* was the most abundant species overall with densities as high as 75 individuals m^{-2} at Galiano reef. The longhorn decorator crab *Chorilia longipes* was seen inside *A. vastus* oscula decorating itself with live sponge tissue. The most common fish observed among the reef sponges were rockfish (*Sebastes* spp.), flatfish, ratfish and pollock (*Theragra* sp.). A six-gill shark (*Hexanchus* sp.) was also seen at Fraser reef in our 2009 survey. Overall, more fauna were visible in images from the Phantom ROV camera compared to those captured by ROPOS (Table 2-6).

2.3 Discussion

By using high resolution ROV imagery, GIS analysis, and small scale sampling, I found distinct patterns of spatial structure at three glass sponge reefs in the Strait of Georgia. My results also reveal differences in usage of reefs by other animals and our quantified data on sponge abundance allows estimation of water and nutrient processing potential of reefs in the Strait of Georgia and highlight the large impacts they have on their environment.

2.3.1 Differences in sponge density and oscula size

The density of sponge populations differed substantially at each reef with the densest cover of live sponges at Galiano reef, and the least dense cover at Howe reef. This suggests there is proportionally more live sponge biomass at Galiano reef compared to Howe and Fraser reefs. Particularly at Howe reef, the live sponges I mapped in 2009 covered far less of the substrate than the structures identified by multibeam echosounding. Whereas acoustic signals used by multibeam echosounding will penetrate into soft sediment (Medialdea et al. 2008), my method of sampling only maps live and dead animals above the sediment surface. Therefore, my observations of large expanses of flat sediment between small clusters of sponges suggests sediment accumulation has buried large portions of Howe reef.

Rates of sediment accumulation are highest in front of the Fraser river outflow and in the southern portions of the Strait of Georgia (~2.0–2.3 g cm^{-2} $year^{-1}$) with less accumulation occuring in Howe Sound and the northern parts of the Strait (~0.2–0.4 g cm^{-2} $year^{-1}$) (Johannessen et al. 2003). The burial of sponges at Howe Reef likely occurs at a much slower rate than at Fraser and Galiano reefs. Therefore, the lower surficial cover and density of live sponges at Howe reef and could be due to several factors such as higher loads of suspended sediments, differences in food availability or impacts of bottom trawling activity. Though I am unable to assess feeding patterns, and do not have data for trawling activity in this region, it has been shown that generally glass sponges do not occur

in regions of high suspended sediments (Leys et al. 2004) and that sediments can clog the aquiferous canals (feeding system) of *A. vastus* (Tompkins-MacDonald & Leys 2008). Furthermore, during the survey at Howe reef, we came across areas of mechanically broken sponges similar to those described for sponge reefs elsewhere in the Strait of Georgia where the cause was suggested to be bottom trawling (Cook et al. 2008).

I also found differences in the size of oscula at each of the three reefs, with the smallest oscula at Howe and Galiano reefs, and the largest at Fraser reef. Conway et al. (2004) commented in particular on the size of oscula at Fraser reef, suggesting they were narrow in comparison to those at the vast northern reefs in Hecate Strait. They suggested that narrow oscula in glass sponges might be an adaptation to high sedimentation rates, but given that I found the smallest oscula in an area of relatively low sediment accumulation (Howe Sound) and larger oscula in areas of comparably higher sediment accumulation (Fraser outflow and southern Strait of Georgia) (Johannessen et al. 2003), this is not likely to be the case. The difference in the area of oscula more likely reflects the local hydrodynamic patterns as sponge oscula are highly plastic over a gradient of flow velocities (Bidder 1923; Warburton 1960; Palumbi 1986). Small scale measurements of benthic current velocities would determine if hydrodyanmic patterns are responsible for the variable oscula found in reef forming glass sponges.

2.3.2 Spatial structure of sponges within a reef

At each reef, live glass sponges characteristically form concentric hotspots in localized patches in which sponge recruitment and growth within a patch is substantially higher than at surrounding regions. My semivariogram analysis and Kriging results indicate the spatially dependent distance within a patch is 42, 58 and 72 m at Fraser, Howe and Galiano reefs respectively when sampled at a 25 m grid resolution. When we sampled at twice the resolution at Galiano (12.5 m grid), the patch size there was halved to 35 m, yet the structural variance explained by both the 25 and 12.5 m semivariogram models remained at

approximately 80%. This suggests that where sponge density is low (Fraser and Howe reefs) patches are well-defined areas of more or less the same size of what I observe as 'mounds'. However, where sponge density is high, as it is at Galiano reef, spatial structuring occurs at multiple scales. When sampled at 25 m resolution, patches merge into one another forming large, less defined mounds 72 m in diameter. When sampled at twice the resolution, smaller patches are resolved. My data further suggests that spatial structuring occurs at even smaller scales and these may be the individual sponge bushes that make up a mound. We do not know the extent to which reef sponges will bud, but asexual reproduction is common in the Porifera and budding commonly occurs in other glass sponges (Barthel & Gutt 1992; Texeidor et al. 2006). If a spatially dependent patch maintains a high recruitment of individuals, then the coalescence of large bushes would form the continuous clumps of sponges observed in our surveys.

The discontinuity of patches within a reef and the geographic separation of entire reefs means that sexual reproduction is responsible for dispersal and recruitment of new sponges, but we do not yet know the extent to which budding and recruitment of new larvae are involved in forming a single reef. Although nothing is known about the disperal ability of dictyonine larvae, larvae of the lyssaccine sponge *Oopsacas minuta* swim much like other sponge larvae *in vitro* and settle anywhere between 24 hours and 3 weeks after release from the parent (S. Leys pers. comm.); therefore it can be presumed that the short pelagic stage of sponge larvae (Maldonado & Bergquist 2002) results in localized recruitment. Local retention of larvae would further enhance patch structuring and development (Parker & Tunnicliffe 1994). This conclusion is supported by the observation that juvenile sponges recruit on the dead skeletons of previous generations (Leys et al. 2004; Krautter et al. 2006), and by the strong correlation I found between live sponge cover and dead sponge skeletons.

The reproductive processes of dictyonine sponges may be partially responsible for creating the characteristic patchy structure of the entire living portion of a glass sponge reef. However, the proportion of larval recruitment to asexual budding in a glass sponge reef remains an open question. To this end, a

microsatellite library is currently being constructed (S. Leys pers. comm.) to compare the genetic relatedness of individuals within a patch, between patches and between reefs. I predict that genetic variability is lowest within a spatially dependent patch with variability increasing as spatial separation between individuals increases.

2.3.3 Reef locations may be determined by hydrodynamics

At Fraser and Galiano reefs, the narrow depth range at which sponges are found may indirectly indicate where flow acceleration occurs over the underlying bathymetry. The lack of a correlation with slope is not surprising as dense non-reef populations of *A.vastus* and *H. calyx* are also found on near vertical fjord walls (Yahel et al. 2007), yet depth was a strong predictor of glass sponge distributions. At each reef, the band of live sponges was within a narrow range of depths and slopes found near the crest of their respective underlying bathymetric feature (ridge or mound). I suggest this is primarily due to flow patterns at that depth in the SOG. When water flows over bathymetric "bumps", it is forced to converge over the ridge, accelerating the fluid at the upper regions of the leeward side, and creating a zone of stagnant water at the lower regions of the leeward side (Dewey et al. 2005). I expect this to be the case at Fraser reef because water flows over the Fraser Ridge in a northern direction (R. Thomson, Institute of Ocean Sciences, pers. comm.), and glass sponges occur on the leeward side of the Fraser Ridge where current velocities are also the highest at the flood tides (Leys et al. in prep.). Leeward side habitats may also act as a shelter from the high suspended sediment loads circulated in the Strait of Georgia. At Galiano reef the live sponges were found on both sides of the ridge where the flow occurs in a predominantly southeastern direction (R. Thomson pers. comm.). Because the flow is parallel to the crest of the ridge, localized smallscale upwelling may occur explaining the distributions of sponges on both sides of the ridge. Topographic amplificaiton of flow explains the increased abundance of other communities of sessile suspension feeders, such as corals (Sebens 1984; Genin et al. 1986). The increased current velocities are beneficial by removing discharged waste waters

and replenishing source waters for suspension feeding (Vogel 1994) which is especially advantageous for the high oscula densities found at reefs as higher flow decreases the probability of adjacent oscula drawing in prefiltered water.

The low percentage of live sponge cover at Howe reef may reflect the suboptimal flow patterns in this area. The relative current velocities at Howe reef are the slowest of the 3 reefs and currents flow in a northwestern direction (R. Thomson pers. comm.). The low current velocity, lack of topographic amplification, and low sponge cover suggests that this reef exists at the lowest tolerable thresholds of flow, but persists because the sedimentation rates here are also low relative to the areas near the Fraser and Galiano reefs (Johannessen et al 2003). The unique bathymetry at the locations where live sponges are found indicates that reefs require a specific ecological niche; a balance of high flow and low sedimentation rates are the strongest abiotic predictors of where glass sponge reefs can exist.

2.3.4 Associations of megafauna with sponge reefs

Where glass sponges dominate the benthic biomass, they have been shown to increase local megafauna abundance by modifying the otherwise soft and flat benthos (Dayton et al. 1974; Barthel 1992a,b; Bett & Rice 1992). My results show that glass sponge reefs also form a massive habitat for other invertebrates and fish. The abundance of megafauna was highest at Galiano which also had the greatest sponge cover and highest density of oscula. Crustaceans such as *M. quadraspina*, decorator crabs and large lithodid crabs were the predominant taxa using the sponges as refuge by hiding in oscula of live and dead sponges and sitting on top of life sponges to feed (Chu pers. obs.). *Sebastes* spp. rockfish also were seen among the glass sponges, using the sponges as refuge (Cook et al. 2008; Marliave et al. 2009), either from predators or perhaps from the high flow above the reef.

Interestingly glass sponge density does not correlate with an increase in all phyla as other sponges and certain molluscs appear to be excluded in the presence of glass sponges. Demosponges were only found on the periphery of large glass

sponge mounds, and it may be that these much smaller individuals are excluded by dictyonine sponges in competition for filtering the same body of water. The majority of molluscs seen were small dendronotid and aeolid nudibranchs and these were usually on the bare substrate between areas of glass sponges or on hydroids growing on dead sponges. Pinnular hexactin spicules of of both *A.vastus* and *H. calyx* have a barbed ornamental ray that protrudes outwards from the outer dermal surface and could impale soft tissue on contact (Austin 2003), so soft-bodied invertebrates may avoid the surface of live glass sponges. The hard exoskeletons of crustaceans and the scales of fish are not damaged by glass sponge spicules and these, not surprisingly, were the only taxa observed in physical contact with live sponges.

In general, past studies on the community structure at reef in the Strait of Georgia suggest increased megafauna abundance in association with the glass sponges across all taxa (Cook et al. 2008; Marliave et al. 2009). However, these studies did not perform statistical analyses on their data to determine if their observations were free from bias or random chance. My results revealed the positive and negative associations the assemblage of megafauna has with glass sponges, and if we take into account distinct spatial patterns of the glass sponges in a reefreef, it is reasonable to assume that the distributions of megafauna are heavily influenced by the patchiness of glass sponges within a reef. In areas of high sponge density, fauna that use sponges will likely form a separate community from the fauna excluded by competition with hexactinellids.

2.3.5 The dorid nudibranch Peltodoris lentiginosa as a predator of glass sponges

The discovery of *P. lentiginosa* (Millen 1982) as a nudibranch predator on glass sponges expands the natural history knowledge of molluscan predators on glass sponges to outside of Antarctica. Although nudibranchs often eat sponges, only one other record shows they eat hexactinellids (Dayton et al. 1974). *P. lentiginosa* appears to be able to withstand contact with the dermal spicules of *A. vastus* and *H. calyx* and also ingest and excrete them.

A. vastus and *H. calyx* proportionally have 80% of their biomass consisting of siliceous spicules (Whitney et al. 2005; Chapter 3). Amazingly, *P. lentiginosa* can grow up to 18 inches in body length (Millen pers. comm.). The large size of *P. lentiginosa*, coupled with the low proportions of organic tissue in their glass sponge diet makes this nudibranch a potentially large impact predator on glass sponge reefs. However, the small population of observed nudibranchs (Table 1-1A in Appendix 1) relative to the enormous amount of glass sponge biomass at each reef suggests *P. lentiginosa* does not play an integral role in controlling glass sponge populations in the Strait of Georgia.

In Antarctica, up to 18 individuals of the dorid nudibranch *Austrodoris mcmurdensis* were observed to be feeding on an individual rosselid glass sponge without killing it (Dayton et al. 1974). The asteroid *Odontaster validus* also predates on glass sponges, but more importantly, controls Antarctic populations of *A. mcmurdensis*, skewing adults to large class sizes, and thus minimizing the impact of *A.mcmurdensis* on local glass sponge populations by preventing larval recruitment. Similarly, the asteroids *Ceramaster* sp., *Henricia* sp., *Mediaster aequalis* and *Pteraster tesselatus* are found with *P. lentiginosa* in glass sponge reefs, but their ecological roles have yet to be revealed. The asteroid *P. tesselatus* may also be a predator of *A. vastus* and *H. calyx*, as *P. tesselatus* has been observed to feed on the lyssacine glass sponge *Rhabdocalyptus dawsoni* which are found elsewhere with *A.vastus* (Leys & Lauzon 1998; Leys et al. 2007). The large size classes and low number of *P. lentiginosa* observed at the 3 glass sponge reefs suggests intraguild interactions of glass sponge predators, analogous to those found in the Antarctic benthos, may be occurring in glass sponge reefs.

Similar to other non-caecate dorid nudibranchs, *P. lentiginosa* may preferentially feed on sponges with more organic biomass (Bloom 1976). The non-caecate dorid, *Peltodoris nobilis* preferentially feeds on the desmacellid sponge *Biemma rhadia* (Bloom 1981). In general, demosponges have proportionally more organic biomass to inorganic skeleton (Barthel 1995). It is likely that *P. lentiginosa* may preferentially feed on the desmacellid *D. austini*,

but also feeds on *A. vastus* and *H calyx* due to the overwhelming abundance of hexactinellid biomass and the epizoic growth of *D. austini* on *H. calyx*.

P. lentiginosa was not observed at the Fraser Reef and could reflect a difference between glass sponge reefs in the Strait of Georgia (Table 1-1A, Appendix 1). Although it is possible a few nudibranchs escaped detection in the video, the systematic surveys used identical methods to survey the 3 reefs within 72 hrs and thus the apparent absence of nudibranchs can not be explained only by food availability or methods used. Glass sponge larvae are short lived when pelagic (Leys et al. 2007) but have established populations in 12 geographically separated reefs throughout the Strait of Georgia (Conway et al. 2007). In comparison, veliger larvae of *P. lentiginosa* are active swimmers (Millen 1982). Likely there are factors affecting successful recruitment of *P. lentiginosa* at Fraser Reef.

2.3.6 Estimates of bentho-pelagic coupling

My high resolution survey of the density of sponges and oscula at Galiano reef, coupled with known pumping and feeding rates for *A. vastus* (Yahel et al. 2006, 2007) allows me to highlight the volume of water and the amounts of carbon and nitrogen processed at a reef. Glass sponges can remove up to 99% of the ultraplankton from the water at excurrent (pumping) velocities of 0.01 m s^{-1} (Yahel et al. 2007). From my measurements of average oscula size and live sponge cover, the entire area we surveyed at Galiano reef would process water at 83,000 l s^{-1}. This estimate assumes continous pumping conditions and similar rates from the closely related *H. calyx*. Based on *in situ* measurements of nearby populations of *A. vastus* (Yahel et al. 2007) total organic carbon (TOC) removal and nitrogen excretion rates would be 0.96 g C m^{-2} day^{-1} and 0.16 g N m^{-2} day^{-1} respectively at Galiano reef. Nutrient flux would likely be greater within the hot spots of sponge density because my conservative approach averages nutrient flux over the entire benthic area we covered in the survey. My carbon uptake calculations greatly exceed those for other glass sponge populations (Pile & Young 2006; Yahel et al. 2007) and among sponge communities, are only

surpassed by calculations for populations of *Baikalospongia bacillifera* in Lake Baikal (Pile et al. 1997).

2.3.7 Summary

My small scale sampling coupling high resolution imagery and ROVs has allowed me to establish the biological patterns live glass sponges create within their ecosystem. The 'patchiness' of reefs may reflect recruitment and growth, allowing us to formulate the hypothesis that sponges within reefs are more closely related to one-another compared to those at other reefs. Sponge cover and density is different between reefs but regardless of sponge density, more animals of certain taxa are found when glass sponges are present. The scale and scope of my study focused on only a small fraction of the total area covered by known glass sponge reefs. The reefs I studied cover several hundred thousand square metres but are dwarfed by the 4 large reefs in Hecate Strait in northern British Columbia, which cover a 1300-fold greater area. A larger quantified survey coupled with a conservative extrapolation of my findings may reveal significant large scale impacts of glass sponges on the abundance of megafauna and nutrient cycling along the western Canadian continental shelf.

2.4 Literature Cited

Austin WC (2003) Sponge Gardens: A hidden treasure in British Columbia. http://mareco.org/khoyatan/spongegardens

Barrie JV, Hill PR, Conway KW, Iwanowska K, Picard K (2005) Georgia Basin: seabed features and marine geohazards. Geosci Can 32:145-156

Barry JP, Dayton, PK (1988) Current patterns in McMurdo Sound, Antarctica and their relationship to local biotic communities. Polar Biol 8:367-376

Barthel D (1992a) Do hexactinellids structure Antarctic sponge associations? Ophelia 36:111-118

Barthel D (1992b) Antarctic hexactinellids: a taxonomically difficult, but ecologically important benthic component. Verh Dtsch Zool Ges 85:271-276

Barthel D, Gutt J (1992) Sponge associations in the eastern Weddell Sea. Antarct Sci 4:137-150

Barthel D (1995) Tissue composition of spongs from the Weddell Sea Antarctica: not much meat on the bones. Mar Ecol Prog Ser 123:149-153

Bett BJ, Rice AL (1992) The influence of hexactinellid sponge (*Pheronema carpenteri*) spicules on the patchy distribution of macrobenthos in the Porcupine Seabight (bathyal NE Atlantic). Ophelia 36:217-226

Beyer HL (2004) Hawth's Analysis Tools for ArcGIS. http://www.spatialecology.com/htools (accessed 1 Nov 2009)

Bidder GG (1923) The relation of the form of a sponge to its currents. Quart J Microsc Sci 67:293-323

Bloom SA (1976) Morphological correlations between dorid nudibranch predators and sponge prey. Veliger 18:289-301

Bloom SA (1981) Specialization and noncompetitive resource partitioning among sponge eating dorid nudibranchs. Oecologia 49:305-315

Burd BJ, Barnes PAG, Wright CA, Thomson, RE (2008) A review of subtidal benthic habitats and invertebrate biota of the Strait of Georgia, British Columbia. Mar Environ Res 66:3-38

Conway KW, Barrie JV, Austin WC, Luternauer JL (1991) Holocene sponge bioherms on the western Canadian continental shelf. Cont Shelf Res 11:771-790

Conway KW, Krautter M, Barrie JV, Neuweiler M (2001) Hexactinellid sponge reefs on the Canadian continental shelf: a unique "living fossil". Geosci Can 28:71-78

Conway KW, Barrie JV, Krautter M (2004) Modern siliceous sponge reefs in a turbid, siliciclastic setting: Fraser River delta, British Columbia, Canada. N Jb Geol Palaont Mh 6:335-350

Conway KW, Barrie JV, Krautter M (2005) Geomorphology of unique reefs on the western Canadian shelf: sponge reefs mapped by multibeam bathymetry. Geo-Mar Lett 25: 205-213

Conway KW, Barrie JV, Hill, PR, Austin WC, Picard K (2007) Mapping sensitive benthic habitats in the Strait of Georgia, coastal British Columbia: deep-water sponge and coral reefs. Geol Surv Can, 2007-A2:1-6

Cook SE (2005) Ecology of the hexactinellid sponge reefs on the Western Canadian continental shelf. MSc thesis, Universisty of Victoria, Victoria, Canada

Cook SE, Conway KW, Burd B (2008) Status of the glass sponge reefs in the Georgia Basin. Mar Environ Res 66: 80-86

Dayton PK, Robilliard, GA, Paine, RT, Dayton LB (1974) Biological accommodation in the benthic community at Mcmurdo Sound, Antarctica. Ecol Monogr 44:105-128

Dewey R, Richmond D, Garrett C (2005) Stratified tidal flow over a bump. J Phy Oceanogr 35:1911-1927

Genin A, Dayton PK, Lonsdale PF, Spiess FN (1986) Corals on seamount peaks provide evidence of current acceleration over deep-sea topography. Nature 322:59-61

Ghiold J (1991) The sponges that spanned Europe. New Sci 2:58-62

Grassle JT (1991) Deep-sea benthic biodiversity. BioScience 41:464-469

Hill PR, Conway K, Lintern DG, Meule S, Picard K, Vaughn Barrie, J (2008) Sedimentary processes and sediment dispersal in the southern Strait of Georgia, BC, Canada. Mar Environ Res 66: 39-48

Johannessen SC, Macdonald RW, Paton DW (2003) A sediment and organic carbon budget for the greater Strait of Georgia. Est Coast Shelf Sci 56: 845-860

Krautter M, Conway KW, Vaughn Barrie J, Neuweiler M (2001) discovery of a "living dinosaur": globally unique modern hexactinellid sponge reefs off British Columbia, Canada. Facies 44: 265-282

Krautter M, Conway KW, Barrie JV (2006) Recent hexactinosidan sponge reefs (silicate mounds) off British Columbia, Canada: frame-building processes. J. Paleontol 80:38-48

Lehnert H, Conway KW, Barrie JV, Krautter M (2005) *Desmacella austini* sp. nov from sponge reefs off the Pacific coast of Canada. Contr Zool 74:265-270

Leinfelder RR, Krautter M, Laternser R, Nose M, Schmid DU, Schweigert G, Werner W, Keupp H, Brugger H, Herrmann R, Rehfeld-Kiefer U, Shröder JH, Reinhold C, Koch R, Zeiss A, Schweizer V, Christmann H, Menges G, Luterbacher H, Leinfelder RR (1994) The origin of Jurassic reefs: Current research developments and results Facies 31:1-56

Legendre P, Thrush SF, Cummings VJ, Dayton PK, Grant J, Hewitt JE, Hines AH, McArdle BH Pridmore RD, Schneider DC, Turner SJ, Whitlatch RB, Wilkinson MR (1997) Spatial structure of bivalves in a sandflat: scale and generating processes. J Exp Mar Biol Ecol 216:99-128

Levin SA (1992) The problem of pattern and scale in ecology: The Robert A. MacArthur Award Lecture. Ecology (USA) 73:1943-1967

Leys SP, Lauzon NRJ (1998) Hexactinellid sponge ecology: growth rates and seasonality in deep water sponges. J Exp Mar Biol Ecol 230:111-129

Leys SP, Wilson K, Holeton C, Reiswig HM, Austin WC, Tunnicliffe V (2004) Patterns of glass sponge (Porifera, Hexactinellida) distribution in coastal waters of British Columbia Canada. Mar Ecol Prog Ser 283:133-149

Leys SP, Mackie GO, Reiswig HM (2007) The biology of glass sponges. Adv Mar Biol 52:1-145

Maldonado M, Bergquist PR (2002) Phylum Porifera. In: Young CM (ed) Atlas of marine invertebrate larvae. Academic, London

Marliave JB, Conway KW, Gibbs DM, Lamb A, Gibbs C (2009) Biodiversity and rockfish recruitment in sponge gardens and bioherms of southern British Columbia, Canada. Mar Biol 156:2247-2254

Medialdea T, Somoza L, León R, Farrán M, Ercilla G, Maestro A, Casas D, Llave E, Hernández-Molina FJ, Fernández-Puga MC, Alonso B (2008) Multibeam backscatter as a tool for sea-floor characterization and identification of oil spills in the Galicia Bank. Mar Geol 249:93-107

Millen SV (1982) A new species of dorid nudibranch (Opisthobranchia: Mollusca) belonging to the genus *Anisodoris*. Can J Zool 60:2694-2705

Palumbi SR (1986) How body plans limit acclimation: responses of a demosponge to wave force. Ecology (USA) 67:208-214

Parker T, Tunnicliffe V (1994) Disperal strategies of the biota on an oceanic seamount: implications for ecology and biogeography. Biol Bull 187:336-345

Pile AJ, Patterson MR, Savarese M, Chernykh VI, Fialkov VA (1997) Trophic effects of sponge feeding within Lake Baikal's littoral zone. 2. Sponge abundance, diet, feeding efficiency,and carbon flux. Limnol Oceanogr 42:178-184

Pile AJ, Young CM (2006) The natural diet of a hexaactinellid sponge: benthic-pelagic coupling in a deep-sea microbial food web. Deep-Sea Res Part I 53:1148-1156

Reiswig HM (2006) Classification and phylogeny of Hexactinellida (Porifera). Can J Zool 84:195-204

Robertson GP, Huston MA, Evans FC, Tiedje JM (1987) Spatial variability in a successional plant community: patterns of nitrogen availability. Ecology (USA) 69:1517-1524

Rossi RE, Mulla DJ, Journel AG, Franz EH (1992) Geostatistical tools for modeling and interpreting ecological spatial dependence. Ecol Monogr 62:277-314

Sebens KP (1984) Water flow and coral colony size: interhabitat comparisons of the octocoral *Alcyonium siderium.* PNAS 81:5473-5477

Tabachnick KR (1994) Distribution of recent Hexactinellida. In: van Soest R, van Kempen B, Braekman G (eds) Sponges in Time and Space. Balkerna, Rotterdam

Teixido N, Gili JM, Uriz MJ, Gutt, J, Arntz, WE (2006) Observations of asexual reproductive strategies in Antarctic hexactinellid sponges from ROV video records. Deep-Sea Res Part II 53:972-984

Thomson RE (1981) Oceanography of the British Columbia Coast. Can Spec Publ Fish Aquat Sci 56:235-258

Tompkins-MacDonald GJ, Leys, SP (2008) Glass sponges arrest pumping in response to sediment: implications for the physiology of the hexactinellid conduction system. Mar Biol 154: 973-984

Vogel SV (1994) Life in moving fluids: the physical biology of flow. Princeton University Press, Princeton

Warburton FE (1960) Influence of currents on form of sponges. Science 132:89

Whitney FA, Conway K, Thomson R, Barrie JV, Krautter M, Mungov G (2005) Oceanographic Habitat of sponge reefs on the Western Canadian Continental Shelf. Cont Shelf Res 25:211-226

Yahel G, Eerkes-Medrano DI, Leys SP (2006) Size independent selective filtration of ultraplankton by hexactinellid glass sponges. Aquat Microb Ecol 45:181-194

Yahel G, Whitney F, Reiswig HM, Eerkes-Medrano DI, Leys SP (2007) In situ feeding and metabolism of glass sponges (Hexactinellida, Porifera) studied in a deep temperate fjord with a remotely operated submersible. Limnol Oceanogr 52:428-440

Table 2-1. Estimates of sponge cover at each of 3 glass sponge reefs. The total survey area represents the benthic area encircled by the entire grid of points respective to each reef survey (Fig. 2-2). The proportion of area covered by all (live and dead) sponges relative to the total sponge reef area is given in parenthesis. The proportion of the reef area relative to that covered in our surveys is indicated by 'proportion'. Areas without sponge cover was bare substrate consisting of patches of mud or exposed bedrock. Area units are given in m^2.

Reef	Total Survey Area	Area of Sponge Reef			Proportion
		Live	Dead	Total	%
Howe	166,500	10,242 (53.0%)	9,083 (47.0%)	19,325	11.6
Fraser	142,775	13,774 (66.5%)	6,945 (33.5%)	20,720	14.5
Galiano	208,250	23,432 (44.0%)	29,799 (56.0%)	53,231	26.0

Table 2-2. Spherical semivariogram model parameters based on UTM coordinates and percent live sponge cover. Model parameters are defined as C_0 = nugget effect, $C_0 + C$ = sill, A_0 (in m) = range, $C/(C_0 + C)$ = proportion of sample variance accounted for by spatial structure, r^2 = coefficient of determination, RSS = residual sum of squares. Galiano 25 m grid data combines ROPOS 2007 and Phantom data.

			Parameters			Goodness of fit		
Reef	Grid	Points	Nugget (C_0)	Sill ($C_0 + C$)	Range (A_0)	Structural variance $C/(C_0 + C)$	r^2	RSS
Howe	25.0 m	309	0.201	1.033	58.00	0.805	0.198	0.0788
Fraser	25.0 m	300	0.241	0.978	42.00	0.754	<0.0001	0.0274
Galiano	25.0 m	753	0.236	1.007	72.00	0.766	<0.0001	0.0248
Galiano	12.5 m	203	0.222	0.994	35.20	0.777	0.350	0.0374

Table 2-3. General characteristics of the distributions of live glass sponges at each reef. Depth (m) and slope (degrees) are reported in mean (± 1 SD). Survey, refers to the "total" set of waypoints (Fig. 2) where images were taken and "present" indicates the number of images in which glass sponges were present. Spearman rank-correlation coefficients (r_s) are provided for each reef; live sponge cover (%) was correlated to dead sponge cover, depth, and slope (*$p < 0.05$, ** $p < 0.0001$, *n.s.* not significant, $p > 0.05$).

	Survey		Depth		Slope		Spearman rank-correlations (r_s)		
Reef	Total	Present	Mean	Range	Mean	Range	Dead Sponge	Depth	Slope
Howe	309	133	79 ± 9	59 - 102	11 ± 6	1 - 30	0.770 **	-0.422 **	-0.027 n.s.
Fraser	300	84	162 ± 9	147 - 180	10 ± 7	1 - 35	0.730 **	-0.180 *	-0.123 n.s.
Galiano	896	497	90 ± 8	69 - 119	16 ± 8	1 - 52	0.689 **	-0.532 **	-0.244 n.s.

Table 2-4. Animals counted living on and within close proximity to dictyonine sponges in images from surveys at Galiano reef in 2008 (Phantom 2008) at all 3 reefs (ROPOS 2009). Identifications were made to lowest possible taxonomic level (taxa). Total counts are shown from Phantom 2008 images (Galiano) and ROPOS 2009 images (pooled across reefs).

Phylum	Class	Taxa	Phantom 2008	ROPOS 2009
Porifera	Hexactinellida	*Rhabdocalyptus dawsoni*	31	3
	Demospongiae	*Desmacella austini*[a]	n.a.	n.a.
		Iophon sp.	13	13
		Poecillastra sp.		2
		Stylissa sp.	110	
		Tetilla sp.	17	65
Cnidaria	Anthozoa	*Cribrinopsis fernaldi*	7	8
		Halipteris willemoesi		118
		Metridium farimen		1
		ORDER: Actiniaria	2	
	Hydrozoa	UNIDENTIFIED sp.	3	
Annelida	Polychaeta	ORDER: Sabellida	6	
		UNIDENTIFIED sp.	42	
Mollusca	Bivalvia	ORDER: Veneroida	29	1
	Cephlapoda	*Octopus* sp.		1
		ORDER: Teuthida		2
	Gastropoda	*Fusitriton oregonensis*	9	5
		Calliostoma sp.	7	3
		Peltodoris lentiginosa		2
		FAMILY: Dendronotidae	53	
		FAMILY: Aeolidioidea	26	
Arthropoda	Malacostraca	*Acantholithodes hispidus*	9	2
		Cancer magister		8
		Chionoecetes sp.		1

		Chlorilia longipes	5	12
		Munida quadraspina	8393	243
		Pandalus platyceros	250	192
		Lopholithodes foraminatus	4	
		FAMILY: Paguridae	53	3
Echinodermata	Asteroidea	*Ceramaster* sp.	3	1
		Henricia sp.	4	8
		Mediaster aequalis	7	11
		Pteraster tesselatus	1	1
		Pycnopodia helianthoides	1	
		Solaster sp.	1	
	Holothuroidea	*Psolus* sp.	1	
	Ophiuroidea	ORDER: Ophiurida	51	
Fish	Osteichthyes	FAMILY: Agonidae	3	
		FAMILY: Bathymasteridae	2	
		FAMILY: Pleuronectidae	3	17
		Sebastes elongates	6	8
		Sebastes maliger	7	14
		Sebastes sp.	30	37
		Theragra chalcogramma		135
	Chondrichthyes	*Hexanchus griseus*		1
		Hydrolagus colliei	10	12

[a]*Desmacella austini* was only observed encrusting on dictyonine sponges and was not recorded as count data.

Table 2-5. Differences in the community composition of glass sponges reefs in the Strait of Georgia. Pairwise Analyasis of Similarity (ANOSIM) were used to compare the community composition between reefs using only abundance data from ROPOS 2009 images. Using only Phantom 2008 images, community composition was compared in the presence and absence of glass sponges.

Community Comparison	R	p
ROPOS 2009		
Howe vs. Fraser	0.193	<0.001
Howe vs. Galiano	0.162	<0.001
Fraser vs. Galiano	0.072	<0.001
Phantom 2008		
Glass sponge Presence vs. Absence	0.246	<0.001

Table 2-6. Density of animals in representative phyla in all reefs identified from ROPOS 2009 (RO) and Phantom 2008 (Ph) images. Area represents total area covered from images (m^2) and Reef/Area represents the proportion of reef area to surveyed area. Density of animals was standardized to image area (individuals m^{-2}) and are grouped by phyla and total fauna. POR = Porifera (not including dictyonine sponges), CNI = Cnidaria, ANN = Annelida, MOL = Mollusca, ART = Arthropoda, ECH = Echinodermata, FIS = Fish. Phantom images revealed more fauna due to the higher resolution and slaved strobe of the camera system.

Reef	ROV	Area	Reef/ Area	POR	CNI	ANN	MOL	ART	ECH	FIS	Total
Howe	RO	1167	0.09	0.0017	0.0069	0	0.0017	0.16	0.00086	0.026	0.28
Fraser	RO	737	0.19	0.11	0.028	0	0.0054	0.14	0.0095	0.014	0.31
Galiano	RO	532	0.39	0.0075	0.0038	0	0.015	0.31	0.026	0.070	0.43
Galiano	Ph	385	0.28	0.45	0.031	0.12	0.32	22.6	0.18	0.13	23.8

Figure 2-1. Map of the Strait of Georgia and relative locations of the Howe, Fraser, and Galiano glass sponge reefs.

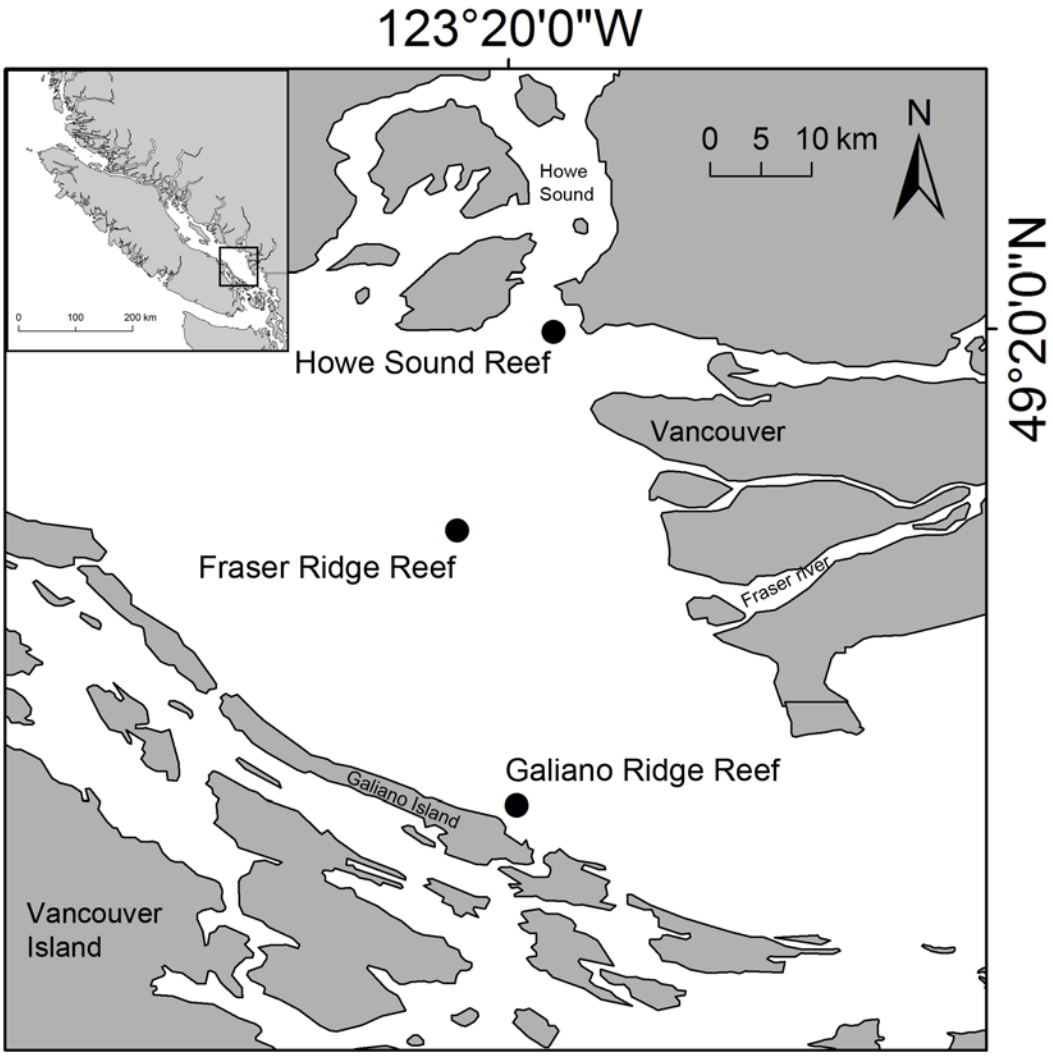
123°20'0"W
49°20'0"N
0 5 10 km
N
Howe Sound
Howe Sound Reef
Vancouver
Fraser Ridge Reef
Fraser river
Galiano Ridge Reef
Galiano Island
Vancouver Island
0 100 200 km

Figure 2-1

Figure 2-2. Schematic showing the field sampling designs at each of the reefs. A downward facing digital image was taken at every point along a stratified 25 m survey grid with ROPOS. (A) Howe (n = 309), (B) Fraser (n = 300), (C, D) Galiano. In (C), the solid box indicates the area covered by the 25 m stratified grid surveyed with ROPOS in 2007 (n = 238), and the transect line points surveyed with the Phantom 2008 (n=515). The dashed line indicates the area sampled at a finer scale. In (D), additional points sampled by ROPOS in 2009 (n=143) are represented by hollow circles (o); these subdivided the original 25 m grid points (solid circles,●) into a 12.5 m grid. Depth contour lines are shown in 10 m intervals.

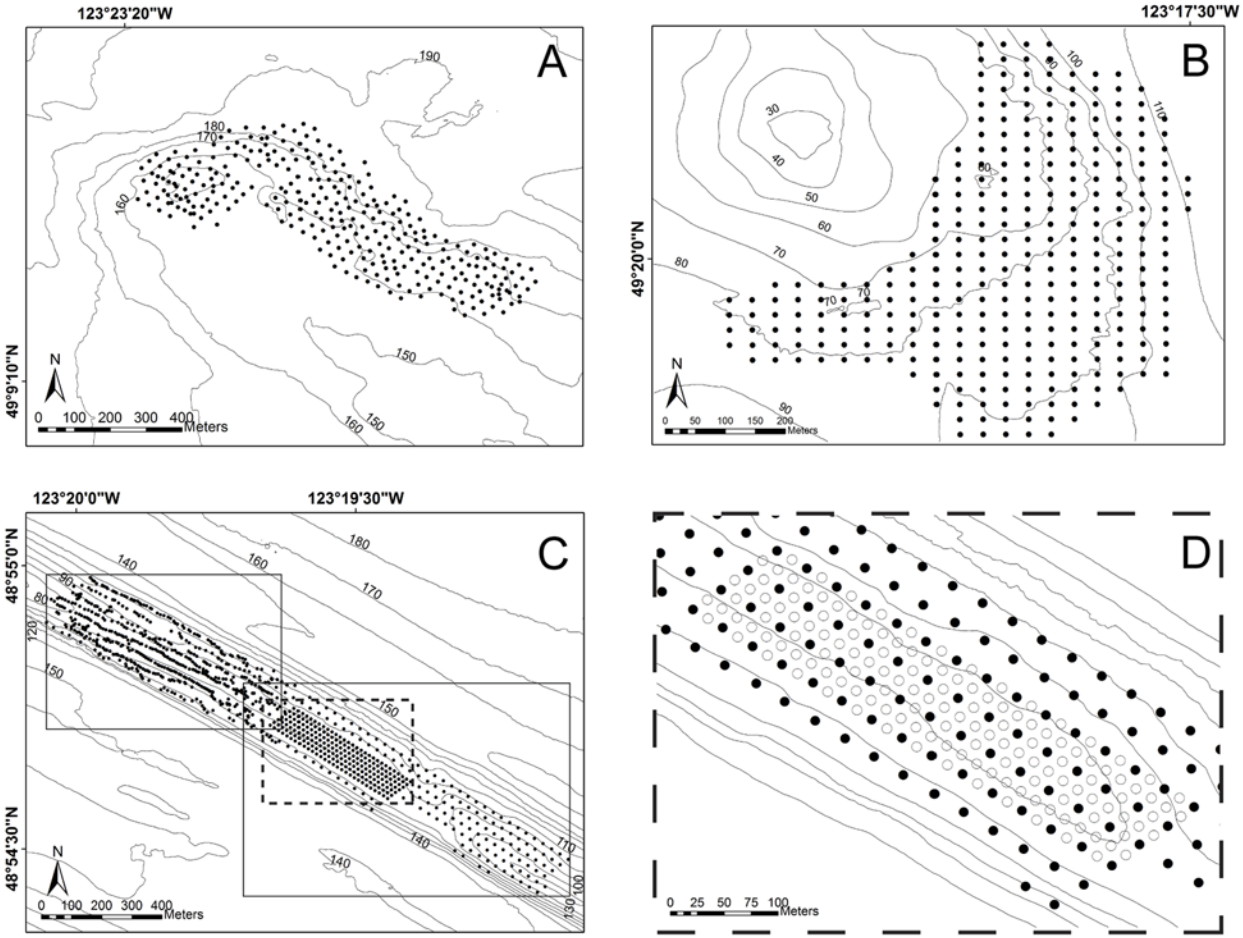
123°23'20"W
A
190
180
170
160
150
150
160
N
0 100 200 300 400
Meters
49°9'10"N
123°17'30"W
B
30
40
50
60
70
80
90
100
110
70
70
80
N
0 50 100 150 200
Meters
49°20'0"N
123°20'0"W
123°19'30"W
C
48°55'0"N
140
160
180
170
90
80
120
150
150
140
170
100
130
140
N
0 100 200 300 400
Meters
48°54'30"N
D
0 25 50 75 100
Meters

Figure 2-2

Figure 2-3. Semivariograms showing spatial structure of sponges within each survey area (created from the model parameters in Table 2-4). (A) Howe Sound 25 m grid sampling. (B) Fraser Ridge 25 m grid sampling. (C) Galiano Ridge 25 m grid & Phantom transect lines sampling. (D) Galiano Ridge 12.5 m grid sampling. Each semivariogram represents the entire spatial structure within the survey area of the respective reef (Fig. 2-2). Dots represent lag distance intervals for each reef survey. Spatial autocorrelation occurred at each reef up to the range distance signified by the sill (dotted line) of each semivariogram. Note the different scales on the x-axis are a result of the different dimensions of the area covered in each survey.

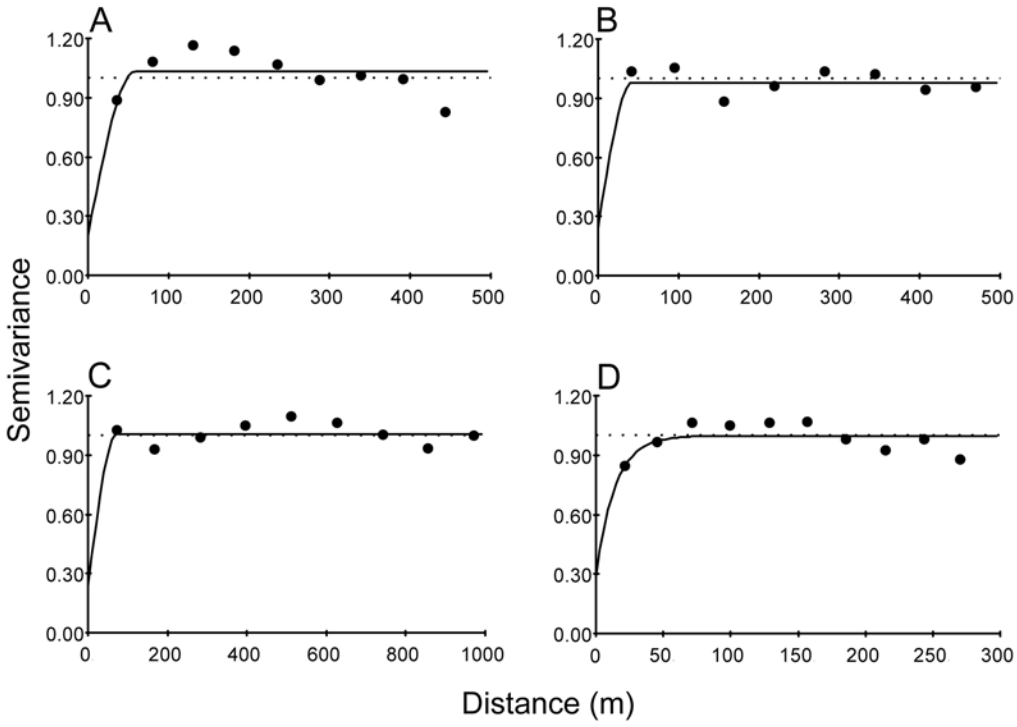
A
B
C
D
Semivariance
Distance (m)
1.20
0.90
0.60
0.30
0.00
0
100
200
300
400
500
600
800
1000
50
150
250

Figure 2-3

Figure 2-4. Distribution maps of live glass sponges at (A) Howe, (B) Fraser, and (C) Galiano reef. Areas were interpolated by Kriging using semivariogram parameters of Table 4. At Howe reef, our survey of live sponge cover is shown as an overlay on top of the bathymetry mapped with multibeam in 2007. Isopleths of live sponge cover are plotted in 5% increments. Note north is different for each reef. Images from each reef correspond to white arrows on their respective Kriging maps. Scale bars in images are 10 cm.

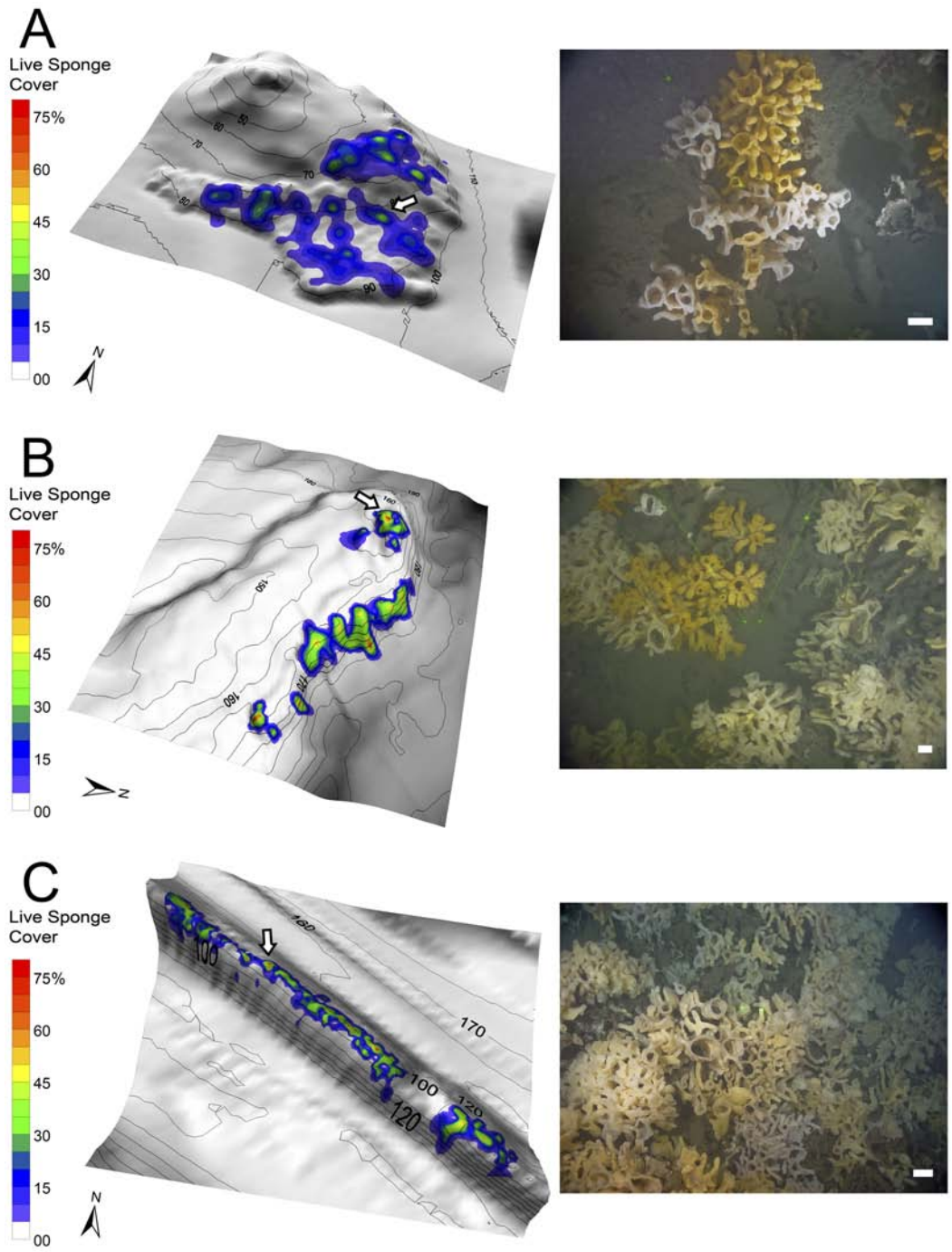
A
Live Sponge Cover
75%
60
45
30
15
00
N
B
Live Sponge Cover
75%
60
45
30
15
00
N
C
Live Sponge Cover
75%
60
45
30
15
00
N
100
120
170

Figure 2-4

Figure 2-5. Distribution of sponges at Galiano reef. (A) The percentage of live sponge cover was greater at slope angles ≥12 ° within the 12.5 m grid survey area. The percent live cover was averaged from slope classes at 4° intervals. Sample sizes are shown in parentheses, error bars indicate 95% C.I. (B) The down slope sponge distributions can be seen in the Kriging results of the 12.5 m grid.

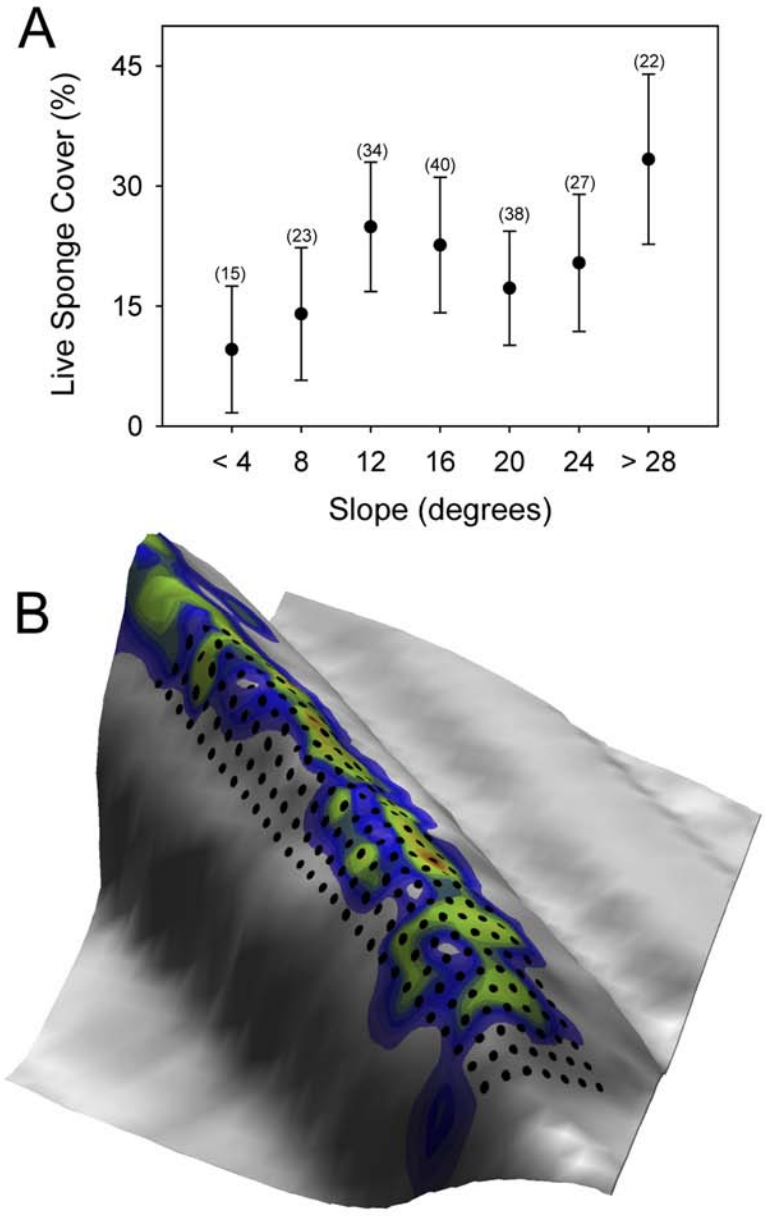
A
Live Sponge Cover (%)
45
30
15
0
(15)
(23)
(34)
(40)
(38)
(27)
(22)
< 4
8
12
16
20
24
> 28
Slope (degrees)
B

Figure 2-5

Figure 2-6. Asexual budding and bush formation observed in dictyonine sponges. (A) A dictyonine sponge at Galiano reef with an extension budding from the base. (B) New oscula form at tips of extensions. (C) Continuous budding forms a characteristic bush of *A. vastus* with densely packed oscula. (D) A dead *A. vastus* bush illustrates the single basal attachment point that supports the entire individual. Scale bars are 5 cm.

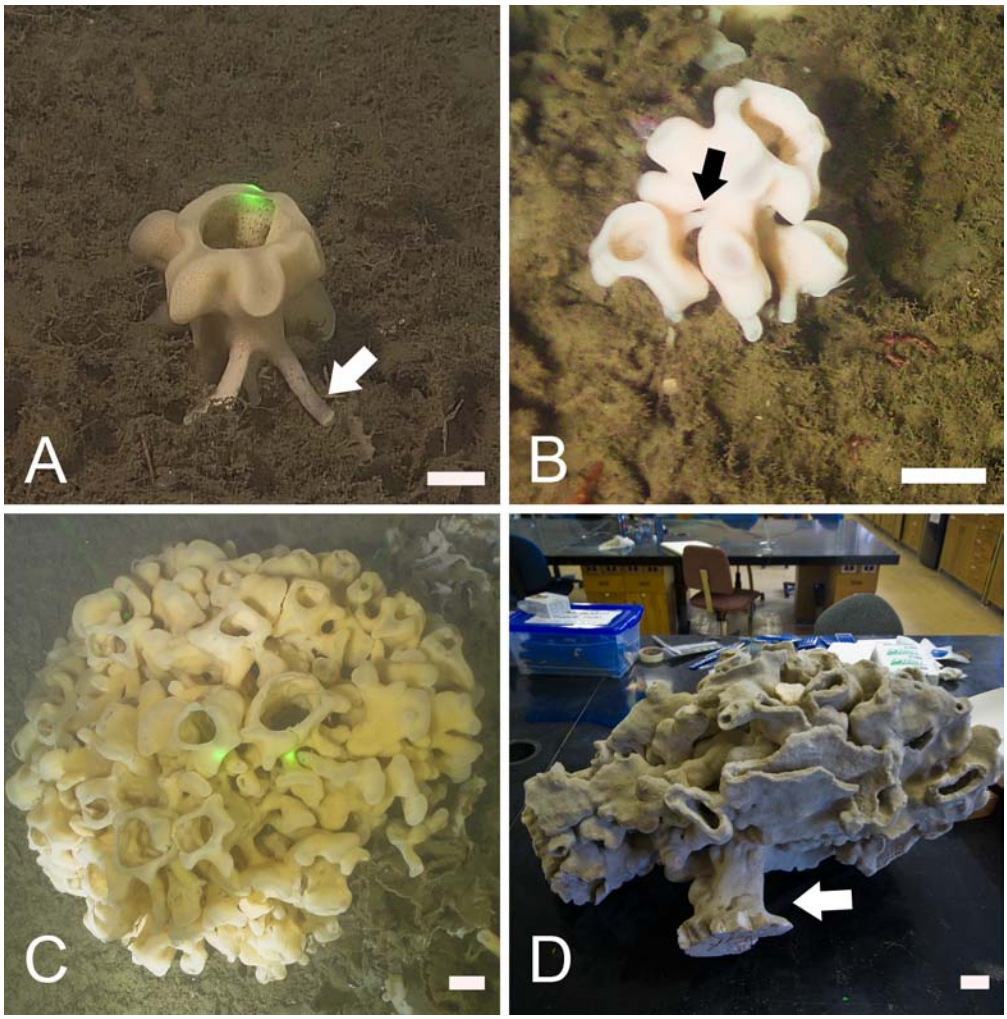

Figure 2-6

Figure 2-7. Comparison of the area and densities of oscula at each reef. (A) Density of sponge oscula relative to benthic area surveyed; graphs show means from 78 images chosen randomly from all captured. (B) Density of oscula in a continuous patch of live sponges; graphs show means from 10 images chosen randomly from all captured. (C) Sponge oscula area among reefs; graphed values show means from 600 random oscula. Error bars are ±1 SE. Letters between columns indicate significant differences ($p < 0.0001$).

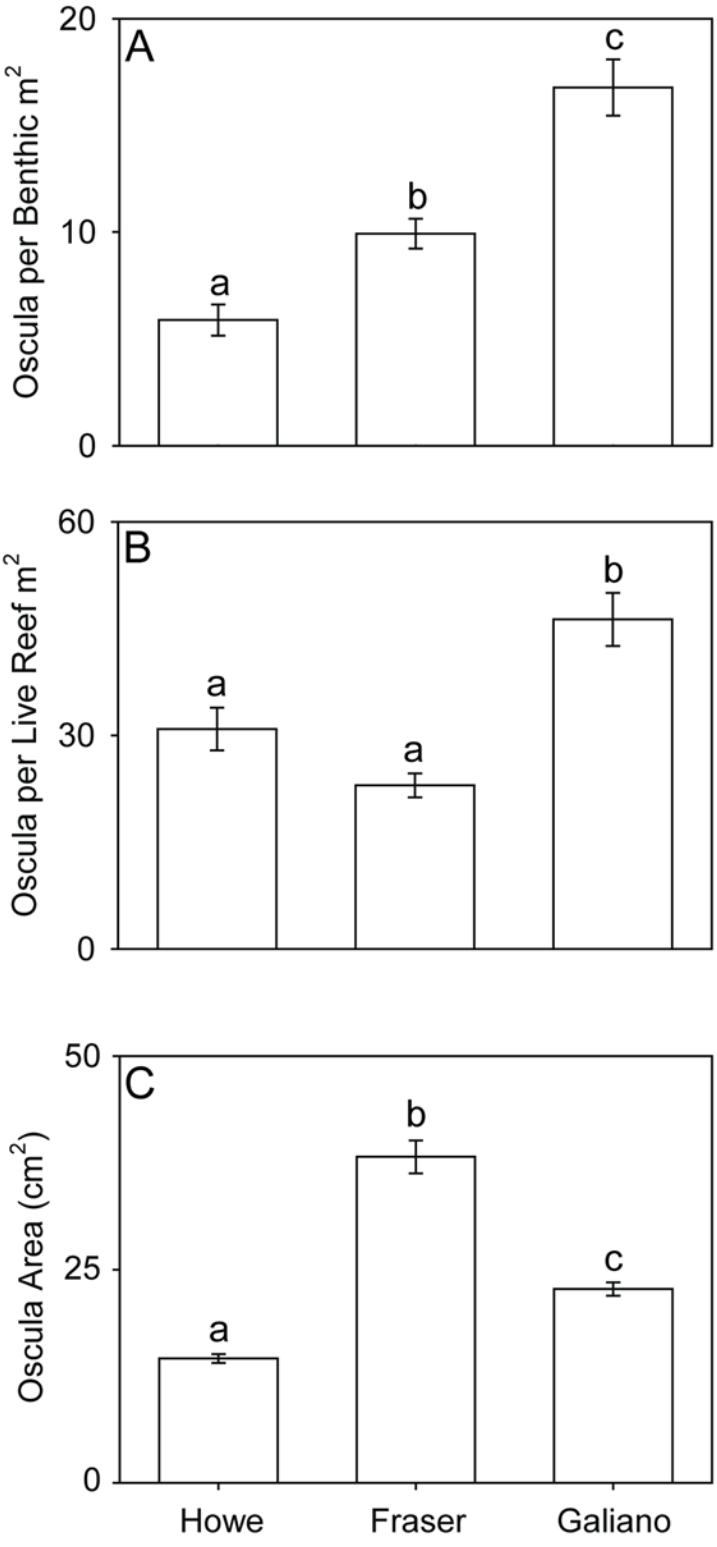
A
Oscula per Benthic m2
20
10
0
a
b
c
B
Oscula per Live Reef m2
60
30
0
a
a
b
C
Oscula Area (cm2)
50
25
0
a
b
c
Howe
Fraser
Galiano

Figure 2-7

Figure 2-8. Size frequency histograms and summary statistics of glass sponge oscula (*A.vastus* and *H. calyx*) at the (A) Howe, (B) Fraser and (C) Galiano reefs. (*) Indicates the distribution of oscula size classes were significantly skewed from 600 randomly chosen oscula (Shapiro-Wilk, $p < 0.0001$ in all cases).

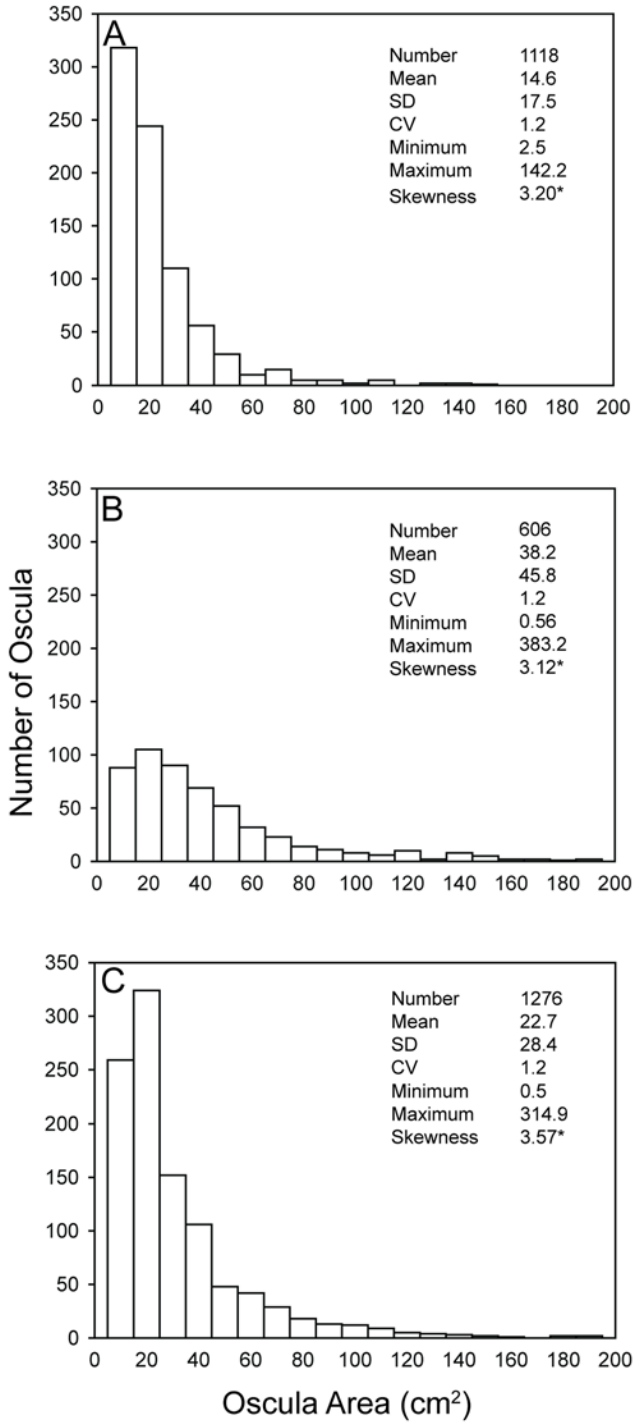
A
Number 1118
Mean 14.6
SD 17.5
CV 1.2
Minimum 2.5
Maximum 142.2
Skewness 3.20*
B
Number 606
Mean 38.2
SD 45.8
CV 1.2
Minimum 0.56
Maximum 383.2
Skewness 3.12*
C
Number 1276
Mean 22.7
SD 28.4
CV 1.2
Minimum 0.5
Maximum 314.9
Skewness 3.57*
Number of Oscula
Oscula Area (cm²)
0 20 40 60 80 100 120 140 160 180 200
0 50 100 150 200 250 300 350

Figure 2-8

Figure 2-9. Comparison of the density of fauna associated with each reef. Counts of fauna were made from ROPOS 2009 images only. Error bars are ± 1 SE. Letters between the columns indicate a significant difference ($p < 0.0001$).

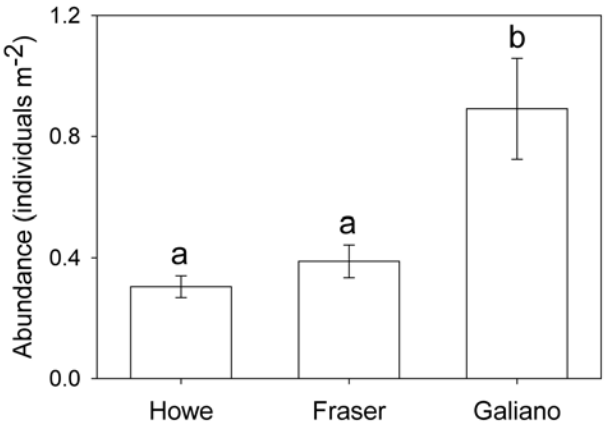
1.2
0.8
0.4
0.0
Abundance (individuals m-2)
a
a
b
Howe
Fraser
Galiano

Figure 2-9

Figure 2-10. Comparisons of the abundances of specific phyla at Galiano reef in the presence and absence of reef sponges (live or dead). Counts were made from Phantom 2008 images only. Comparisons include the total (combined fauna) and individual phyla. Error bars are ±1 SE. P-values indicate significant differences (α=0.05).

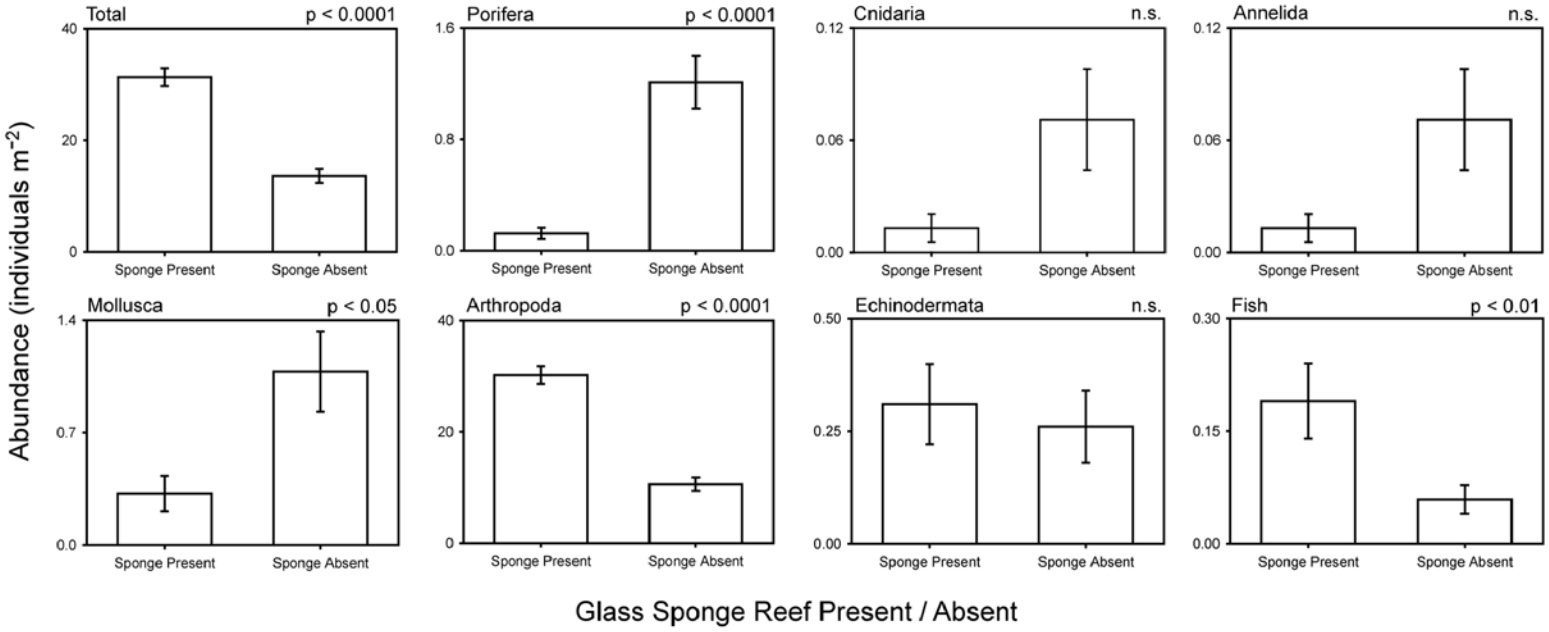
Total
p < 0.0001
Porifera
p < 0.0001
Cnidaria
n.s.
Annelida
n.s.
Mollusca
p < 0.05
Arthropoda
p < 0.0001
Echinodermata
n.s.
Fish
p < 0.01
Sponge Present
Sponge Absent
Abundance (individuals m-2)
Glass Sponge Reef Present / Absent

Figure 2-10

Figure 2-11. The dorid nudibranch *Peltodoris lentiginosa*. *P. lentiginosa* was found to be a predator on both reef forming glass sponge species (*Aphrocallistes vastus* and *Heterochone calyx*) and the demosponge *Desmacella austini*.

Figure 2-11

Figure 2-12. Sponge spicules found in fecal and gut contents analysis of *P. lentiginosa*. (A**)** oxyhexaster microsclere of *Aphrocallistes vastus* (fecal). (B) Fused skeleton likely of *A. vastus* (fecal) (C) pinnular hexactin microsclere of *A. vastus* (fecal) (D**)** tylostyle megascleres and sigma microscleres of *Desmacella austini* (fecal) (E**)** fused skeleton and tylostyles (gut) (F**)** hexactin megasclere of *Heterochone calyx* (gut) (G**)** forked scopule microsclere of *H. calyx* (gut). Scale bars = 50 µm. For spicule processing methods, see Appendix 1.

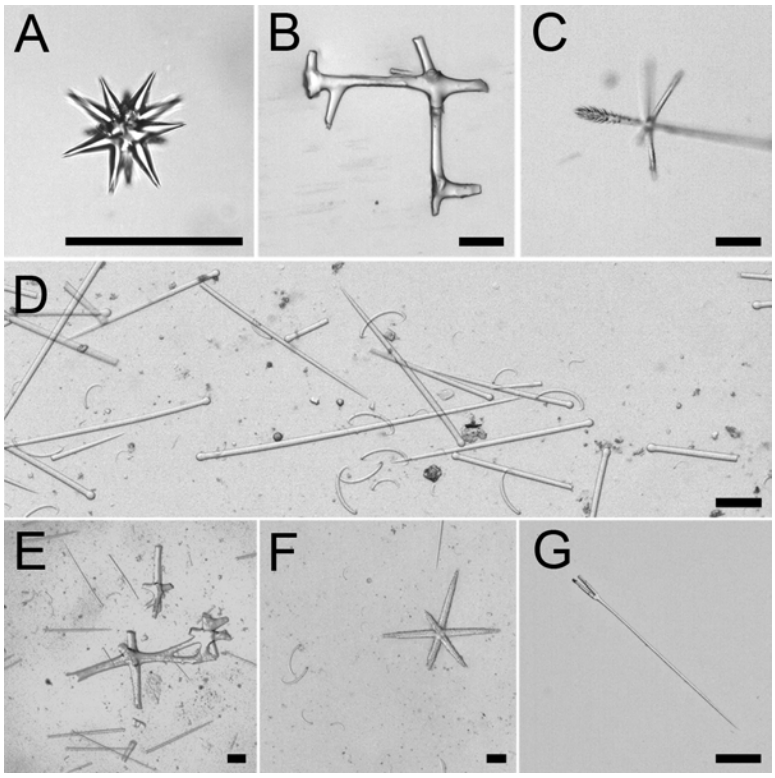

Figure 2-12

Chapter 3

Glass sponge reefs as a silica sink

3.0 Introduction

Sponges are overlooked as important contributers to biological silicon (Si) cycling in the world's oceans. In the marine environment, Si is highly under saturated (Perry 2003), where diatoms represent the entire biological part of the current global marine Si balance producing an estimated 240 teramoles (10^{12}) of biogenic silica per year (Tréguer et al. 1995). Diatoms incorporate Si into their cell walls by polymerizing silicic acid into an amorphous hydrated form, silica (Raven & Waite 2004). After death, silica from frustules dissolves back into an available form, silicic acid ($SiO_{2\,(s)} + H_2O_{\,(l)} \rightarrow H_4SiO_{4\,(aq)}$), in a thermodynamically favored forward reaction (Williams et al. 1985). The rapid growth and dissolution of diatom frustules annually cycles half of the biogenic silica in the photic zone with the rest sinking to deeper waters by pathways such as fecal pellet transport (Nelson et al. 1995; Schrader 1971). Diatoms are estimated to be responsible for 35% of global primary productivity and thus the role of silicon (Si) cycling has direct consequences in our understanding of CO_2 sequestering in the world's oceans (Nelson et al. 1995; Tréguer & Pondaven 2000). The overwhelming importance of diatoms in the silica balance has resulted in the generally ignored role of other siliceous organisms, such as sponges, in silica cycling.

Recent studies indicate that siliceous sponges on continental margins may play a relevant role in Si cycling at a regional scale (Maldonado et al 2005, 2010). Like diatoms, sponge spicules are made from hydrated amorphous silica (Sandford 2003). However, whereas dissolution in diatom frustules occurs within days after cell death (Kamatani 1982), sponge spicules are surprisingly resistant to dissolution even after months (Kamatani 1971; Maldonado et al. 2005). Maldonado et al. (2005) first quantified the large difference between long term

dissolution of diatom frustules and sponge spicules in axenic water and proposed that sponges represent an overlooked component of the oceanic silica balance.

Glass sponges (class Hexactinellida), are heavily silicified with up to 95% of their biomass made up of spicules (Barthel 1995). In regions where live sponges and the spicules from dead individuals cover large areas of the seafloor, they create three-dimensional habitats for other organisms (Dayton et al. 1974; Barthel 1992; Bett & Rice 1992; Beaulieu 2001). Glass sponges are characteristically deep water animals (Tabachnick 1994), but are found in shallow (~50 m) waters in a few places worldwide, in particular, Antarctic (Dayton et al. 1974) and the northeast Pacific Ocean where densities as high as 240 individuals per 10 m^2 are found in fjords of British Columbia (Leys et al. 2004). Also in coastal British Columbia, glass sponge reefs are found where siliceous mounds up to 21 m high cover a discontinuous benthic area of > 700 km^2 (Conway et al. 2001, 2005; Krautter et al. 2001). The framework of the reefs in the Strait of Georgia (SOG) is built from the fused skeletons of *Aphrocallistes vastus* and *Heterochone calyx*. After death, tissue and loose spicules are lost, but the fused skeletons remain as hard substratum for recruitment of subsequent sponge generations and other fauna (Leys et al. 2004). If we consider the long-lived nature of glass sponges (Leys & Lauzon 1998; Fallon et al. 2010), and their potentially dissolution resistant spicules, glass sponge reefs could represent a significant silica sink in northeastern Pacific waters.

The goal of this study, therefore, was to assess the importance of glass sponge reefs as a potential silica sink. First, I determined the amount of silica locked into glass sponge biomass in each of 3 reefs in the SOG and the amount of silicic acid in waters over the reefs. I then determined the long term (months) dissolution potential of glass sponge skeletons. The presence of bacteria has been shown to accelerate the dissolution of diatom frustules (Bidle 1999; Bidle & Azam 2001) by degrading the organic components within the biogenic silica matrix (Smith et al. 1995). Therefore, as a contrast to the experiments performed by Maldonado et al. (2005), natural sea water containing bacteria was used in the dissolution experiments. In nature, sponge skeletons naturally experience

diagenesis which slowly blacken spicules with precipitates because the surface of the silica is negatively charged and attracts positive ions such as Fe^{3+} and Mn^{2+} (Hurd 1973). Because diagenetic skeletons have already had extended exposure dissolution conditions, these "blackened skeletons" were also included in the experiments and examined for evidence of dissolution. Results show that while the skeletons from freshly killed sponges are resistant to dissolution, dissolution is found in the diagenetic skeletons indicating that dissolution will occur over the long term. Nevertheless, my calculations of silica locked into each reef suggest that, at these dissolution rates, glass sponge reef represent a significant silica sink on the western continental shelf waters of Canada.

3.1 Materials and Methods

3.1.1 The SOG glass sponge reefs

Field work in the Strait of Georgia was carried out in October 2007 onboard the Canadian Coast Guard Ship (CCGS) Vector and in October 2009 onboard the CCGS John P Tully using the remotely operated vehicle (ROV) ROPOS. We visited three reefs (Fig. 3-1); the Fraser reef (49°9'15.673"N, 123°23'3.705"W), Howe reef (49°19'57.672"N, 123°17'42.297"W) and Galiano reef (48°54'51.468"N, 123°19'27.654"W). The live sponge populations grow above the sediment surface at each reef (Fig. 3-2A) and are found in characteristic, highly clustered patches covering areas of 10,242 m^2, 13,774 m^2, and 23,432 m^2 respectively at Howe, Fraser, and Galiano reef (Chapter 2).

3.1.2 Field Sampling

To determine the amount of sponge biomass within a reef, dense patches of live *A. vastus* (Fig. 3-2B) were identified and sampled with an Ekman grab (3.54×10^{-3} m^3). The grab was manually pushed into the sponges and closed with ROPOS' manipulator arms. Eight grabs (Howe: 2, Fraser: 3, Galiano: 3) were retrieved in 2007 and 4 additional grabs (Howe: 2, Fraser: 1, Galiano: 1) were retrieved in 2009. The sponge biomass (Fig. 3-2C) was gently rinsed with

seawater onboard the ship to remove sediment and frozen at -20°C until processed.

In 2007, water was sampled *in situ* at the sediment-water interface, approximately 5 cm above the bottom without disturbing the sediment (hereafter refered to as 0 metres above bottom (MAB) to maintain unit consistency) using SIP water samplers (Yahel et al. 2007), at 2 MAB using 2.5 L Niskin bottles mounted on the forward brow of ROPOS with ROPOS sitting on the bottom, and at 10 MAB with ROPOS hovering above the sponges. We sampled among and ~160 m away from the reefs (where no sponges were found) as a comparative control. Five-litre Niskin bottles were lowered over the side of the ship to sample sea water throughout the water column. Water samples were syringe filtered through 0.22 µm Millipore membrane filters, frozen on board and analyzed for silicic acid at the Institute of Ocean Sciences (IOS) in Sidney, British Columbia using a Technicon AAII Autoanalyzer with modified Technicon procedures (Barwell-Clarke & Whitney 1996; courtesy of F. Whitney, Institute of Ocean Sciences). A Mann-Whitney U test was used to compare levels of silicic acid at the sediment water interface (0 MAB) between areas with sponges and areas away from sponges. Due to the low replication of water samples taken in areas away from sponges, samples were pooled for meaningful statistical analysis.

Water used for dissolution experiments was collected from ~150 m with 5 one-litre Niskin bottles, immediately filtered with nominal 1-5 µm cartridge filters and stored in polyethylene carbuoys at 10°C until used.

3.1.3 Measurements of sponge biomass

The entire contents of each Ekman grab were oven-dried at 60°C and weighed. To determine silica content, preweighed subsamples (n=5 per grab) were placed in preweighed 1.5 ml Eppendorf tubes and treated with 5% hydrofluoric acid (HF) for 24 hrs. Samples were centrifuged at 13,000 rpm for 2 minutes, the supernatant was removed and the tissue was rinsed three times with distilled water using the same procedure. The tubes were oven-dried at 60°C and reweighed and the loss in weight (percent silica) was used to extrapolate the total

silica in each Ekman grab. A second method was used to confirm results: in this method, subsamples from 2007 grabs (n=10 per grab) were weighed before and after combustion at 500°C for 12 hrs to determine the inorganic (silica) to organic (tissue) ratio of biomass. To compare the proportions of silica in *A. vastus* between reefs, data was arcsine square root transformed and analyzed with a nested ANOVA using the reef as a fixed factor and each Ekman grab as nested factors.

To determine the relative proportions of spicule to organic tissue in *A. vastus*, 20 pieces were haphazardly sampled from the remaining Ekman grab material. Oven-dried samples were weighed, placed in glass test tubes, and cleaned with a small volume of hot concentrated nitric acid at 95°C for 5 minutes. The acid was diluted with ~5.0 ml of distilled water and the entire contents of each tube were filtered onto preweighed 0.22 µm Millipore membrane filters. Filters were dried at 60°C until a constant weight was achieved and the proportion of weight loss was determined as the organic tissue lost through acid digestion.

3.1.4 Silica dissolution experiments

For dissolution experiments, I used a batch design with 5 identical, independent experiments lasting 1, 2, 3, 6 and 8 months. Each experiment consisted of 4 treatments with 8 replicates per treatment: (1) blank control with just seawater, (2) loose spicules from freshly killed sponges (loose), (3) fused skeleton from freshly killed sponges (fused) and (4) fused skeleton from dead sponges that I describe as blackened (black) from natural *in situ* diagenesis and had already experienced extended dissolution (Fig. 3-2D). All spicules and skeletons were cleaned in 5% sodium hypochlorite for 24 hrs, rinsed three times with distilled water with the supernatant decanted, and dried at 60°C until a constant mass was achieved. For each replicate, 25.5 ± 0.3 mg of spicules was added to capped polyethylene tubes with 50 ml of sea water. Because it was difficult to keep bacteria while also removing siliceous particulates, the seawater was filtered through 0.45 µm pore sized Millipore membrane filters to prioritize particulate removal but maintain some bacteria. The bacterial diversity and

abundance would have been skewed toward smaller class sizes (<0.45 µm) and likely reduce the potential effect on dissolution. Scanning electron microscopy (SEM) of the seawater confirmed presence of bacteria but no unicellular eukaryotes such as diatoms. Tubes were sealed with Parafilm™ and stored in the dark at 10°C for the duration of the experiments to be similar to the deep water environment of the reefs. Dissolution experiments were required to begin at different times because of the time, equipment and space constraints as well as the different end dates of the experiments.

Silicic acid in all samples was measured at the start and end of each experiment using the method of Strickland and Parsons (1978). Tubes were gently shaken, fused skeletons were carefully removed with forceps, placed on aluminum weigh boats, and oven dried at 60°C. For treatments with loose spicules, the seawater was filtered through 0.22 µm Millipore membrane filters to recover spicules prior to measuring the levels of silicic acid. To ensure consistency of technique, subsamples of each tube were measured in triplicate with glass cuvettes using a UV spectrophotometer (Ultrospec 2100 pro UV/Visible spectrophotometer) at a wavelength of 810 nm. Seawater pH was 8.1 at the start of the experiments and 7.5 at the end. Non-parametric analyses of variance were used on all data from dissolution experiments because parametric assumptions were not met even after transformations. Individual Kruskal-Wallis with Dunn pairwise tests (Zar 1999) were used to compare between spicule groups within each experiment. Individual Mann-Whitney U tests were used to compare dissolutions of diatom frustules to seawater controls, and a Kruskal-Wallis test with Dunn pairwise tests was used to compare dissolution of diatoms between experiments. Within each experiment, silicic acid levels in control bottles were compared to the initial silicic acid levels to confirm no change in silicic acid levels occurred (Mann-Whitney U, $p > 0.05$) and a Kruskal-Wallis test with Dunn pairwise tests was used to compare spicule treatments to the control blanks and (Zar 1999).

To compare dissolution between hexactinellid and diatom silica, the diatom *Thalassiosira weissflogii* (CCMP 1336 strain; Centre for Culture of

Marine Phytoplankton, Maine, USA) was cultured in 2 l batches using artificial seawater (Instant Ocean® dissolved in distilled water) with added f/2-enriched media (Guillard & Ryther 1962) and 0.013 mg l^{-1} sodium metasilicate. When cultures reached ~50,000 cells ml^{-1}, they were filtered onto 5 µm polycarbonate membrane filters, rinsed with distilled water into 50 ml capped polyethelene bottles, and dried at 50°C to a constant weight. Four separate sets of experiments using blank controls (n=2 per group) and diatom frustules (n=3 per group) were carried out simultaneously for 1, 2, 3 and 4 month time trials and stored at 10°C. Samples were processed following the same protocol as the spicule dissolution experiments. Within each diatom experiment, individual Mann-Whitney U tests were used to compare diatom frustules to the control blanks and a Kruskal-Wallis with Dunn pairwise tests was used to compare dissolution of frustules over time.

3.1.5 Microscopy

Sponge spicules and diatom frustules were dried at 60°C to a constant weight, mounted on aluminum stubs, gold coated and examined for qualitative signs of dissolution using SEM (JEOL 6301F field emission microscope). To evaluate the effect of cleaning and a visual comparison for silica etching, spicules cleaned with sodium hypochlorite (no dissolution) were artificially etched with 5 % HF for 3 minutes and studied by SEM. The elemental composition of the adsorbed blackened material on diagenetic skeletons was analyzed using energy dispersive x-ray spectroscopy (EDX) with a specific resolution of 138 eV.

To determine if bacteria were present in the seawater used for dissolution experiments, water was fixed with 5% glutaraldehyde and filtered through 0.02 µm Millipore membrane filters. Filters were post fixed in 1% osmium for 30 minutes, dehydrated in ethanol and critical point dried. Filters were fixed to aluminum stubs, coated with gold and examined by SEM.

3.2 Results

3.2.1 Biomass of live sponges in reefs

The biomass of live *A. vastus* recovered in the Ekman grab was highly variable both within a reef and between reefs (Table 3-1) due to the amorphous shapes of the clumps of sponges we sampled. Within the live biomass of A. vastus consists of the tissue components (organic) and spicule components (inorganic silica). The relative proportion of silica in the biomass ranged between 88-92% among all 3 reefs but was significantly lower at Fraser reef (88%) compared to Howe and Galiano reefs (92%) (Table 3-1, 3-2). Ashed samples were proportionally 80-83% inorganic in the biomass composition (Table 3-1), the ~10% difference between methods is proportional to the water content found in *A. vastus* spicules (Sandford 2003) which is lost during combustion (Mortlock & Froelich 1989). The biomass of *A. vastus* is mostly made of spicules with more fused skeleton (62.7 %) than organic tissue (20.7%) or loose spicules (16.6%) (Table 3-3).

For my estimates of the amount of silica in a reef, I used the more conservative proportions derived from ashing (Table 3-1). The live populations of sponges in the SOG grow to 1.2 m in height (Conway et al. 2005), therefore I used a conservative 0.6 m height coupled with the respective areas of Howe, Fraser and Galiano reefs (10,242 m^2, 13,774 m^2, and 23,432 m^2; Chapter 2) to calculate the volume of biomass at each reef. Live sponges consist of both fused and loosed spicules (79.3%, Table 3-3) and dead skeletons contain only fused spicules (62.7%). Live sponge biomass is found in approximately 17.0, 19.6 and 26.6 kg m^{-3} at Howe, Fraser and Galiano reefs respectively and thus the biomass reservoirs at Howe, Fraser and Galiano reefs contain 141, 180 and 595 tonnes of silica respectively (Table 3-4).

3.2.2 Silicic acid in the water column

During our fall sampling in the SOG, the levels of silicic acid ranged from 48-52 µM in the water column (Fig. 3-3A). The lowest levels of silicic acid were

found at ~2 m depths in surface waters (48 µM) with significantly higher levels (52 µM) at depths >50 m (Mann-Whitney U, $p < 0.05$). Water sampled at the sediment-water interface had significantly higher levels of silicic acid at sponge reef compared to areas away from reefs and without sponges (Fig. 3-3B; Mann-Whitney U, $p < 0.05$).

3.2.3 Dissolution potential of sponge spicules

The initial levels of silicic acid were significantly different between the three starting periods of the experiments (63.2, 65.7, and 64.5 µM) and prevented us from comparing results between experiments (Kruskal-Wallis, $p < 0.001$). There was no significant difference in the initial and final levels of silicic acid between blank controls from the start and end of each experiment (Mann-Whitney U, $p > 0.05$). Also, there was no significant difference between the blank controls and the final levels of silicic acid in loose or fused spicules in all dissolution experiments (Fig. 3-4A-E). However, the diagenetically blackened skeleton treatments showed small, but significant, increases in silica compared to the controls in all experiments with a maximum increase in silicic acid levels of ~10 µM after 8 months (Fig. 3-4A-E; Kruskal-Wallis, $p > 0.001$). Slightly negative dissolution values in some of the treatments indicated that there must have been some adsorption of silicic acid onto the insides of the experiment bottles. In comparison diatom frustules showed a 200-fold increase in the levels of silicic acid after only 1 month and showed continued significant dissolution after 4 months (Fig. 3-4F: Kruskal-Wallis, $p < 0.0001$).

Diatom frustules observed under SEM had severe signs of dissolution after 1 month (Fig. 3-5A-B). In comparison, the initial morphology of fresh loose spicules showed no appreciable changes in morphology after 8 months of dissolution (Fig. 3-5C-H). Similarly, on fresh fused skeleton (Fig. 3-5I), sharp beam spikes (Fig. 3-5J) and exposed cross sections of broken beams (Fig. 3-5K) also showed no appreciable evidence of dissolution (Fig. 3-5L-M). The SEM-EDX showed that the diagenetically blackened skeleton was coated with iron and manganese (Fig. 3-6A). These minerals adsorb to the fused skeleton under

natural field conditions and cause other particulates (Fig. 3-6B), such as diatomaceous material (Fig. 3-6B inset), to adhere to the spicules. Pre-dissolution cleaning with sodium hypochlorite removed most, but not all, of the adsorbed minerals (Fig. 3-6C). Even after rinses of hot nitric acid, adsorbed precipitates will sometimes remain (Chu pers. obs.) and thus I can not entirely attribute the change in silicate acid to be from sponge silica alone.

However by SEM, at the cross sections of broken beams of the fused skeleton pitting could been seen, revealing the colloidal nature of the nanoparticle substructure of the spicule silica (Fig. 3-6D) which had been previously identified in the nanoscale structure of diatom frustules (Noll et al. 2002) and demosponge spicules (Weaver et al. 2003). Similarly, the HF etching showed the same pitting patterns at the cross sections of broken beams (Fig. 3-6E) and the hollow cavity where the axial organic filament used to be was larger after being etched with HF (Fig. 3-6E inset). In comparison, intact loose spicules etched with HF showed no change in morphology (Fig. 3-6F-G). The presence of bacteria was confirmed in both the initial sea water used for dissolution experiments (Fig. 3-6H) and at the end of dissolution experiments (Fig. 3-6I).

3.3 Discussion

Glass sponge reefs are found in waters with relatively high levels of silicic acid which has been directly correlated with the increased abundance of hexactinellid populations (Leys et al. 2004; Whitney et al. 2005a). The large benthic area covered by glass sponge reefs and the high proportion (80%) of silica in their biomass concentrates large amounts of Si in a relatively small area of the world's oceans. Furthermore, the Si retained in a reef is high because spicules are strongly resistant to dissolution. The slow growing and long-lived nature of glass sponges (Leys & Lauzon 1998; Fallon et al. 2010) suggests silica is continually locked into the living portions of the reefs creating significant sinks of silica.

3.3.1 Glass sponge reefs as Si reservoirs

Glass sponge reefs are sustained in their environment probably because of the high levels of silicic acid in the water which correlates to the amount of biogenic silica produced by glass sponges (Leys et al. 2004; Whitney et al. 2005a). The seasonal upwelling along the continental shelf replenishes the silicic acid supply (Whitney et al. 2005a) which would further promote growth of the sponges. Although our surface water measurements for silicic acid were relatively high (~ 48 µM), summer diatom blooms can decrease surface silicic acid levels down to 10 µM (Whitney et al. 2005b). In comparison, silicic acid levels in the bottom waters of the Strait of Georgia are above 50 µM throughout the year (Masson 2006) and thus our measurement of silicic acid levels near the benthos (~50 µM) fall within the values from past studies. Silicic acid levels in water samples taken at the Fraser reef during summer months were ~48 µM (Leys pers. comm.) supporting the seasonal consistency of silicic acid levels in bottom waters and suggests that benthic silicic acid levels do not experience the wide seasonal fluctuations characteristic of surface waters. I can only hypothesize that the small increase (~4 µM) of silicic acid levels in waters over sponge reef compared to waters away from the reef may be caused by the release of Si from skeletons of long dead sponges indicating a slight localized enrichment of Si over the reefs. Our single time point measurement and the small increase permits only cautious interpretations and would require sampling at multiple spatial and temporal time points at a reef to determine that this difference was not an artifcat of seasonal or spatial variability. However, diatomaceous material from surface waters would settle on the benthos regardless of the presence of glass sponges and thus sponge spicules are a likely source of localized enrichment of Si over the reefs. The slightly lower proportions of silica in the biomass of the sponges from Fraser reef were a result of sampling newer sponge growth, as less spicules are found in newer tissue and in areas such as the oscula (Chu, unpublished). Nevertheless, the proportion of silica in the biomass of *A. vastus* is higher than in demosponges and similar to other hexactinellids (Barthel 1995) and thus *A. vastus* can be considered a heavily silicified sponge.

The amounts of silica sequestered in the Howe (145 tonnes), Fraser (180 tonnes) and Galiano (595 tonnes) reefs equate to 2.4 x 10^6, 3.0 x 10^6, and 9.9 x 10^6 moles of Si respectively retained in glass sponge biomass. In bottom sediments, only the upper 0.2-0.3 m will experience Si dissolution and at very low rates (Hurd 1973; Demaster 2002). On average, 8 m of the Fraser reef is buried (Conway et al. 2005) and therefore, the bulk of the Si reservoir of a glass sponge reef is unavailable for dissolution. Under optimal growth conditions, the longevity of hexactinellids and the resistance of their spicules to dissolution would continually increase the amounts of Si locked into a reef compared to the rapid regeneration of Si by diatoms in surface waters.

3.3.2 Dissolution potential of glass sponge silica

Hexactinellid spicules are significantly more resistant to dissolution compared to diatom frustules. Although the lack of detectable dissolution on fresh spicules may have been a result of low statistical power, the pitting observed on the diagenetically blackened spicules supports evidence from past studies which showed dissolution occurring in sponge spicules (Katamani 1971; Maldonado et al. 2005) but still represents a miniscule amount of Si released back into the sea water compared to the relative rates measured for diatoms. Artificially coating diatom frustules with ions of Fe has been shown to slow their rate of dissolution (Lewin 1961) and it is therefore reasonable to assume that the diagenesis of dead sponge skeletons will also function to slow down dissolution. It is important to note the incomplete removal of diatomaceous material from the diagenetic skeletons could be reflected in what was measured as the dissolution rate of the sponge skeletons and thus be a slight overestimate of the Si released from spicules. However, considering that the dead skeletons in my study had already undergone extended dissolution prior to my 8 month experiments, the rates I measured can be cautiously interpreted as being in the upper range of dissolution rates and that the dissolution of hexactinellid spicules occurs at extremely slow rates over the timescale of years.

Pitting was observed only in areas normally not exposed to sea water (broken spicules) which suggests that intact spicules have an external coating that prevents dissolution. Both diatom frustules and sponge spicules are made of amorphous hydrated silica and so a difference in organic subcomponents is likely responsible for the large difference in dissolution potential between frustules and spicules. Diatoms have an organic layer, partially made of the polysaccharide pectin (Desikachary & Dweltz 1961), which protects frustules from dissolution (Lewin 1961; Kamatani 1982). After cell death, the organic layer is degraded by the hydrolytic ectoenzymes of bacteria (Smith et al. 1995) which significantly enhances the dissolution of the frustule silica (Bidle & Azam 1999). Recently a different polysaccharide, chitin, has been discovered as an organic component within the nanoscale silica matrix of spicules from the reef forming hexatinellid, *Farrea occa* (Ehrlich et al. 2007). The chitin-protein complexes found in the exoskeletons of other marine invertebrates are highly insoluble in water (Hunt 1970; Weiner et al. 1983). If chitin is found within the hydrated layers of the spicules of *A. vastus*, the insolubility of chitin (Hock 1940; Austin et al. 1981) would explain the 200-fold difference in dissolution potential between sponge spicules and diatom frustules.

In marine systems, chitin is degraded by chitinovorous bacteria, widely distributed in marine sediments (Zobell & Rittenberg 1937). I cannot determine if bacteria caused the dissolution in my experiments, but if chitinvorous bacteria enhances the dissolution of sponge spicules, this may be an important but overlooked mechanism that promotes Si cycling in benthic waters. The combined effects of diagenesis, natural resistance to dissolution and burial of skeletons at a reef effectively prevents the release of Si and creates a silica sink at a glass sponge reef.

3.3.3 Silica flux of glass sponge reefs

To quantify the silica sink created by glass sponges, I used the Fraser reef to calculate a Si flux (Fig. 3-7). Leys & Lauzon (1998) monitored a population of glass sponge in a fjord off the coast of British Columbia and found growth rates

of ~2 cm $year^{-1}$. Using a more conservative 1 cm $year^{-1}$ growth rate, the live sponge population at Fraser reef would incorporate Si into new biomass at a rate of 3.5 x 10^4 mol Si $year^{-1}$. Based on my maximum observed dissolution rate (10 µmol l^{-1} over 8 months) Si would be released at a rate of 0.083µmol Si day^{-1} per gram of dead sponge skeleton. Under favorable conditions of dissolution, the dead sponges at Fraser reefs would release 1.3 x 10^3 mol Si $year^{-1}$. The rate of Si sequestering is 27-fold greater compared to the rate of Si released and highlights the magnitude of the sink effect at Fraser reef. The Fraser reef represents only a small fraction of the total benthic area covered by glass sponge reefs (700 km^2). A conservative extrapolation of my calculations would be useful to address whether glass sponge reefs affect the cycling of Si at a global scale. If I assume a conservative 50:50 ratio of live to dead sponges occurs over the 700 km^2, a considerable reservoir of 9.7 x 10^8 mol Si is locked into the biomass of glass sponges that sequesters 9.0 x 10^6 mol Si $year^{-1}$ and releases 7.9 x 10^5 mol Si $year^{-1}$, a significant silica sink where Si sequestering is 11-fold greater than Si release.

Although my calculation is negligible relative to the biogenic silica budget of the entire world's oceans (2.4 x 10^{14} mol Si $year^{-1}$, Tréguer et al.1995), the sink effect created by glass sponge reefs illustrates an important, but overlooked, component of the environment when calculating the Si balance at regional scales on the continental shelf. For example, marine silica budgets are calculated under the assumption that removal occurs from only the burial of biogenic silica debris (e.g. diatoms) and most of which occurs in the Antarctic (Tréguer et al. 1995; DeMaster 2002). Further dissolution prior to burial recycles 95% of this Si back up to surface waters for primary production (Tréguer et al. 1995). The removal part of the global balance primarily occurs around the Southern ocean, where dense populations of demosponges and hexactinellids (Dayton et al 1974; 1979) also contribute substantially to the local biogenic Si production (Maldonado et al. 2005). By not taking into account the silica sink created by heavy silicified sponges, the amount of Si reaching surface waters from vertical transport in areas with dense sponge populations maybe much lower than previously assumed.

Modern reefs are analogous to the largest siliceous structures ever created, sponge reefs that dominated areas of the northern Tethys Sea that existed during the Jurassic (~160 million years ago) with the largest spanning over 7,000 km (Ghiold 1991; Leinfelder et al. 1994). The disappearance of siliceous reefs during the Cretaceous has been attributed to Si competition occurring when diatoms established their dominance in the silica cycle (Maldonado et al. 1999). The relatively shallow depths of the reefs in the Strait of Georgia (Chapter 2) create an equivalent setting where this silica competition hypothesis could be empirically tested. Further work bridging the surface water silica cycling by diatoms with the silica sink created by glass sponge reefs would provide useful insight into past ecological conditions.

3.4 Literature Cited

Austin PR, Brine CJ, Castle JE, Zikakis JP (1981) Chitin: New facets of research. Science 212:749-753

Barthel D (1992) Do hexactinellids structure Antarctic sponge associations? Ophelia 36:111-118

Barthel D (1995) Tissue composition of sponges from the Weddell Sea, Antarctica: not much meat on the bones. Mar Ecol Prog Ser 123:149-153

Beaulieu SE (2001) Life on glass houses: sponge stalk communities in the deep sea. Mar Biol 138:803-817

Bett BJ, Rice AL (1992) The influence of hexactinellid sponge (*Pheronema carpenteri*) spicules on the patchy distribution of macrobenthos in the porcupine seabight (bathyal NE Atlantic). Ophelia 36:217-226.

Bidle KD, Azam F (1999) Accelerated dissolution of diatom silica by marine bacterial assemblages. Nature 397:508-512

Bidle KD, Azam F (2001) Bacterial control of silicon regeneration from diatom detritus: significance of bacterial ectohydrolases and species identity. Limnol Oceanogr 46:1606-1623

Conway KW, Krautter M, Barrie JV, Neuweiler M (2001) Hexactinellid sponge reefs on the Canadian continental shelf: a unique “living fossil” Geosci Can 28:71-78

Conway KW, Barrie JV, Krautter M (2005) Geomorphology of unique reefs on the western Canadian shelf: sponge reefs mapped by multibeam bathymetry. Geo-Mar Lett 25: 205-213.

Dayton PK, Robilliard, GA, Paine, RT, Dayton LB (1974) Biological accommodation in the benthic community at Mcmurdo Sound, Antarctica. Ecol Monogr 44:105-128

Dayton PK (1979) Observations of growth, dispersal and population dynamics of some sponges in McMurdo Sound, Antarctica. Colloques internationaux du CNRS 291:271-282

DeMaster DJ (2002) The accumulation and cycling of biogenic silica in the Southern Ocean: revisiting the marine silica budget. Deep-Sea Res Part II 49:3155-3167

Desikachary TV, Dweltz NE (1961) The chemical composition of the diatom frustules. Proc Plant Sci 53:157-165

Ehrlich H, Krautter M, Hanke T, Simon P, Knieb C, Heinemann S, Worch H (2007) J Exp Zool B Mol Dev Evol 308:473-483

Fallon SJ, James K, Norman R, Kelly M, Ellwood MJ (2010) A simple radiocarbon dating method for determining the age and growth rate of deep-sea sponges. Nucl Instrum Methods in Phys Res B 268:1241-1243

Ghiold J (1991) The sponges that spanned Europe. New Sci 2:58-62

Guillard RRL, Ryther JH (1962) Studies of marine planktonic diatoms. I. *Cyclotella nana* Hustedt and *Detonula confervacea* Cleve. Can J Microbiol 8:229-239

Hock CW (1940) Decomposition of chitin by marine bacteria. Biol Bull 79:199-206

Hunt S (1970) Polysaccharide-protein complexes in invertebrates. Academic Press, New York.

Hurd DC (1973) Interactions of biogenic opal, sediment and seawater in the Central Equatorial Pacific. Geochim Cosmochim Acta 37:2257-2282

Kamatani A (1971) Physical and chemical characteristics of biogenous silica. Mar Biol 8:89-95

Kamatani A (1982) Dissolution rates of silica from diatoms decomposing at various temperatures. Mar Biol 68:91-96

Krautter M, Conway KW, Barrie JW, Neuweiler M (2001) Discovery of a "living dinosaur" globally unique modern hexactinellid sponge reefs off British Columbia, Canada. Facies 44:265-282

Leinfelder RR, Krautter M, Laternser R, Nose M, Schmid DU, Schweigert G, Werner W, Keupp H, Herrmann R, rehfeld-Kiefer, U, Schröder JH, Reinhold C, Koch R, Zeiss A, Schweizer V, Christmann H, Menges G, Luterbacher (1994) The origin of Jurassic reefs: current research developments and results. Facies 31:1-56

Lewin JC (1961) The dissolution of silica from diatom walls. Geochim et Cosmochim Acta 21:182-198

Leys SP, Lauzon NRJ (1998) Hexactinellid sponge ecology: growth rates and seasonlity in deep water sponges. J Exp Mar Biol Ecol 230:111-129.

Leys SP, Wilson K, Holeton C, Reiswig HM, Austin WC, Tunnicliffe V (2004) Patterns of glass sponge (Porifera, Hexactinellida) distribution in coastal waters of British Columbia Canada. Mar Ecol Prog Ser 283:133-149.

Leys SP, Mackie GO, Reiswig HM (2007) The biology of glass sponges. Adv Mar Biol 52:1-145.

Maldonado M, Carmona MC, Uriz MJ, Cruzado A (1999) Decline in Mesozoic reef-building sponges explained by silicon limitation. Nature 401:785-788

Maldonado M, Carmona MC, Velásquez Z, Puig A, Cruzado A (2005) Siliceous sponges as a silicon sink: An overlooked aspect of benthopelagic coupling in the marine silicon cycle. Limnol Oceanogr 50:799-809

Maldonado M, Riesgo A, Bucci A, Rützker K (2010) Revisiting silicon budgets at a tropical continental shelf: Silica standing stocks in sponges surpass those in diatoms. 55:2001-2010

Masson D (2006) Seasonal water mass analysis for the Strait of Juan De Fuca and Georgia. Atmos-Ocean 44:1-15

Mortlock RA, Froelich PN (1989) A simple method for the rapid determination of biogenic opal in pelagic marine sediments. Deep-Sea Res 36:1415-1426

Nelson DM, Tréguer P, Brzezinski MA, Leynaert A, Quéguiner B (1995) Production and Dissolution of biogenic silica in the ocean: revised global estimates, comparison with Regional data and relationship to biogenic sedimentation. Global biogeochem 9:359-372

Noll F, Sumper M, Hampp N (2002) Nanostructure of diatom silica surfaces and of biomimetic analogues. Nano Lett 2:91-95

Perry CC (2003) Silicification: The processes by which organisms capture and mineralize silica. Rev Mineral and Geochem 54:291-327

Raven JA, Waite AM (2004) The evolution of silicification in diatoms: inescapable sinking and sinking as escape? New Phytol 162: 45-61

Sanford F (2003) Physical and chemical analysis of the siliceous skeletons in six sponges of two groups (Demospongiae and Hexactinellida) Microsc Res Tech 62:336-355

Schrader HJ (1971) Fecal pellets: role in sedimentation of pelagic diatoms. Science 174: 55-57

Smith DC, Steward GF, Long RA, Azam F (1995) Bacterial mediation of carbon fluxes during a diatom bloom in a mesocosm. Deep-Sea Res II 42:75-97

Strickland JD, Parsons TR (1978) A practical handbook of seawater analysis. Bull Fish Res Board Can, Ottawa, Canada p311

Tabachnick, KR (1994) Distribution of recent Hexactinellida. In: van Soest RWM, van Kempen B, Braekman G (eds) Sponges in time and space. Balkema Rotterdam p 225-232

Tréguer P, Nelson DM, Bennekom AJV, DeMaster DJ, Leynaert A, Quéguiner B. (1995) The silica balance in the world ocean: a reestimate. Science 268: 375-379.

Trégeur P, Pondaven P (2000) Silica control of carbon dioxide. Nature 406:358-359.

Weaver JC, Pietrasanta LI, Hedin N, Chmelka BF, Hansma PK, Morse DE (2003) Nanostructural features of demosponge biosilica. J Struc Biol 144:271-281

Weiner S, Traub W, Lowenstam HA (1983) Organic matrix in calcified exoskeletons. In: Westbroek P, de Jong EW (eds) Biomineralization and biological metal accumulation. Reidel, Amsterdam

Whitney FA, Conway K, Thomson R, Barrie JV, Krautter M, Mungov G (2005a) Oceanographic habitat of sponge reefs on the Western Canadian Continental Shelf. Cont Shelf Res 25:211-226.

Whitney FA, Crawford DW, Yoshimura T (2005b) The uptake and export of silicon and nitrogen in HNLC waters of the NE Pacific Ocean. Deep-Sea Res Part II 52:1055-1067

Williams LA, Parks GA, Crerar DA (1985) Silica diagenesis; I, solubility controls. J Sediment Res 55:301-311

Yahel G, Whitney F, Reiswig HM, Eerkes-Medrano DI, Leys SP (2007) In situ feeding and metabolism of glass sponges (Hexactinellida, Porifera) studied in a deep temperate fjord with a remotely operated submersible. Limnol Oceanogr 52:428-440.

Zar JH (1999) Biostatistical analysis 4 ed. Prentice Hall, New Jersey 663 p

Zobell CE and Rittenberg SC (1937) The occurrence and characteristics of chitinoclastic bacteria in the sea. J Bacteriol 35:275-287

Table 3-1. The proportion of silica in the biomass sampled at each of 3 reefs in the SOG. An Ekman grab (3.54×10^{-3} m^3) was used to sample live sponges at each of the reefs and the proportion of Si in the biomass was determined from subsamples using two methods. The HF dissolution method to determine proportional Si in biomass was done with combined 2007 and 2009 grabs. Ashing was only done with 2007 grabs. Number of grabs used in each method is in parentheses.

				HF Dissolution Method			Ashing Method[a]		
	Grab Dry Weight (g)			Proportion of Si in biomass (%)			Proportion of Si in biomass (%)		
Reef	N	Mean	SD	N	Mean*	SD	N	Mean*	SD
Howe	4	60.2	35.7	20(4)	92.8 (b)	2.4	30(3)	82.1 (ab)	7.7
Fraser	4	69.3	62.3	20(4)	88.9 (a)	3.0	20(2)	80.0 (a)	2.2
Galiano	4	94.2	58.7	20(4)	92.3 (b)	2.3	30(3)	83.1 (b)	3.4

[a]only done with 2007 Ekman grabs

*letters in parentheses indicate significant differences (Table 3-2)

Table 3-2. Nested ANOVA comparing the proportion of silica in *A. vastus* between reefs.

Factor	df	MS	F	p
HF Method				
Reef	2	0.0185	25.75	<0.0001
Ekman (Reef)	9	0.0062	8.66	<0.0001
Residual	48	0.0007		
Combustion				
Reef	2	0.00763	4.24	0.018
Ekman (Reef)	5	0.00581	3.23	0.011
Residual	72	0.001800		

Table 3-3. Proportions of the differenet components (loose spicules, fused skeleton, organic tissue) in the biomass of *A. vastus*.

	Percentage of dryweight (%)	
Biomass component	Mean	SD
Fused skeleton	62.7	3.4
Loose spicules	16.6	1.6
Organic tissue	20.7	3.5

Table 3-4. The amount of silica in each of 3 glass sponge reefs in the SOG.

	Biomass ($kg\ m^{-3}$)	Volume of Reef (m^3)[a]		Mass of Silica (kg)		Silica Reservoir (tonnes)
Reef		Live	Dead	Live[b]	Dead[b]	
Howe	17.0	6,145	5,450	82,841	58,092	141
Fraser	19.6	8,264	4,167	128,446	51,209	180
Galiano	26.6	14,059	17,879	296,558	298,190	595

[a] calculated using areas in Table 2-1 (Chapter 2) and a 0.6 m average height
[b] calculated using proportions of silica of 79.3% in live and 62.7% in dead sponges (Table 3-3)

Figure 3-1. Study locations (glass sponge reefs) in the Strait of Georgia.

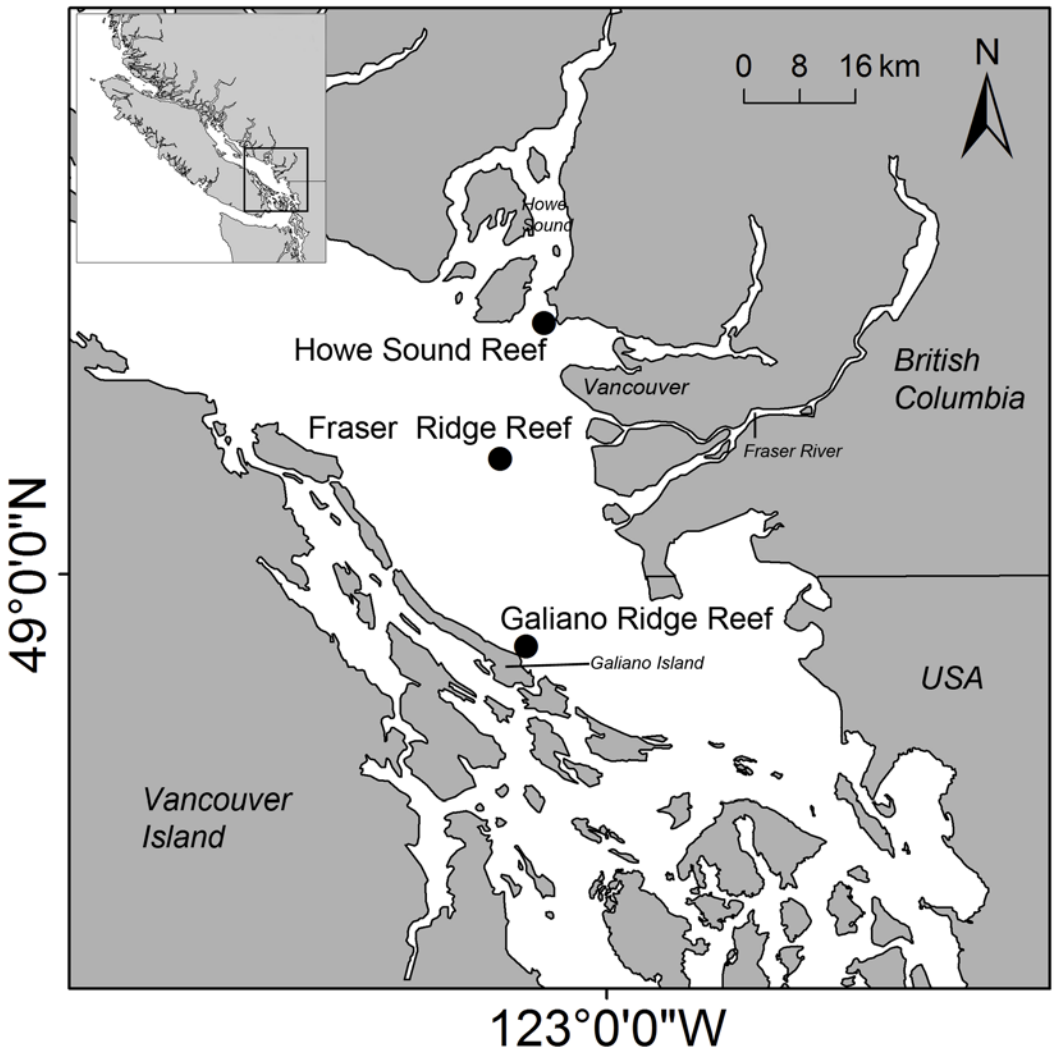
0 8 16 km
N
Howe Sound
Howe Sound Reef
Vancouver
British Columbia
Fraser Ridge Reef
Fraser River
Galiano Ridge Reef
Galiano Island
USA
Vancouver Island
49°0'0"N
123°0'0"W

Figure 3-1

Figure 3-2. Field sampling of silica at a glass sponge reef. (A) *A. vastus* and *H. calyx* form dense bushes that cover the seafloor in patches within a reef. (B) Live sponges are cream colored. (D) An Ekman grab sample of biomass from live *A. vastus*. (E) Dead sponges eventually "blacken" after death but the fused skeleton persists, retaining original shape of the sponge. Scale bars are 10 cm.

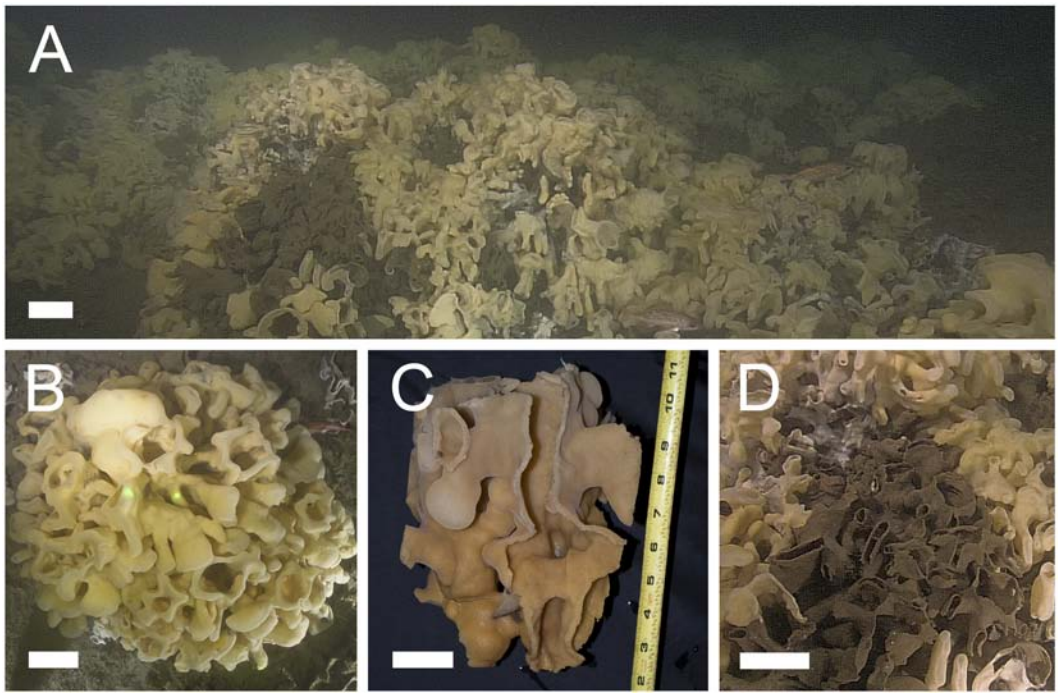

Figure 3-2

Figure 3-3. Levels of silicic acid in the waters above and around the glass sponge reefs. (A) Silicic acid ranged from 48-52 μM throughout the water column. There was a slight decrease in the upper 50 m of surface waters with the highest silicic acid levels from at 80-100 m where the glass sponges are located. (B) Silicic acid levels at the sediment-water interface were significantly higher at the reefs compared to areas away from the reefs (Mann-Whitney U, $p < 0.05$). Data are shown in mean ± SE with sample sizes shown in parentheses.

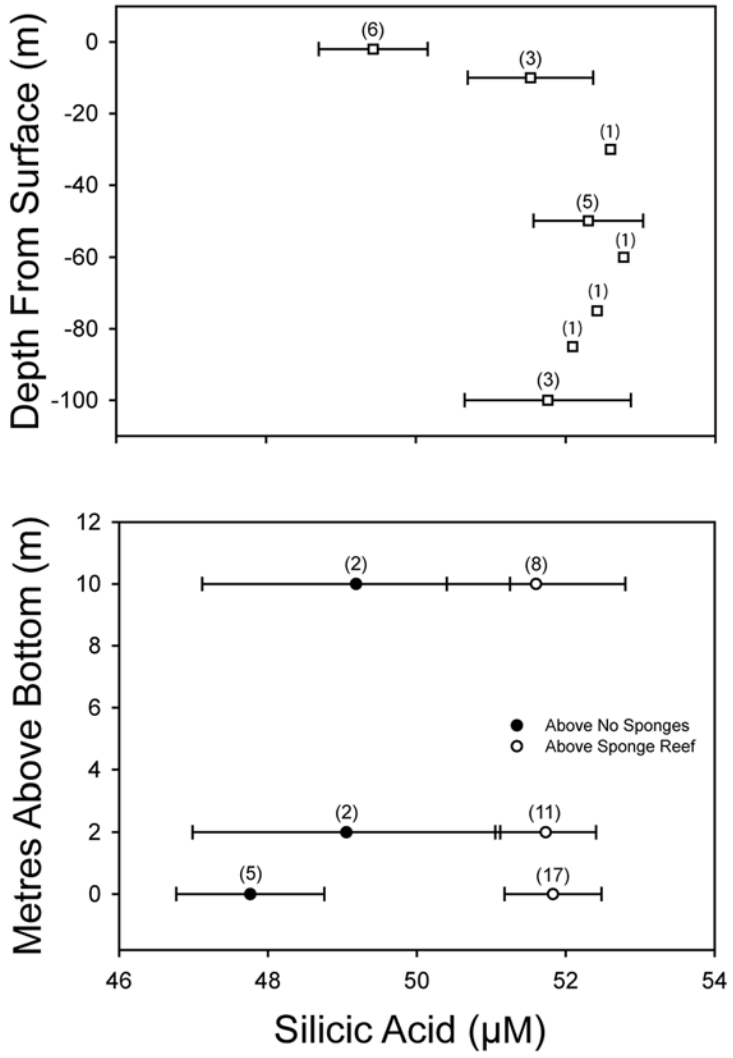
Depth From Surface (m)
0
-20
-40
-60
-80
-100
(6)
(3)
(1)
(5)
(1)
(1)
(1)
(3)
Metres Above Bottom (m)
12
10
8
6
4
2
0
(2)
(8)
Above No Sponges
Above Sponge Reef
(2)
(11)
(5)
(17)
46
48
50
52
54
Silicic Acid (µM)

Figure 3-3

Figure 3-4. Dissolution experiments of the spicules of *A. vastus*. Independent sets of replicates were run for the duration of (A) 1 month (B) 2 months (C) 3 months (D) 6 months (E) or 8 months. All bars are mean ± 1 SE. Note that all control blanks were not significantly different than initial concentrations at the end of dissolution period (t-test, $p > 0.05$) and that the slight negative values in some treatments were likely from the adsorption of silicic acid onto the inside surfaces of the experimental bottles. Within an experiment, different letters among columns indicate significant differences (Dunn's test, α 0.05). (F) Diatoms significantly dissolved compared to controls after only 1 month (Mann Whitney U, $p < 0.0001$) and showed significant amounts of dissolution over time (Kruskal-Wallis, $p < 0.0001$). Letters among columns indicate differences in dissolution of frustules between experiments (Dunn's test, α 0.05).

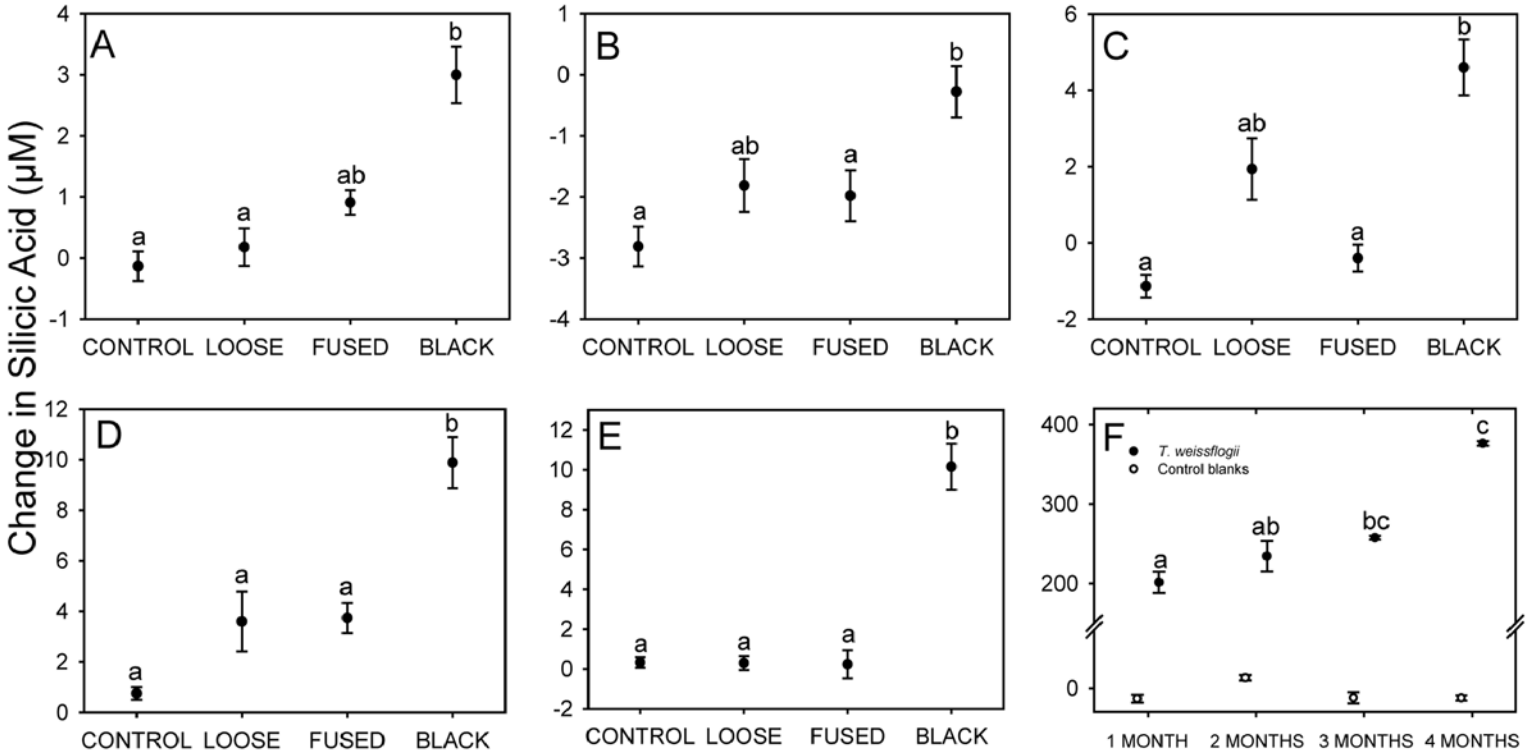
Change in Silicic Acid (µM)
A
B
C
D
E
F
CONTROL LOOSE FUSED BLACK
T. weissflogii
Control blanks
1 MONTH 2 MONTHS 3 MONTHS 4 MONTHS

Figure 3-4

Figure 3-5. Evidence of silica dissolution in biogenic substrates observed by scanning electron microscopy. (A) Frustules of the diatom *T. weisfloggii* before dissolution showed intricate surface morphology. (B) Surface morphology of frustules was lost after 1 month of dissolution in seawater. (C-H) Loose spicules of *A. vastus* showed no signs of dissolution after 8 months of dissolution in seawater: (C) Initial oxyhexaster morphology, (D) oxyhexaster retained sharp features after dissolution, (E) initial pinnular hexactin morphology, (F) pinnular hexactin also retained sharp features after dissolution, (G) initial forked scopule morphology, (H) forked scopule retained sharp features (inset) after dissolution 8 months. (I-M) Similarly, fused skeleton of *A. vastus* showed no signs of dissolution: (I) initial fused skeleton, (J) initial ornamental spines on beams, (K) initial exposed cross section of a broken beam, (L) beam spine after dissolution, and (M) exposed cross section after dissolution. Note the axial cavity (arrow) of the organic filament is visible.

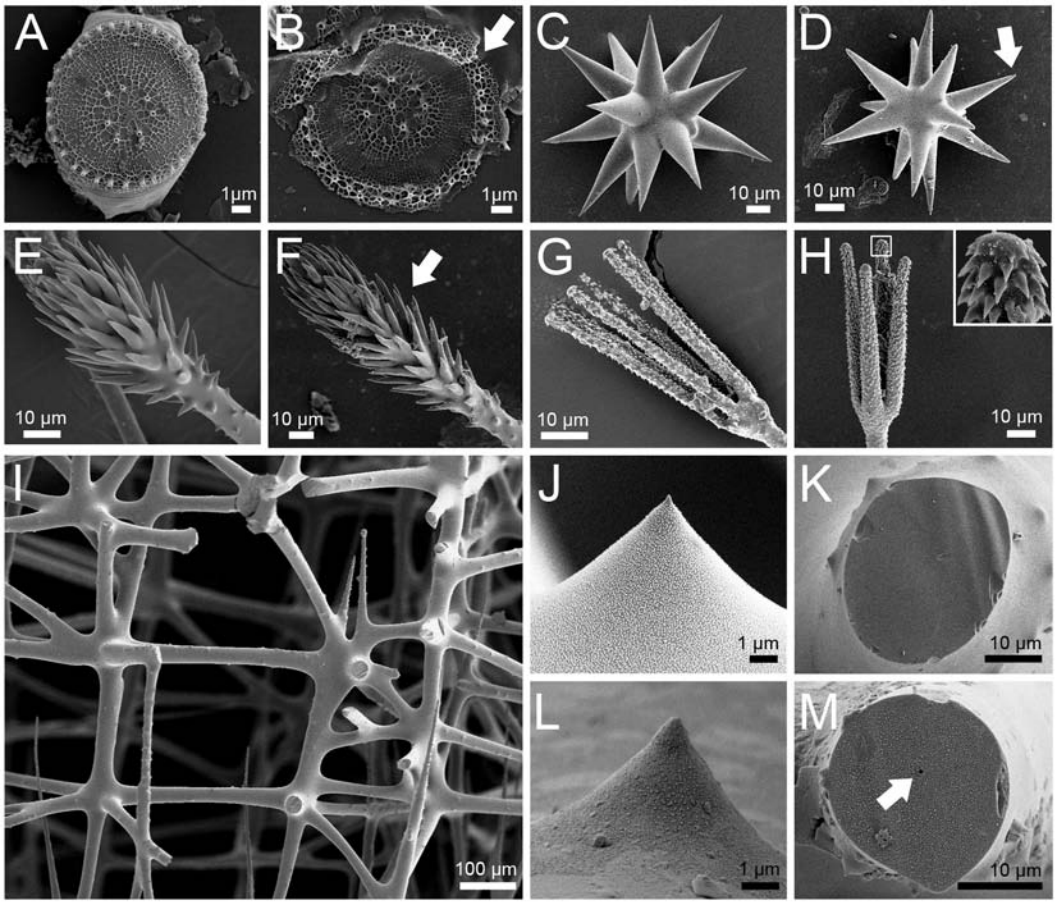
A
1µm
B
1µm
C
10 µm
D
10 µm
E
10 µm
F
10 µm
G
10 µm
H
10 µm
I
100 µm
J
1 µm
K
10 µm
L
1 µm
M
10 µm

Figure 3-5

Figure 3-6. Evidence of silica dissolution in diagenetically blackened skeletons of *A. vastus* observed by scanning electron microscopy. (A) EDX analysis showed composition of the blackening was mainly adsorbed precipitates of iron (Fe) and manganese (Mn). The peaks of silica and gold are from the spicule and the gold coating for scanning electron microscopy. (B) Skeletons were completely coated by precipitates which adhered diatomaceous material to the spicule (inset) (C) Most of the precipitates were removed after cleaning with sodium hypochlorite but small amounts remained. (D) Blackened skeleton had pitting at the exposed cross sections of skeletal beams but not on the outer surface of beams after 8 months of dissolution in sea water. (E-G) The effects of artificially etching spicules with HF. (E) Artificially induced etching with a 3 minute rinse in dilute HF showed similar patterns of etching at cross sections as the 8-month dissolution experiment and also resulted in enlargement of the axial cavity (arrow) where the organic filament previously resided. There were no obvious changes in the morphology of (F) oxyhexasters or (G) pinnular hexactins from HF rinses. (H) Bacteria were present in the initial filtered (0.45 μm) sea water used for dissolution experiments. (I) Bacteria was also present in the sea water at the end of dissolution experiments.

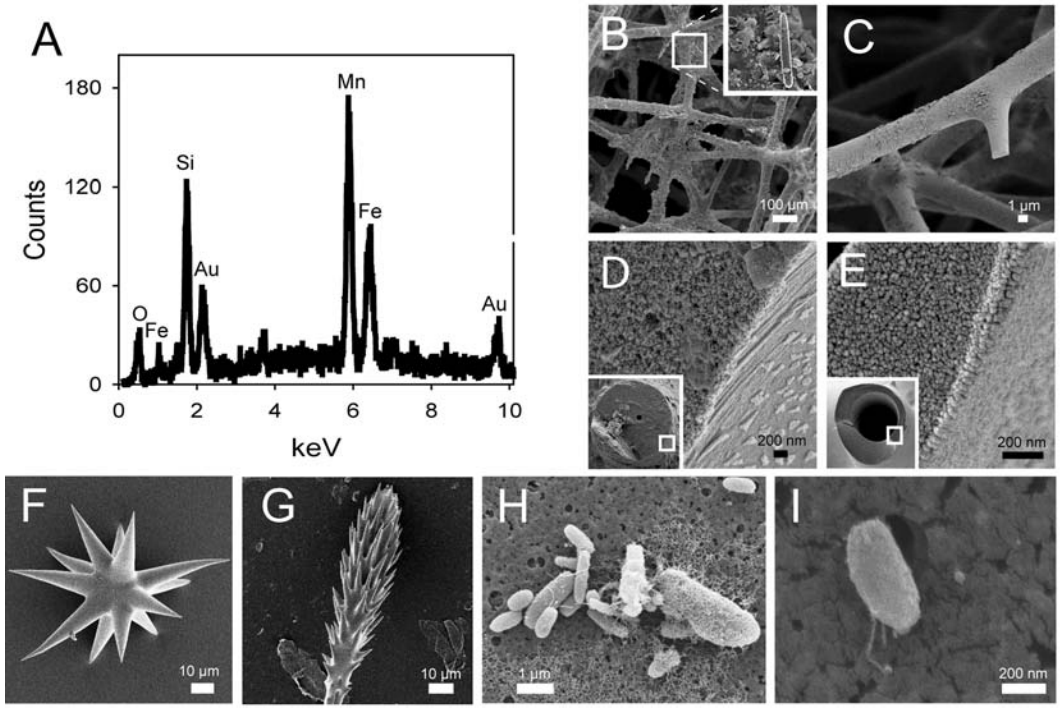
A
Counts
180
120
60
0
0
2
4
6
8
10
keV
O
Fe
Si
Au
Mn
Fe
Au
B
100 µm
C
1 µm
D
200 nm
E
200 nm
F
10 µm
G
10 µm
H
1 µm
I
200 nm

Figure 3-6

Figure 3-7. Estimated silica flux of the Fraser glass sponge reef. A reservoir of 2.98×10^6 mol of Si is locked into the biomass of live (2.12×10^6 mol Si) and dead (8.55×10^5 mol Si) glass sponges. The rate of Si sequestering from growth (35,453 mol Si $year^{-1}$) exceeds the rate of Si released from dissolution (1,557 mol Si $year^{-1}$) and thus a sink effect occurs at the reef. In surface waters (<50 m), Si levels seasonally range from 10 µM (Whitney et al. 2005) to 48 µM. In bottom waters, Si levels are higher in areas above reefs (52 µM) compared to areas of bare substrate.

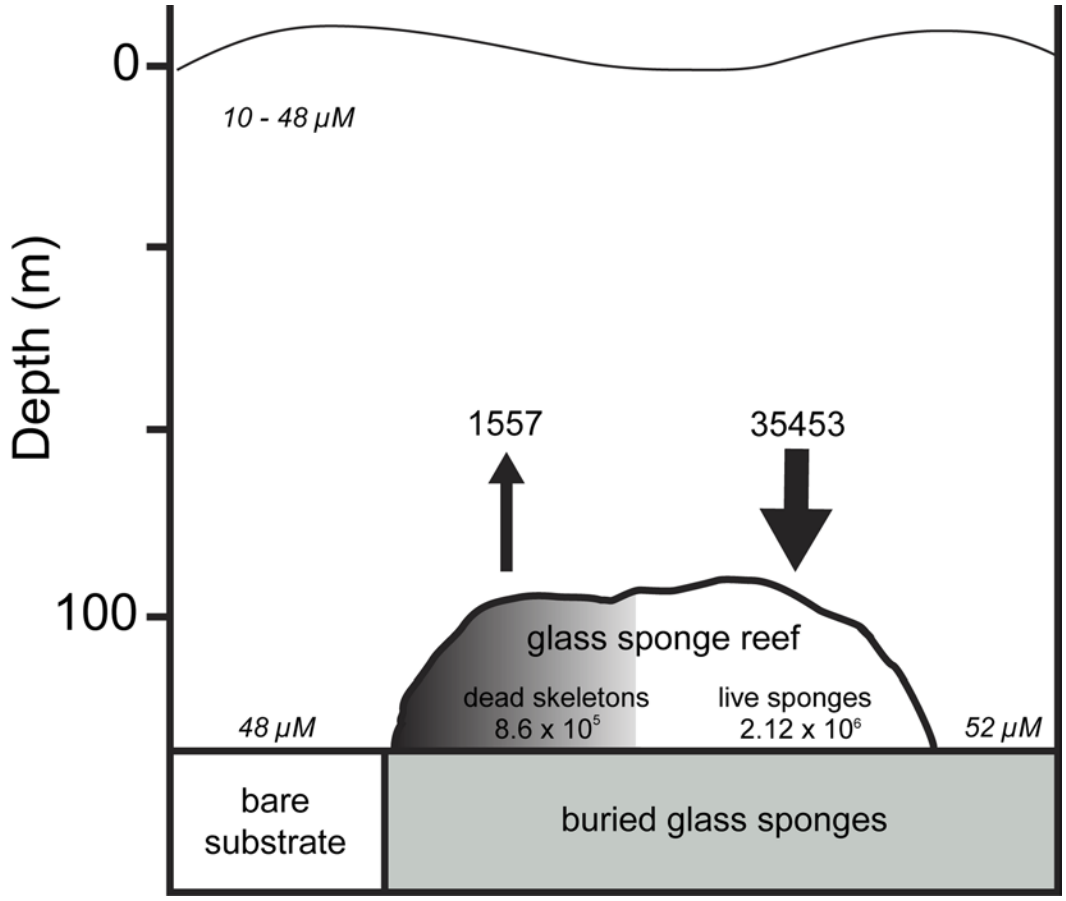
0
10 - 48 µM
Depth (m)
100
1557
35453
glass sponge reef
dead skeletons
8.6 x 10^5
live sponges
2.12 x 10^6
48 µM
52 µM
bare substrate
buried glass sponges

Figure 3-7

Chapter 4

Differences in trophic patterns between glass sponge reefs: spatial variation in $\delta^{13}C$ and $\delta^{15}N$ of *Aphrocallistes vastus*

4.0 Introduction

Benthic sponge communities have important functional roles in the transfer of nutrients between pelagic and benthic environments (for a review see Gili & Coma 1998). Of these, glass sponges (Porifera, Hexactinellida) are found in high abundance in waters of the Antarctic (Dayton 1979), Europe (Vacelet 1995), Hawaii (Pile & Young 2006) and the Northeast Pacific Ocean (Conway et al. 2001; Leys et al. 2004), but only recently has their feeding ecology been well understood (Reiswig 1990; Pile & Young 2006; Yahel et al. 2006, 2007). Glass sponges are highly efficient consumers of non-photosynthetic bacteria and heterotrophic protists, which dominate the ultraplankton (<10 µm) in their detrital food web (Pile & Young 2006; Yahel et al. 2006, 2007). Thus, the microbial community responsible for transporting half of the ocean's primary productivity into benthic waters via the 'microbial loop' (Azam et al. 1983) is strongly coupled with glass sponges.

One of the highest densities of glass sponges is found in the unique reefs on the Pacific coast of Canada (Conway et al. 2001, 2007) where populations of *Aphrocallistes vastus* and *Heterochone calyx* form dense patches in relatively shallow depths (59 to 180 m, Chapter 2). For sessile suspension feeders, an increase in the availability of food particles is determined by increasing flow intensity and frequency (Wildish & Kristmanson 1997). In the case of glass sponges, this may directly control the growth, maintenance, and biomass in a glass sponge reef. However, the food source supporting the populations of glass sponges in the reefs has not been investigated. For sessile suspension feeders, living carbon is preferentially assimilated over detrital particulate organic carbon (Wotton 1994), but the diet will reflect the availability of food sources. Shifts in

diet are not uncommon as an adaptive strategy in sponges (Ribes et al. 1999) and in suspension feeders such as ascidians (Ribes et al. 1998) and corals (Slattery et al. 1997). The relative differences in dictyonine sponge abundance (Chapter 2) and biomass (Chapter 3) between glass sponge reefs may be a reflection of the availability and quality of suspended food in the Strait of Georgia (SOG).

Glass sponge reefs in the SOG, due to their relatively shallow depths and close proximity to the city of Vancouver, may feed on food sources normally not available to glass sponge populations inhabiting deeper waters. Such influences on the food web can be revealed from the use of stable isotopes ($\delta^{13}C$ and $\delta^{15}N$). $\delta^{13}C$ allows us to trace the flow of primary production (Peterson & Fry 1987) and $\delta^{15}N$ allows an inference to trophic level because of a predictable stepwise enrichment of $\delta^{15}N$ up a food chain (~3 to 4‰, Minagawa & Wada 1984). Furthermore, $\delta^{13}C$ has been used to determine anthropogenic input into benthic food webs where the typical -15‰ to -22 ‰ range of marine phytoplankton detritus (Gearing et al. 1984) shifts towards more negative values because of the presence of sewage derived organic matter (OM, -22‰ to -26‰, Conlan et al. 2006 and references therein) or terrestrial C3 plant OM (-27‰ to -25.5‰, Hedges & Mann 1979; Rau et al. 1989; Macdonald et al. 1991). Recent sediment samples taken from regions near (~1 km) two of the three reefs in my study (Howe and Fraser reefs) had low $\delta^{13}C$ values (-25%) pointing to potential input of terrestrial carbon from nearby (~13 km) municipal sewage outfalls and the Fraser River (Macdonald et al. 2008). Because of the input of terrestrial OM into the SOG, it is reasonable to expect that the glass sponges, low order suspension feeders in a detritus based food web, will have negative shifts in the $\delta^{13}C$ values of their tissue.

The goal of my study, therefore, was to document the variability of isotopic composition ($\delta^{13}C$ and $\delta^{15}N$) in *A. vastus* between 3 glass sponge reefs in the SOG and examine the potential differences in feeding and trophic structure between reef and non-reef populations. I collected tissue from *A. vastus* and particulate organic matter (POM) in near-bottom waters at 3 reefs in the SOG (Howe, Fraser and Galiano reefs) with two reefs (Fraser and Galiano reefs)

sampled over two years. *A. vastus* from non-reef populations were also sampled to compare the isotopic compositions between reef and non-reef habitats. Potential differences in the $\delta^{13}C$ and $\delta^{15}N$ between reef and non-reef populations of *A.vastus* would likely reflect the food supply in the SOG.

4.1 Materials and Methods

4.1.1 Description of sampling locations

The Strait of Georgia (SOG, Fig.4-1 inset) is approximately 28 km wide by 222 km long with an average depth of 155 m (Thomson 1981). Water residence time of bottom waters is ~300 days compared to 100 days for the upper 50 m of the surface waters (Waldichuk 1983). Outflow from the Fraser River spreads over the surface waters of the SOG causing stratification until wind vertically mixes the water column (LeBlond et al. 1991). Summer intrusion of offshore waters in the Pacific enters through the deeper portions of the Juan de Fuca Strait, replenishing the lower (>100 m) and intermediate water layers of the SOG (LeBlond et al. 1991; Thomson et al. 2007). The Fraser River is responsible for 80% of the terrestrial particulate load and 65% of the freshwater flowing into the SOG (Thomson 1981; Thomas & Bendell-Young 1999; Thomson et al. 2007). The glass sponge reefs in the SOG are found on hard bedrock features elevated from the surrounding mud. In this study, I focused only on the more abundant *A. vastus* and did not compare between the two reef forming species.

4.1.2 Field sampling

Glass sponges were sampled at 5 distinct locations along the coast of British Columbia and Washington, including 3 glass sponge reefs (Howe, Fraser, and Galiano reefs) in the Strait of Georgia (Fig. 4-1, Table 4-1) from 2007 to 2009. Sponges were sampled at Fraser and Galiano reefs in October 2007 and October 2009, to compare isotopic composition between years. Collections from non-reef populations were taken from fjord walls in Barkley Sound and isolated

individual sponges found off the coast of Washington within the boundaries of the Olympic Coast National Sanctuary.

Sponges were sampled as ~4 cm^2 sized pieces (n = 46) and retrieved at depth with the remote operated vehicle ROPOS by either suction sampler or by manipulator arm. The species identity of each specimen was confirmed by microscopy using the identifying characteristics of *A. vastus*' microsclere spicules and their arrangement within the tissue (Reiswig 2002). Water samples were retrieved with 2-litre Niskin bottles mounted onto the forward brow of ROPOS and 5-litre Niskin bottles lowered over the side of the ship to the depths of the sponges. Water samples were prefiltered through 180 µm nitex mesh to remove small zooplankton (e.g. copepods) and vacuum filtered onto precombusted (500°C for 12 hrs) Whatman GF/F filters (nominal 0.7 µm pore size). All samples were labelled, georeferenced, and stored at -80°C until processed.

4.1.3 Isotope analysis

Sponge tissue and POM samples were oven-dried at 60°C for 4 days, then ground into a homogenous powder using a Wig-L-Bug grinder (Crescent Dental Co., Chicago, Illinois). The instruments used during sample processing were carefully rinsed with 95% ethanol between replicates to prevent cross contamination. Five mg of each sample was packaged into tin capsules which were processed for continuous-flow isotope ratio mass spectrometry (CF-IRMS) analysis of carbon and nitrogen using a PDZ Europa 20-20 isotope ratio mass spectrometer (Sercon Ltd., Chesire, UK) at the Stable Isotope Facility at the University of California Davis. Carbon and nitrogen isotope data are expressed in ppt (‰) calculated as the ratio of the heavy to light isotope according to the formula: $\delta^{H}X = [(R_{sample} / R_{standard} - 1)] \times 1000$, where the ratio ($\delta^{H}X$) represents $^{13}C/^{12}C$ for carbon and $^{15}N/^{14}N$ for nitrogen and standards were Pee-Dee Belemnite for $\delta^{13}C$ and air for $\delta^{15}N$. Measurement precision was approximately 0.05‰ and 0.09 ‰ for $\delta^{13}C$ and $\delta^{15}N$ respectively.

The synthesis and accumulation of lipids can cause negative values of $\delta^{13}C$, masking the true effects of an animal's diet (DeNiro & Epstein, 1977;

McConnaughey & Roy, 1979). There was a strong negative correlation between $\delta^{13}C$ values and C:N ratios among sponge tissue samples ($r = -0.47$, $p<0.001$), therefore, the $\delta^{13}C$ values were normalized with C:N ratios (Post et al. 2007) and analyses were run on both normalized and non-normalized data. The outcome of the statistical analyses did not change after normalization and thus results are presented using non-normalized values. To establish a meaningful sample size for statistical comparison, samples from Barkley Sound and the coast of Washington were pooled in a 'non-SOG' group. All data met parametric assumptions, except the values of $\delta^{15}N$ for POM which met assumptions after applying square root transformations. One-way ANOVA with Tukey post-hoc tests were used to compare between groups. All statistical analyses were done in JMP v7.0.

4.2 Results

4.2.1 Benthic particulate organic matter (POM) at glass sponge reefs in the SOG

In the waters sampled near the sponges at each reef, $\delta^{13}C$ and $\delta^{15}N$ values were between -25.2 to -22.5‰ (a 2.7‰ range) and 5.3 to 12.0‰ (a 6.7‰ range) respectively (Table 4.2, Fig. 4.2A). $\delta^{13}C$ was not significantly different between reefs (ANOVA, $F_{2,27}=1.83$, $p = 0.18$). $\delta^{15}N$ values were significantly higher in sponges from Galiano reef compared to Howe reef, but not Fraser reef (ANOVA, $F_{2,27}=3.78$, $p = 0.04$).

4.2.2 Isotopic composition of glass sponges

The $\delta^{13}C$ of *A. vastus* tissue was between -21.3 to -19.5‰ (a 1.8‰ range) and the $\delta^{15}N$ were between 14.4 to 17.5‰ (a 3.1‰ range) (Table 4.2, Fig. 4.2B)

Differences between years - Sponges sampled in 2009 from both the Fraser reef and Galiano reef had significantly higher $\delta^{13}C$, by 0.9‰ and 0.3‰ respectively, compared to samples from 2007 (Fig 4.3A, ANOVA, $F_{5,45} = 94.94$, $p < 0.0001$). Only sponges sampled in 2009 from Galiano reef had significantly higher $\delta^{15}N$,

by 2.3‰, compared to 2007 sponges (Fig 4.3B, ANOVA, $F_{5,45} = 51.12$, $p < 0.0001$).

Differences between reefs in the SOG – In 2009, Galiano reef had significantly higher $\delta^{13}C$ (by 1.6‰) compared to both Fraser and Howe reefs (Fig 4.3A) and significantly higher $\delta^{15}N$ compared to Howe (by 2.1‰) and Fraser (by 2.2‰) reefs (Fig. 4.3B).

Differences between populations outside of the SOG- $\delta^{13}C$ values of Galiano sponges were more similar to non-SOG populations than to those from Howe and Fraser reefs (Fig. 4.3A). All sponge samples from the SOG were significantly lower in $\delta^{15}N$ compared to non-reef populations except for sponges sampled in 2009 at Galiano reef which were significantly higher in comparison (Fig. 4.3A, B).

4.2.3 C:N ratio of POM and glass sponges

The C:N ratio of POM samples was the same in near-bottom waters between reefs (ANOVA, $F_{2,27} = 1.004$, $p = 0.38$) and averaged 6.4±0.8. The C:N ratio of sponge tissue was the same across all locations and sampling years (ANOVA, $F_{5,45} = 1.047$, $p = 0.40$). The pooled average C:N ratio from all tissue samples (n=46) was 4.7±0.2.

4.3 Discussion

In general, there is low variability in the isotopic composition of *A. vastus* within a glass sponge reef at a given point in time. However, $\delta^{13}C$ and $\delta^{15}N$ values shifted between years within a reef and the differences in the isotopic composition between areas suggest that different populations of glass sponges are feed on different food supplies.

4.3.1 Feeding patterns of glass sponges

The lower C:N ratio of *A. vastus* tissue (4.7:1) relative to the POM in the ambient water near the sponges (6.4:1) shows a preferential retention of carbon

and the excretion of nitrogen. This supports past observations of elevated ammonium levels measured in the exhaled water from *A. vastus* (Yahel et al. 2007). Only one previous study had documented $\delta^{13}C$ (-17.25‰) and $\delta^{15}N$ (17.93‰) values for an unidentified hexactinellid (n=5, Iken et al. 2001). The $\delta^{15}N$ of the sampled POM in their study was 8.15‰, a stepwise difference of 9.8‰. This indicates an unusual 3 trophic levels above the POM base and suggests this unidenfitifed sponge is uncoupled with the POM.

The $\delta^{13}C$ values of *A. vastus* are more similar to those of demosponges (1 species, -22 ‰, Kaehler et al. 2000; 3 species, -22 to -24‰, Thurber 2007). The $\delta^{15}N$ values of *A. vastus* lie between the range of reported value for these demosponges (17.9‰, Kaehler et al. 2000; 5-11‰, Thurber 2007). It is important to note that the sampling design in these studies did not factor in the seasonal difference found in sponge diets (Ribes et al. 1999) and occurred in areas with kelp derived subsidies (Kaehler et al. 2000) and sewage waste (Thurber 2007) in the ambient water. The strong interspecific differences of isotopic composition within these studies limit their comparability to the values of *A. vastus* in my study.

In *A. vastus*, the differences in $\delta^{13}C$ and $\delta^{15}N$ between both years of sampling at both Fraser and Galiano reefs reveals that complete shifts in diet can occur within 2 years indicating that glass sponges are actively growing in the reefs. Despite the highly selective feeding of *A. vastus* (Yahel et al. 2006, 2007), the isotopic composition was different between populations which shows strong intraspecific variability of $\delta^{13}C$ and $\delta^{15}N$ in *A. vastus.* A population of *A. vastus*, within a range of <0.5 km can be considered to be filtering a relatively homogenous pool of water, but sponges separated by >20 km are probably filtering different source waters or showing a difference in isotope fractionation.

The range of $\delta^{15}N$ found in the POM (~6.7) indicates that two trophic levels occur at the base of the reef food web where *A. vastus* can be considered a 2^{nd} or 3^{rd} order consumer in the SOG. The 5‰ stepwise enrichment of $\delta^{15}N$ between POM and glass sponges at Howe and Fraser reef indicates a difference of ~1 trophic level. However, the 8.5‰ enrichment of $\delta^{15}N$ between POM and

sponges sampled in 2009 from Galiano reef indicates a difference of ~2 trophic levels. The diet of *A. vastus* consists of selective removal of free living non-photosynthetic bacteria and heterotrophic protists with a minor contribution from detrital POM (Yahel et al. 2007). The higher trophic position detected in Galiano reef sponges may be explained by selective feeding on the living component of the POM but may also indicate a lower abundance of live cells within the POM at Howe and Fraser reefs. The similarity of $\delta^{15}N$ between Galiano reef and non-SOG sponges indicates that offshore POM is likely supplied to the southern portions of the SOG through the intrusion of offshore waters through the Juan de Fuca Strait (LeBlond 1991; Johannessen et al. 2005; Thomson et al. 2007). If offshore waters supply a subsidy of living cells to the diet of sponges from Galiano reef, this may explain the greater relative abundance of live sponge cover (Chapter 2) and biomass (Chapter 3) at Galiano reef compared to Howe and Fraser reef.

4.3.2 Terrestrial input to glass sponge reefs

The lower $\delta^{13}C$ values in glass sponges from the Howe and Fraser reefs may also point to a contribution of terrestrial OM in the sponge diet. The range of $\delta^{13}C$ in the sampled POM (-25.2 to -22.5‰) is more depleted compared to the typical range of -15‰ to -22 ‰ found in marine phytoplankton (Gearing et al. 1984; Risk et al. 1994) suggesting the presence of terrestrial carbon. In the SOG, up to 40% of the bottom sediments can be derived from terrestrial OM (Macdonald et al. 1991) because of the multiple input sources from pulp mills, sewage outfalls, and the Fraser River (Kay 1989, Macdonald et al. 1991, Yunker et al. 1999, Johannessen et al. 2005; Macdonald et al. 2008). Lower $\delta^{13}C$ found in bottom sediments near Howe (-24‰) and Fraser (-25‰) reefs compared to Galiano reef (-22‰) is explained by the input of terrestrial OM from the nearby Lions Gate and Iona sewage outfalls and the Fraser River (Macdonald et al. 2008). In shallow water corals elsewhere, lower $\delta^{13}C$ values have been found in populations of inshore corals compared to offshore corals (Risk et al. 1994). Similarly, lower $\delta^{13}C$ values have been found in deposit feeders and sponges close

to sewage outfalls on the eastern coast of the United States and Antarctica (Van Dover et al. 1992; Thurber 2007). It is, therefore, highly likely the lower $\delta^{13}C$ values found in glass sponges from the Howe and Fraser reefs are a result of their close proximity to local input sources of terrestrial carbon.

Although I cannot correlate the contribution of specific carbon sources to each reef, the spatial patterns of $\delta^{13}C$ and $\delta^{15}N$ suggests the diets of the sponges at Howe and Fraser reefs have a larger terrestrial component relative to Galiano reef. The immediate focus on conservation and protection of glass sponge reefs has been on the impact of trawling fisheries (Jamieson & Chew 2002), yet subtle shifts in diet as a result of their local environment may be placing a previously undetected stressor on this sensitive benthic ecosystem.

4.4 Literature Cited

Azam F, Fenchel T, Field JG, Gray JS, Meyer-Reil LA, Thingstad F (1983) The ecological role of water-column microbes in the sea. Mar Ecol Prog Ser 10:257-263

Conlan KE, Rau GH, Kvitek RG (2006) $\delta^{13}C$ and $\delta^{15}N$ shifts in benthic invertebrates exposed to sewage from McMurdo Station, Antarctica. Mar Poll Bull 52:1695-1707

Conway KW, Krautter M, Barrie JV, Neuweiler M (2001) Hexactinellid sponge reefs on the Canadian continental shelf: a unique "living fossil". Geosci Can 28:71-78

Conway KW, Barrie JV, Hill, PR, Austin WC, Picard K (2007) Mapping sensitive benthic habitats in the Strait of Georgia, coastal British Columbia: deep-water sponge and coral reefs. Geol Surv Can, 2007-A2:1-6

Dayton PK (1979) Observations of growth, dispersal and population dynamics of some sponges in McMurdo Sound, Antarctica. Colloques Internationaux du CNRS 291:271-282

DeNiro MJ, Epstein S (1977) Mechanism of carbon isotope fractionation associated with lipid synthesis. Science 197:261-263

Gearing JN, Gearing PJ, Rudnick DT, Requejo AG, Hutchins MJ (1984) Isotopic variability of organic carbon in a phytoplankton-based temperate estuary. Geochim Cosmochim Acta 48:1089-1098.

Gili JM and Coma R (1998) Benthic suspension feeders: their paramount role in littoral marine food webs. Trends Ecol Evol 13:316-321

Hedges JI, Mann DC (1979) The lignin geochemistry of marine sediments from the southern Washington coast. Geochim Cosmochim Acta 43:1809-1818

Iken K, Brey T, Wand U, Voight J, Junghans P (2001) Food web structure of the benthic community at the Porcupine Abyssal Plain (NE Atlantic): a stable isotope analysis. Prog Oceanogr 50:383-405

Jamieson GS, Chew L (2002) Hexactinellid sponge reefs: Areas of interest as marine protected areas in the north and central coast areas. Can Sci Adv Secretariat. Department of Fishers and Oceans p1-78

Johannessen SC, Masson D, Macdonald RW (2005) Distribution and Cycling of Suspended particles inferred from transmissivity in the Strait of Georgia, Haro Strait and Juan de Fuca Strait. Atmos-Ocean 44:17-27

Kaehler S, Pakhomov EA, McQuaid CD (2000) Trophic structure of the marine food web at the Prince Edward Islands (Southern Ocean) determined by $\delta^{13}C$ and $\delta^{15}N$ analysis. Mar Ecol Prog Ser 208: 13-20

Kay BH (1989) Pollutants in British Columbia's marine environment: a status report. SOE Rep. 89-1, 59pp.

LeBlond PH, Ma H, Doherty F, Pond S (1991) Deep and intermediate water replacement in the Strait of Georgia. Atmos-Ocean 29:288-312

Leys SP, Wilson K, Holeton C, Reiswig HM, Austin WC, Tunnicliffe V (2004) Patterns of glass sponge (Porifera, Hexactinellida) distribution in coastal waters of British Columbia Canada. Mar Ecol Prog Ser 283:133-149

Macdonald RW, Macdonald DM, O'Brien MC, Gobeil C (1991) Accumulation of heavy metals (Pb, Zn, Cu, Cd), carbon and nitrogen in sediments from Strait of Georgia. Mar Chem 34:109-135

Macdonald RW, Johannessen SC, Gobeil C, Wright C, Burd B, Van Roodselaar A, Pedersen TF (2008) Sediment redox tracers in Strait of Georgia

sediments – can they inform us of the loadings of organic carbon from municipal wastewater? Mar Environ Res 66:87-100

McConnaughey T, McRoy CP (1979) Food-web structure and the fractionation of carbon isotopes in the Bering Sea. Mar Biol 53:257-262

Minagawa M, Wada E (1984) Stepwise enrichment of ^{15}N along food chains: Further evidence and the relation between $^{\delta 15}N$ and animal age. Geochim Cosmochim Acta 48:1135-1140

Peterson BJ, Fry B (1987) Stable isotopes in ecosystem studies. Annu Rev Ecol Syst 18:293-320

Pile AJ, Young CM (2006) The natural diet of a hexactinellid sponge: benthic-pelagic coupling in a deep-sea microbial food web. Deep-Sea Res Part I 53:1148-1156

Post DM, Layman CA, Arrington DA, Takimoto G, Quattrochi J, Montana CG (2007) Getting to the fat of the matter: models, methods and assumptions for dealing with lipids in stable isotope analyses. Oecologia 152:179-189

Rau GH, Takahashi T, Des Marais DJ (1989) Latitudinal variation in plankton $\delta^{13}C$: implication for CO_2 and productivity in past oceans. Nature 341:516-518

Reiswig HM (1990) In situ feeding in two shallow-water Hexactinellid sponges. In: Rutzler K (ed) New perspectives in sponge biology. International Conference on the Biology of Sponges, Smithsonian Institution Press

Reiswig HM (2002) Family Aphrocallistidae Gray, 1867. In: Hooper JNA, van Soest RWM (eds) Systema Porifera: A guide to the classification of sponges, Vol 2, Plenum, New York

Ribes M, Coma R, Gili JM (1998) Seasonal variation of in situ feeding rates by the temperate ascidian *Halocynthia papillosa.* Mar Ecol Prog Ser 175:201-213

Ribes M, Coma R, Gili JM (1999) Natural diet and grazing rate of the temperate sponge *Dysidea avara* (Demospongiae, Dendroceratida) throughout an annual cycle. Mar Ecol Prog Ser 176:179-190

Risk MJ, Sammarco PW, Schwarcz HP (1994) Cross-continental shelf trends in $\delta^{13}C$ in coral on the Great Barrier Reef. Mar Ecol Prog Ser 106:121-130

Slattery M, McClintock JB, Bowser SS (1997) Deposit feeding: a novel method of nutrition in the Antarctic colonial soft coral *Germesia antarctica*. Mar Ecol Prog Ser 149:299-304

Thomas CA, Bendell-Young LI (1999) The significance of diagenesis versus riverine input in contributing to the sediment geochemical matrix of iron and manganese in an intertidal region. Est Coast Shelf Sci 48:635-647

Thomson RE (1981) Oceanography of the British Columbia coast. Can. Spec. Publ. Fish. Aquat. Sci. 56 291pp. Dep. Of Fish. And Oceans. Ottawa, Ont. Canada.

Thomson RE, Mihaly SF, Kulikov EA (2007) Estuarine versus transient flow regimes in Juan de Fuca Strait. J Geophys Res 112:1-25

Thurber AR (2007) Diets of Antarctic sponges: links between the pelagic microbial loop and benthic metazoan food web. Mar Ecol Prog Ser 351:77-89

Vacelet J, Boury-Esnault N, Harmelin JG (1994) Hexactinellid cave, a unique deep-sea habitat in the scuba zone. Deep-Sea Res Part I 41:965-973

Van Dover CL, Grassle JF, Fry B, Garritt RH, Starczak VR (1992) Stable isotope evidence for entry of sewage-derived organic material into a deep-sea food web. Nature 360:153-156

Waldichuk M (1983) Pollution in the Strait of Georgia: a review. Can J Fish Aquat Sci 40:1142-1167

Wildish D, Kristmanson D (1997) Benthic suspension feeders and flow. Cambridge University Press, Cambridge 409pp

Wotton RS (1994) The biology of particles in aquatic systems. 2nd ed. CRC Press, Boca Raton, 325 pp

Yahel G, Eerkes-Medrano DI, Leys SP (2006) Size independent selective filtration of ultraplankton by hexactinellid glass sponges. Aquat Microb Ecol 45:181-194

Yahel G, Whitney F, Reiswig HM, Eerkes-Medrano DI, Leys SP (2007) In situ feeding and metabolism of glass sponges (Hexactinellida, Porifera) studied in a deep temperate fjord with a remotely operated submersible. Limnol Oceanogr 52:428-440

Yunker MB, Macdonald RW, Goyette D, Paton DW, Fowler BR, Sullivan D, Boyd J (1999) Natural and anthropogenic inputs of hydrocarbons to the Strait of Georgia. Sci Total Environ 225:181-209

Table 4-1. Locations and dates of glass sponge sampling for isotope analysis. Depth (m) is the average depth sponges were sampled at with SD in parentheses. Glass sponges are constrained to a small band of depths at each location hence the limited variability at each location. Distance represents the distance (m) separating the two samples furthest from each other within a study location.

Location	Date	Latitude	Longitude	Depth (SD)	Distance
SOG					
Fraser Reef	Oct 2007	49°9.485'N	123°23.081'W	167 (2)	250
Galiano Reef	Oct 2007	48°54.477'N	123°19.168'W	85 (9)	510
Fraser Reef	Oct 2009	49°9.485'N	123°23.081'W	167 (3)	294
Galiano Reef	Oct 2009	48°54.477'N	123°19.168'W	90 (3)	127
Howe Reef	Oct 2009	49°19.901'N	123°17.647'W	72 (9)	344
Non-SOG					
Barkley Sound	Jun 2008	48°54.262'N	125°2.637'W	152 (11)	821
Washington Coast	Jul 2009	48°22.676'N	125°3.056'W	135 (6)	239

Table 4-2. Stable isotope composition ($\delta^{13}C$ and $\delta^{15}N$) of *A. vastus.* Sponge samples (n=46) came from locations in Fig. 4-1 and sampling was done over the course of 3 years (2007 to 2009). Sponges from Fraser and Galiano reef were sampled in two different years (2007, 2009). Samples from non-reef (Non-Strait of Georgia) populations came from fjord wall populations at Barkley Sound and isolated individuals found off the coast of Washington. POM filtered from near-bottom waters at Howe, Fraser and Galiano reefs was also sampled (n=28) in 2009. $\delta^{13}C$ and $\delta^{15}N$ values are given in ‰.

		$\delta^{13}C$		$\delta^{15}N$		C:N Ratio		
Location	Type	Mean (SD)	Range	Mean (SD)	Range	Mean (SD)	Range	N
Non-Strait of Georgia								
2008								
Barkley Sound	Sponge	-19.7 (0.1)	-19.8, -19.5	16.1 (0.4)	15.5, 16.4	4.7 (0.1)	4.5, 4.8	4
Washington Coast	Sponge	-19.8 (0.3)	-20.1, -19.5	16.8 (0.7)	16.0, 17.5	4.7 (0.4)	4.5, 5.0	2
Strait of Georgia								
2007								
Fraser Reef	Sponge	-21.2 (0.1)	-21.3, -21.1	15.0 (0.3)	14.6, 15.4	4.8 (0.2)	4.7, 5.0	5
Galiano Reef	Sponge	-19.8 (0.2)	-20.0, -19.5	14.7 (0.3)	14.4, 15.0	4.6 (0.2)	4.3, 4.8	5
2009								
Howe Reef	Sponge	-20.3 (0.2)	-20.7, -20.1	15.2 (0.5)	14.5, 16.1	4.8 (0.2)	4.4. 5.2	10
Fraser Reef	Sponge	-20.3 (0.1)	-20.4, -20.1	14.7 (0.3)	14.4, 15.2	4.8 (0.3)	4.3, 5.3	10
Galiano Reef	Sponge	-19.5 (0.1)	-19.8, -19.4	17.0 (0.3)	16.6, 17.5	4.8 (0.2)	4.4, 5.0	10
Howe Reef	POM	-23.5 (0.7)	-24.9, -22.7	10.2 (1.0)	8.7, 12.0	6.4 (0.8)	5.1, 7.5	10
Fraser Reef	POM	-23.8 (1.1)	-25.2, -22.6	9.6 (2.1)	5.3, 11.6	6.7 (1.1)	5.7, 9.2	9
Galiano Reef	POM	-23.1 (0.7)	-24.5, -22.5	8.5 (1.0)	7.2, 10.3	6.2 (0.4)	5.4, 6.8	9

Figure 4-1. Sampling locations along the coast of British Columbia and Washington. *A. vastus* was sampled at 3 glass sponge reefs in the Strait of Georgia: (*H*) Howe reef, (*F*) Fraser reef, and (*G*) Galiano reef as well as in 2 non-reef populations: (*B*) Barkley Sound, Vancouver Island, British Columbia and (*W*) Washington Coast - Olympic Coast National Marine Sanctuary.

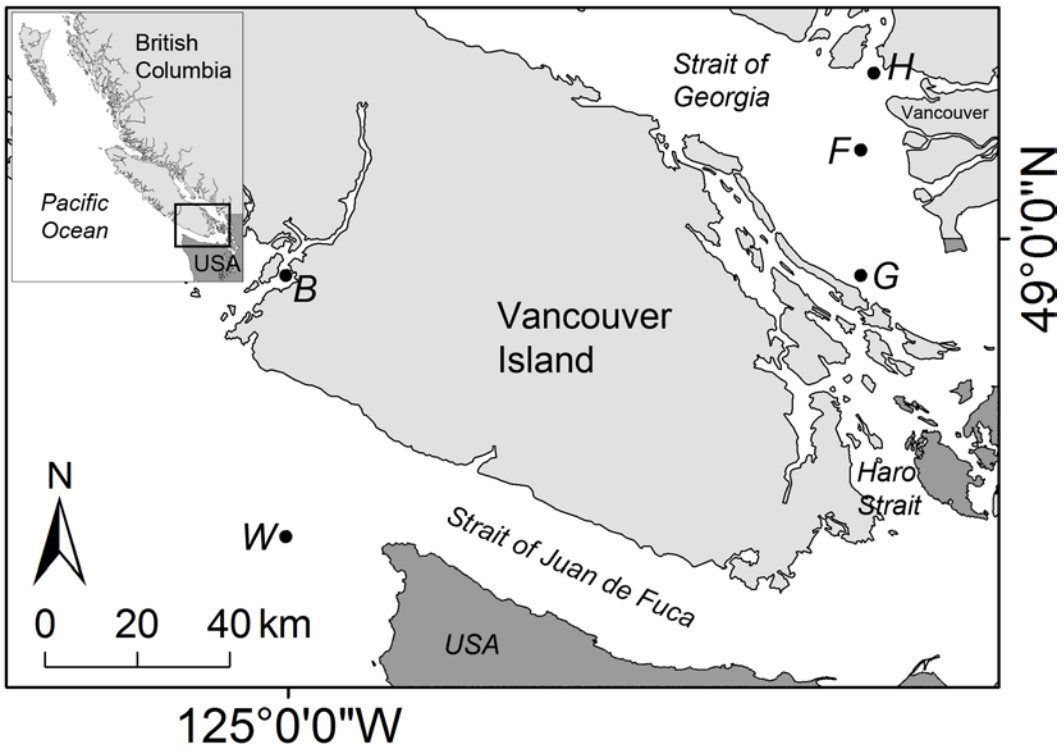
British
Columbia
Pacific
Ocean
USA
B
Strait of
Georgia
H
Vancouver
F
G
Vancouver
Island
Haro
Strait
N
W
Strait of Juan de Fuca
0 20 40 km
USA
125°0'0"W
49°0'0"N

Figure 4-1

Figure 4-2. $\delta^{13}C$ and $\delta^{15}N$ of glass sponge tissue (hollow boxes) and POM (solid boxes) from all sample sites in and out of the SOG. Letters and sampling years represent locations in Fig. 4-1. (A) POM samples from 2009 show ~2 trophic levels within POM found in near bottom waters at the 3 reefs in the Strait of Georgia. Sponges at Howe and Fraser reefs show stepwise enrichment of $\delta^{15}N$ of 1 trophic level above the POM. However, sponges from Galiano reef show stepwise enrichment of $\delta^{15}N$ of 2 trophic levels above the POM. (B) Differences in $\delta^{13}C$ and $\delta^{15}N$ from sponges tissue suggests (1) the diet of the glass sponges is different between reefs in the Strait of Georgia and (2) sponges at Fraser and Galiano reef were feeding differently between years (2007 to 2009). Boxes are means with ±1 SD and sample sizes are given in table 4-1.

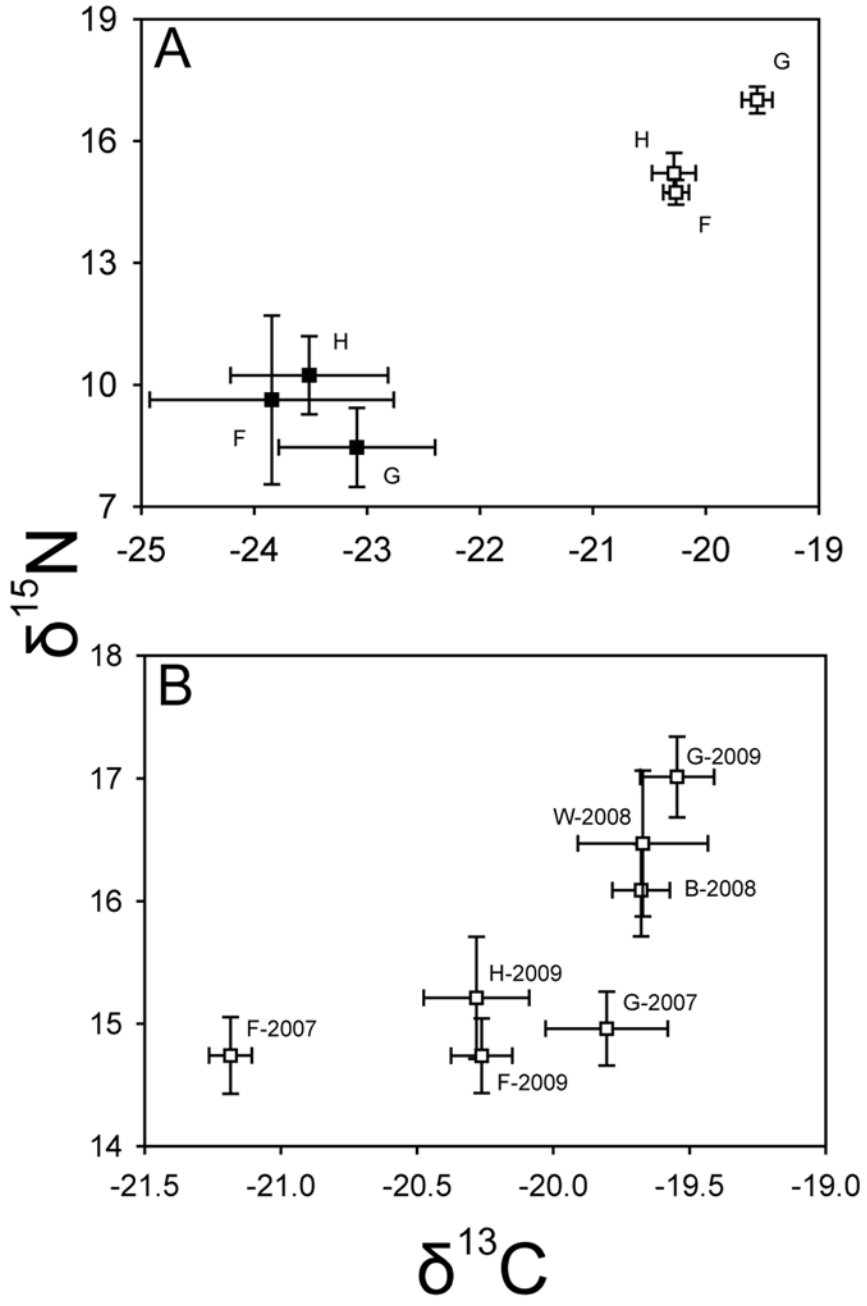
A
B
G
H
F
H
F
G
G-2009
W-2008
B-2008
H-2009
G-2007
F-2007
F-2009
19
16
13
10
7
-25
-24
-23
-22
-21
-20
-19
18
17
16
15
14
-21.5
-21.0
-20.5
-20.0
-19.5
-19.0
δ15N
δ13C

Figure 4-2

Figure 4-3. Mean differences in $\delta^{13}C$ and $\delta^{15}N$ values in populations of *A. vastus*. (A) $\delta^{13}C$ values indicate sponges at Galiano reef have carbon signatures more similar to non-reef populations than sponges at either Howe and Fraser reefs. (B) $\delta^{15}N$ values indicate that sponges from non-reef populations and from Galiano reef (2009) had significantly enriched nitrogen signatures relative to sponges at Howe and Fraser reefs and sponges sampled from Galiano reef in 2007. Data are presented in Mean ± 1 SD and sample sizes are in table 4-1. Horizontal bars indicate statistically indistinguishable groups (ANOVA with Tukey post hoc tests, $p < 0.001$).

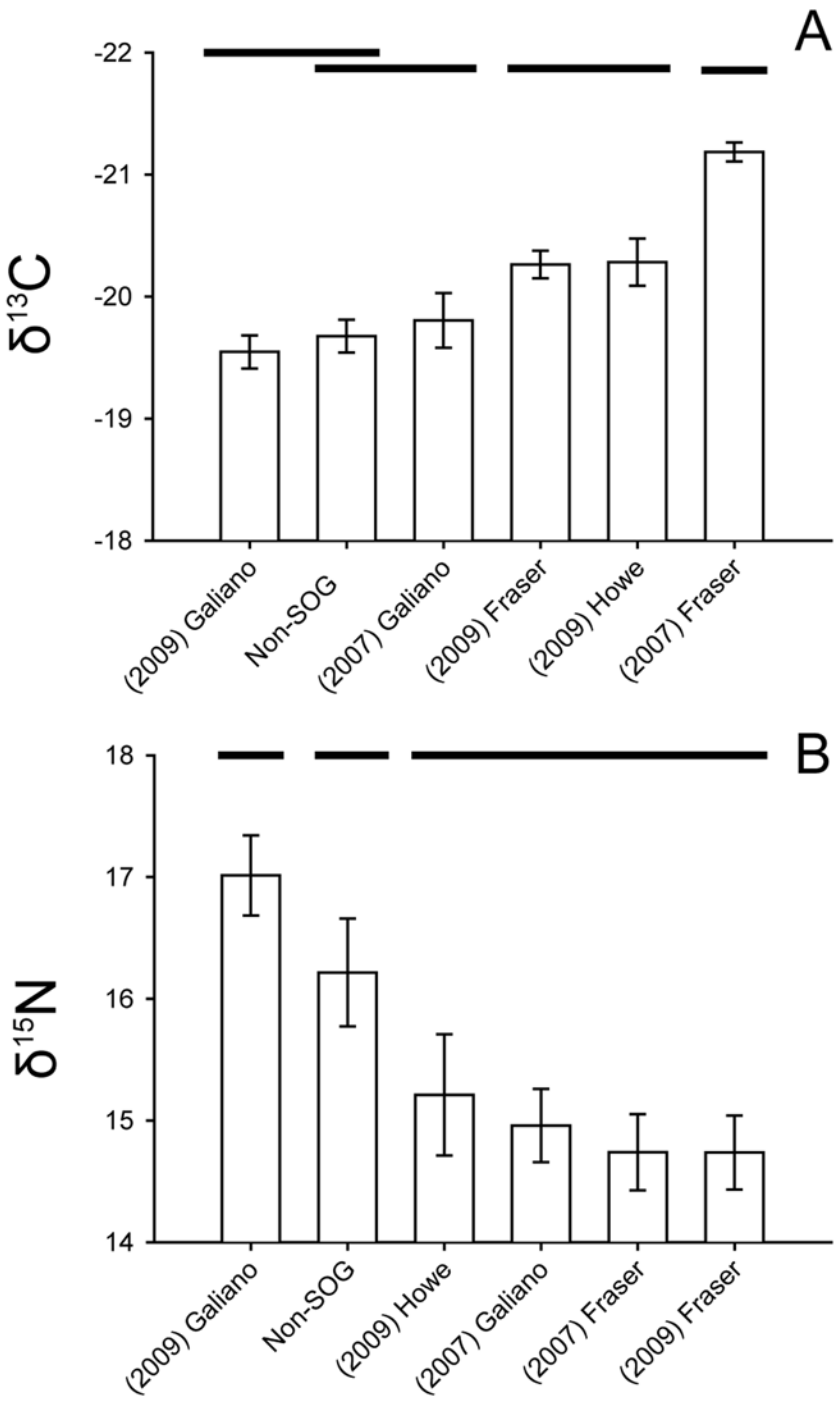
A
-22
-21
-20
-19
-18
δ13C
(2009) Galiano
Non-SOG
(2007) Galiano
(2009) Fraser
(2009) Howe
(2007) Fraser
B
18
17
16
15
14
δ15N
(2009) Galiano
Non-SOG
(2009) Howe
(2007) Galiano
(2007) Fraser
(2009) Fraser

Figure 4-3

Chapter 5

A General Discussion

5.0 Overview

Glass sponges are one of the oldest known metazoan lineages with extant representatives. Hexactine spicules found in the fossil record show the existence of hexactinellids during the Neoproterozoic (~543-549 mya, Gehling & Rigby 1996; Brasier et al. 1997) and molecular evidence suggests siliceous sponges (demosponges and hexactinellids) were the earliest diverging animals (Sperling et al. 2009; Philippe et al. 2009). Temporal persistence could mean glass sponges are specialized to a narrow ecological niche and have remained relatively unchanged since their first appearance as one of the earliest derived branches in the metazoan tree of life (Dohrmann et al. 2008; Pick et al. 2010). Glass sponges have syncytial tissue and lack both muscles and nerves in a simple body plan designed to pump and filter water. The high abundance and density of hexactinellids in the Strait of Georgia (SOG) suggest the sponge populations are supported by optimal conditions found at the reef locations, making the sponge reefs ideal systems to further our understanding of glass sponge ecology.

Several patterns of the glass sponges were quantified in my thesis and represent a biological baseline of 3 reefs in the SOG. Chapter 2 revealed the large and small scale patterns of distributions and community structure of glass sponges and their associated assemblage of animals. Chapter 3 focused on silica, the main component of glass sponge biomass and therefore an entire reef, and suggests glass sponge reefs are a substantial silica sink in the north-eastern Pacific Ocean. Chapter 4 revealed distinct spatial patterns in feeding of *A. vastus*, a reflection of the input from their surrounding environments. Based on these patterns, I discuss several new questions as areas of future research on glass sponges and glass sponge reefs.

5.1 Abiotic factors affecting glass sponges

5.1.1 The effects of flow on the range limits of glass sponges

Glass sponges are common in deep water (300-600 m, down to 6200 m, Tabachnick 1994; Leys et al. 2007) throughout the world's oceans, but there are only 4 regions (Table 1-1, Chapter 1), where glass sponges not only flourish, but are found in relatively shallow waters (20-200 m). The high density and shallow water nature of these populations suggests depth does not directly influence where glass sponges may exist but other abiotic factors will control their range limits (Leys et al. 2004).

In Chapter 2, I suggested that patterns of water flow are a strong predictor of where glass sponge reefs can establish. The hydrodynamics of water flow, acceleration and displacement are both essential and harmful for organisms found in shallow waters (Vogel 1981; Denny 1988). The sponge body plan is optimized to pump water for both feeding and waste excretion. The lower limits of flow velocities would partially determine the energetic requirements of the glass sponges because sufficient flow will determine the food availability and the efficiency of the removal of wastes expelled by the sponge. However, along the west coast of British Columbia, where we find extremely dense populations of glass sponges in uncharacteristically shallow waters (Leys et al. 2004), is there an upper threshold to the hydrodynamic processes they can experience and would this determine their distributions?

In the ocean, pressure generated by surface waves propagate and diminish down the water column (Denny 1988). For shallow water suspension feeders such as reef corals, hydrodynamic processes will break and dislodge larger size classes during episodic storm events (Tunnicliffe 1982; Madin 2005; Madin & Connolly 2006). Similar patterns have not been addressed for glass sponges as they are normally considered deep sea fauna. As hexactinellids are made of biogenic silica, a naturally brittle substance in nature and are found in unusually shallow waters along the coast of British Columbia (<50m), this may expose them to the hydrodynamic processes of shallower waters. Breakage or dislodgement of

glass sponges found in shallow waters may occur during storm events when the forces created by maximum flow reaches a critical threshold that exceeds the structural tolerance of the glass sponge body plan.

5.1.2. Morphological adaptations to hydrodynamic processes

Within a range of tolerable hydrodynamic forces, glass sponges may have morphological adaptations to a life in moving water. For example, demosponges show considerable plastic responses to different flow conditions (Bidder 1923; Warburton 1960; Palumbi 1986). Under a gradient of flow conditions, thin and tall morphologies predominate at the slower velocities and wide and short moprhologies are found in faster moving water (Kaandorp 1999; Bell & Barnes 2000). Similarly, *A. vastus* and *H. calyx* are found in a range of morphologies (Chu pers. obs.) yet to establish a similar link between flow and form, hydrodynamic patterns and flow velocities must be measured and correlated with measurements of morphology (morphometrics). I predict that the morphological adaptations of dictyonine sponges are similar to those of demosponges in that, within the tolerable range limits set by flow velocities, the continuum of glass sponge morphotypes will reflect the gradient of flow.

5.1.3 Structural adaptations to hydrodynamic processes

In other marine organisms, structural design falls into two main categories, those designed to be rigid, such as invertebrates with structures made from calcium carbonate ($CaCO_3$) and those designed to promote flexibility, such as the stipes of some seaweeds (Denny 1988). Although they are constrained to a glass body, *A. vastus* would need to be structurally adapted to survive in the potentially hydrodynamically active areas of shallower waters similar to other marine organisms found in wave swept or high flow areas. How are glass sponges structurally adapted to varying flow patterns?

As an aside to my thesis work, I began to address this question by examining the mechanical properties of the dictyonine skeleton of *A. vastus* (see Appendix 2 for methods). Empirical measurements of mechanical properties

require application of engineering theory because the stiffness of a material is measured by the Young's modulus (E). High Young's moduli represent stiff materials (e.g. E = 1.9 to 3.8 x 10^{10} N m^{-2} for tropical coral $CaCO_3$ skeletons, Chamberlain 1978), while flexible materials have values that are several magnitudes lower (e.g. E = 1.7 to 3.8 x 10^{7} N m^{-2} for kelp, Johnson & Koehl 1994). The exponent is the important indicator of relative stiffness (or flexibility) between materials. I predicted the individual spicules of *A. vastus* would be stiff and similar to the reported values of other glass sponges (Levi et al. 1989; Sarikaya et al. 2001; Woesz et al. 2006) but the fused dictyonine skeleton of *A. vastus* would likely reduce stiffness, in other words greatly increase flexibility as an adaptation to shallow water processes.

By using engineering theory of static beam bending (Denny 1988), I discovered that the individual spicules of *A. vastus* were indeed stiff, E = 2.68 x 10^{11} ± 2.35 x 10^{11} N m^{-2} (mean ± sd, n=12). However, the dictyonine skeleton was more flexible. Young's modulus values for the dictyonine skeleton were between 2.76 x 10^{6} to 10.04 x 10^{6} N m^{-2} which is a 10,000-fold increase in flexibility over the individual stiff spicules (Table A2-2 in Appendix 2). Interestingly, the presence of tissue does not affect the stiffness of the skeleton but rehydrating the skeleton significantly increased stiffness compared to the dried samples (Table A202 inAppendix, ANOVA, $F_{3,36} = 52.80$, $p < 0.0001$). The tissue is proportionally only 20.7% of *A. vastus*' biomass and, unsurprisingly, has little effect on the structural properties of a sponge that is 80% inorganic (silica). Although the dictyonine skeleton is 62.7% of *A. vastus*' biomass, 17.7% of the biomass consists of loose spicules imbedded within the tissue (Chapter 3). In demosponges, loose spicules imbedded in the tissue increases structural stiffness of the sponge body plan (Koehl 1982). However, this was not the case for *A. vastus* and thus loose spicules likely have another role such as a deterrent to predators as suggested in Chapter 2.

In comparison to other naturally occurring biological materials, the dictyonine skeleton of *A. vastus* can be considered to be similar in stiffness to some biological rubbers (Table 5-1). The dictyonine skeleton is most likely

optimally designed to maximize the use of a highly limited building material in the marine environment (Si) but also minimize the environmental effects of being exposed to hydrodynamic forces found in shallow waters.

5.1.4 Thermal tolerance and the effects of climate change on sponge distributions

The narrow operational range (7-12°C) of the action potential that controls the pumping in the glass sponge, *Rhabdocalyptus dawsoni*, (Leys & Meech 2006) indicates glass sponges are markedly stenothermal (narrow thermal tolerance). At temperatures below ~7°C, sponges are unable to resume arrested pumping and at temperatures above ~12°C, sponges are unable to arrest their pumping. The inability to control water pumping behaviour would incur energetic costs and increase the susceptibility of the water canal system to clogging from sediments. How would ocean warming from climate change affect the relatively shallow glass sponge populations found in the SOG?

The upper 150 m in the SOG has experienced ~1°C rise in average water temperature within the last 20 years (Masson & Cummins 2007). Warming in the SOG is only a small part of the global trend of rising surface temperatures and is predicted to rise an additional 1-5° C by 2099 (IPCC 2007). If water temperature continually rises, we may see a decline in the live sponge populations in the shallower reefs (79 m at Howe reef, 90 m at Galiano reef) where surface warming has the strongest effect, compared to the deeper reefs (169 m at Fraser reef) which exist below the shallow sills (100 m) splitting the surface with deeper water flow patterns in the SOG (Masson 2002). However, deeper reefs are also susceptible to intermittent fluctuations in temperature from strong El Ninõ events where warm offshore waters, travelling up the North American coast, enter the deep-water renewal of the SOG (LeBlond et al. 1991) and cause deep water warming in the SOG (Masson 2002). Although individual *A. vastus* are documented to show normal pumping and arresting activity at temperatures up to 19°C (Tompkins-Macdonald & Leys, 2008), both chronic and stochastic warming events may diminish the shallower glass sponge populations in the SOG and select towards thermal tolerant glass sponges.

5.2 Species interactions with glass sponges

Species interactions within a system will structure the community of animals and can be categorized into the direct effects of consumption and competition (Hutchinson 1959; Paine 1980) or the multitude of indirect effects such as shifts incurred from changes in feeding, behaviour, and the environment (Menge 1995). In chapter 2, I established the community of animals within a glass sponge reef and the positive and negative relationships they have with the glass sponges. However, the types of interactions occurring within the community of animals of a glass sponge reef have yet to be explored.

As a first step in this direction, I have illustrated a conceptual food web based on all known direct interactions within a glass sponge reef community (Fig. 5-1). This conceptual food web currently consists of 4 trophic levels where the lowest 2 levels are found within the POM. *A. vastus* is a low order consumer on the POM and *P. lentiginosa* represents a predator on *A. vastus*. Considering the diversity of animals I identified within the reefs, the glass sponges are probably not the only direct consumers of the POM and my conceptual food web probably only identifies a subweb (Paine 1966) within the entire reef community. A stable isotope study expanded to include the diversity of animals found within the glass sponges (Chapter 2) would allow us to trace the flow of energy between all residents in a glass sponge reef.

P. lentiginosa (Chapter 2) is currently known as the top predator in the glass sponge reef system yet, as suggested in chapter 2, the sea stars *Pteraster tesselatus* and *Mediaster* sp. may also be predators of the glass sponges because they are commonly found within the reefs, in non-reef populations, and *P. tesselatus* has been documented to feed on the boot sponge *Rhabdocalyptus dawsoni* (Leys et al. 2007). The proportion of observed *P. lentiginosa* (Appendix 1), *P. tesselatus* and *Mediaster* (Chapter 2) compared to the sheer abundance of glass sponge biomass suggests predation is unlikely to directly contribute to structuring the glass sponge abundance as it does in Antarctic glass sponge populations (Dayton et al. 1974). However, another known direct interaction with

glass sponges involves the demosponge *Desmacella austini* which exists as an epizoic growth on living *H. calyx* (Lehnert et al. 2005). *D. austini* may also encrust on *A. vastus* but would require sampling for spicule identifications. In the reefs, *D. austini* appears to kill the live glass sponges by encrusting over the dictyonine skeletons of their host (Fig. 5-2). The extent of the *D. austini* population in glass sponge reefs has not been measured but in comparison to *P. lentiginosa*, *D. austini* is present at Howe, Fraser and Galiano reefs (Chu pers. obs). If the rate of *D. austini* growth exceeds that of the glass sponges at a reef, this could severely diminish the glass sponge populations.

Nevertheless, based on the diverse assemblage of animals found in a reef, the key species interactions with glass sponges in a reef are probably non-consumptive (indirect), and therefore, the control on glass sponge populations is not predator induced. I suggest the network of species interactions within a reef community is as follows: The majority of species interactions with glass sponges are facilitative (indirect, Bruno et al. 2003), where animals are provided with refuge, habitat, or a hard substratum for settlement (Leys et al. 2007). The species interactions within the associated community of animals (not including the glass sponges) are direct forms of predation and competition. Although these interactions exist in non-reef populations of glass sponges, their frequency is amplified due to the localized concentration of animals at a reef and thus glass sponges can be thought of as the facilitators of direct interactions within a reef. As such, the detritus base of the glass sponge food web is more than likely supporting the other low order consumers inhabiting a reef.

5.3 Glass sponge reefs as a system for conservation

5.3.1 Threats from fisheries and glass sponge reefs as MPAs

The ecological importance of deep sea communities has increased interest in their conservation as they are threatened by fishing practices (Watling & Norse 1998; Thrush & Dayton 2002). Mobile fishing equipment, such as otter trawls (Engel & Kvitek 1998), will indiscriminately scour large expanses of the seafloor

to catch commercial species while effectively tearing, crushing, and upturning all other benthic life.

Cold water coral beds have been the primary focus of deep sea conservation research (Freiwald et al. 2004) because they form habitats for commercial fish and non-commercial species and their prey. The benthic complexity created by cold water corals also increases the local abundance of the commercially important species (Husebo et al. 2002; Kriegerand & Wing 2002). The extreme longevity and slow growing nature of corals (Roark et al. 2009) results in the inability of deep sea coral beds to recover from the severe disturbance (Auster & Langtom 1999; Roberts & Hirshfield 2004). Considering that glass sponges share similar natural history characteristics with deep sea corals and that glass sponge reefs are also benthic habitats for other species (Chapter 2), reefs are just as susceptible to benthic disturbance and are worthy of conservation and protection.

Physical destruction of biogenic structures on the seafloor removes the positive associations between associated animals and their benthic habitats (Watling & Norse 1998; Thrush & Dayton 2002). Such would be the case with the positive relationships I revealed between the glass sponges and their associated fauna in reef communities. Shrimp otter trawls are active in the SOG (http://www.dfo-mpo.gc.ca/science/publications/uww-msm/articles/shrimp-crevette-eng.htm) and, although there is no direct evidence of trawling activity at the glass sponge reefs, I have observed mechanically broken glass sponges at Howe reef (Fig 5-3).

In July 2008, I participated in a Canadian Healthy Oceans Network (CHONe, http://www.marinebiodiversity.ca/CHONe) expedition to explore Learmonth Bank, Dixon Entrance (Fig. 5.4) which is an area of heavy trawling activity (J. Boutillier, Department of Fisheries and Oceans, pers. comm.). The objective of this cruise was to document the diversity of biogenic structuring organisms such as deep water corals and glass sponges. Several discoveries relating to glass sponges were made during this cruise. We discovered dense, mixed populations of lyssacine and dictyonine glass sponges (Fig. 5.5A) at the

shallowest depths we explored (~150 m) in densities as high as 36 individuals per 10 m^2, over 615 m^2 of scouted area but no reefs were discovered. The majority of lyssacine sponges were asexually budding and formed double-oscula morphologies (Fig. 5.5B). Individuals of the dictyonine sponge, *Heterochone calyx*, had tissue extensions (Fig. 5.5C) formed at their base that appeared to form new oscula (Fig. 5.5D) similar to the budding mechanism I described for *Aphrocallistes vastus* (Chapter 2). However, the most noteworthy discovery may have been the sponge graveyard (Fig 5.6) where the accumulation of dead glass sponges created a ridge 7 m high at the base of Learmonth Bank at a depth of 344 m. The southern portions of Learmonth Bank are heavily trawled and bycatch material likely gets transported by bottom currents and trapped against the bank. Because of the natural long term persistence of their skeletons (Chapter 3), it is reasonable to assume such severe mechanical damage to glass sponges is due to bottom disturbances from fishing activity.

My observations of broken glass sponge debris in reefs and non-reef locations suggest glass sponges are actively destroyed by disturbances of the seafloor. Glass sponge reefs do not have federal conservation status, yet there is current interest in establishing the Hecate Strait reefs as Marine Protected Areas (MPA, Jamieson and Chew 2002; http://www.dfo-mpo.gc.ca/media/back-fiche/2010/hq-ac31b-eng.htm). An MPA is defined as 'an area of inter-tidal or sub-tidal terrain, together with its overlying water and associated flora, fauna, historical, or cultural features, which has been reserved by law or other effective means to protect part or all of the enclosed environment' (Kelleher & Kenchington 1992) with direct goals of conserving commercial and non-commercial fisheries and their habitats (Juanes 1994). However, the implementation of MPAs often bypasses the need to first firmly empirically establish the ecological and socio-economical patterns underlying the need for conservation science on the proposed system (Agardy et al. 2003).

A past study highlighted the important increases in biodiversity at the reefs in Hecate Strait and provided the initial insight into the functional importance of the glass sponge reef system (Cook 2005). Unfortunately this

study did not establish a biological baseline of the glass sponges that would allow monitoring of temporal changes and used only video transects without accounting for the spatial structure of the glass sponges. This was largely in part to the difficulties associated with the large reef size, remote location and challenges of ROV research at the reefs in Hecate Strait. The reefs in the SOG represent much smaller, accessible and tractable research systems to allow the ecology of glass sponge reefs to be thoroughly examined. The increased abundance of crustaceans and fish within the glass sponges in the SOG include several commercially caught species such as flatfish, rockfish (*Sebastes* spp.), pollock (*Theragra chalcogramma*), the Dungeness crab (*Cancer magister*) and the spot prawn (*Pandalus platyceros*). Although they cover much smaller areas in comparison to the reefs in Hecate Strait, the glass sponge reefs in the SOG are just as susceptible to fishing activity and should also be in consideration for federal conservation and protection status.

5.3.2 Temporal monitoring of the Howe, Fraser and Galiano reefs

One of the most important achievements of my thesis is that my detailed mapping establishes biological baselines for the glass sponge communities at the Howe, Fraser and Galiano reefs and will allow changes in the reef biology to be revealed from future studies. Although the logistical difficulties of researching this deep water system remain, technological advances during the course of my thesis will enable expansion on my work. The recent completion (2008) of the Victoria Experimental Network Under the Sea (VENUS; http://www.venus.uvic.ca) provides *in situ* instrumentation to monitor several environmental variables in the SOG. During the course of my thesis, the implementation of high definition (1080i) video recordings on ROPOS (http://www.ropos.com) increased the resolution and data made available for image analysis. The coupling of these two new technologies with repeated future surveys would establish a timescale to the biological processes in a reef. Future quantified mapping would reveal whether the sponge populations are growing at a reef or in decline giving us an indicator of reef health.

5.4 Concluding Thoughts

The enigmatic nature of glass sponges adds layers of complexity to the glass sponge reef system. By following the research path established by past research on other deep sea communities, the results of my thesis has greatly advanced our knowledge of the glass sponge reefs. I have empirically defined the patterns of community structure of three glass sponge reefs and established a baseline for ecological monitoring. Also, we now have further evidence on the important ecological roles glass sponge reefs have on providing habitat for other animals, new insight into their significance in silica cycling, and their coupling with localized input from the surrounding environments. The remarkable discovery of glass sponge reefs within close proximity to the city of Vancouver represents the wealth of knowledge still to be gained from exploration of the deep ocean.

5.5 Literature Cited

Auster PJ, Langton RW (1999) The effects of fishing on fish habitat. In: Benaka L (ed) Fish habitat: essential fish habitat and rehabilitation. American Fisheries Society, Bethesda, Maryland p 150-187

Barrie JV, Conway KW (1999) Late Quaternary glaciations and postglacial stratigraphy of the northern Pacific margin of Canada. Quat Res 51:113-123

Bell JJ, Barnes DKA (2000) The influences of bathymetry and flow regime upon the morphology of sublittoral sponge communities. J Mar Biol Ass U K 80:707-718

Bidder GG (1923) The relation of the form of a sponge to its currents. Quart J Microsc Sci 67:293-323

Brasier M, Green O, Shields G (1997) Ediacarian sponge spicule clusters from southwestern Mongolia and the origins of the Cambria fauna. Geol 25:303-306

Bruno JF, Stachowicz JJ, Bertness MD (2003) Inclusion of facilitation into ecological theory. Trends Ecol Evol 18:119-125

Chamberlain JA (1978) Mechanical properties of coral skeleton: compressive strength and its adaptive significance. Paleobiology 4:419-435

Cook SE (2005) Ecology of the hexactinellid sponge reefs on the Western Canadian continental shelf. MSc thesis, University of Victoria, Victoria Canada pp127.

Dayton PK, Robilliard, GA, Paine, RT, Dayton LB (1974) Biological accommodation in the benthic community at Mcmurdo Sound, Antarctica. Ecol Monogr 44:105-128

Denny MW (1988) Biology and the mechanics of the wave-swept environment. Princeton University Press, Princeton.

Dohrmann M, Janussen D, Reitner J, Collins AG, Wörheide G (2008) Phylogeny and evolution of glass sponges (Porifera, Hexactinellida). Syst Biol 57:388-405

Engel J, Kvitek R (1998) Effects of otter trawling on a benthic community in Monterey Bay National Marine Sanctuary. Conserv Biol 12:1204-1214

Freiwald A, Fossa JH, Grehan A, Koslow T, Roberts JM (2004) Cold-water coral reefs. UNEP-WCMC, Cambridge UK.

Gehling JG, Rigby JK (1996) Long expected sponges from neoproterozoic Ediacara fauna of South Australia. J Paleontol 70:185-195

Husebo A, Nottestad L, Fossa J, Furevik D, Jorgensen S (2002) Distribution and abundance of fish in deep-sea coral habitats. Hydrobiologia 471:91-99

Hutchinson GE (1959) Homage to Santa Rosalia or why are there so many kinds of animals? Am Nat 93:145-159

IPCC (Intergovernmental Panel on Climate Change) (2007) Climate change 2007: the physical science basis. Contribution of Working Group I to the 4th assessment report of the Intergovernmental Panel on Climate Change. Cambridge University Press, Cambridge

Jamieson GS, Chew L (2002) Hexactinellid sponge reefs: Areas of interest as marine protected areas in the north and central coast areas. Can Sci Adv Secretariat. Department of Fishers and Oceans p1-78

Johnson AS, Koehl MAR (1994) Maintenance of dynamic strain similarity and environmental stress factor in difference flow habitats: thallus allometry and material properties of a giant kelp. J Exp Biol 195:381-410

Juanes F (1994) Mediterranean marine protected areas. Trends Ecol Evol 16:169-170

Kaandorp JA (1999) Morphological analysis of growth forms of branching marine sessile organisms along environmental gradients. Mar Biol 134: 295-306

Kelleher G, Kenchington R. 1992. Guidelines for Establishing Marine Protected Areas. A Marine Conservation and Development Report. IUCN: Gland, Switzerland, 79pp.

Koehl MAR (1982) Mechanical design of spicule-reinforced connective tissue: stiffness. J Exp Biol 98:239-267

Krieger KJ, Wing BL (2002) Megafauna associations with deepwater corals (Primnoa spp.) in the Gulf of Alaska. Hydrobiologia 471:83-90

LeBlond PH, Ma H, Doherty F, Pond S (1991) Deep and intermediate water replacement in the Strait of Georgia. Atmos-Ocean 29:288-312

Lehnert H, Conway KW, Barrie JV, Krautter M (2005) *Desmacella austini* sp. nov from sponge reefs off the Pacific coast of Canada. Contr Zool 74:265-270

Levi C, Barton JL, Guillemet C, Le Bras E, Lehuede P (1989) A remarkably strong natural glassy rod: the anchoring spicule of the *Monorhaphis* sponge. J Mater Sci Lett 8:337-339

Leys SP, Wilson K, Holeton C, Reiswig HM, Austin WC, Tunnicliffe V (2004) Patterns of glass sponge (Porifera, Hexactinellida) distribution in coastal waters of British Columbia Canada. Mar Ecol Prog Ser 283:133-149

Leys SP, Meech RW (2006) Physiology of coordination in sponges. Can J Zool 84:288-306

Leys SP, Mackie GO, Reiswig HM (2007) The biology of glass sponges. Adv Mar Biol 52:1-145

Madin JS (2005) Mechanical limitations of reef corals during hydrodynamic disturbances. Coral Reefs 24:630-635

Maddin JS, Connolly SR (2006) Ecological consequences of major hydrodynamic disturbances on coral reefs. Nature 444:470-480

Masson D (2002) Deep water renewal in the Strait of Georgia. Est Coast Shelf Sci 54:115-126

Masson D, Cummins PF (2007) Temperature trends and interannual variability in the Strait of Georgia, British Columbia. Cont Shelf Res 5:634-649

Menge BA (1995) Indirect effects in marine rocky intertidal interaction webs: patterns and importance. Ecol Monogr 65:21-74

Paine RT (1966) Food web complexity and species diversity. Am Nat 100:65-75

Paine RT (1980) Food webs: linkage, interaction strength and community structure. J Anim Ecol 49: 667-685

Palumbi SR (1986) How body plans limit acclimation: responses of a demosponge to wave force. Ecology (USA) 67:208-214

Philippe H, Derelle R, Lopez P, Pick K, Borchiellini C, Boury-Esnault N, Vacelet J, Deniel Em, Houliston E, Quéinnec E, Da Silva, C, Wincker P, Le Guyader H, Leys S, Jackson DJ, Schreiber F, Erpenbeck D, Morgenstern B, Wörheide G, Manuel M (2009) Phylogenomics revives traditional views on deep animal relationships. 19:706-712

Pick KS, Philippe H, Schreiber F, Erpenbeck D, Jackson DJ, Wrede P, Wiens M, Alié A, Morgenstern B, Manuel M, Wörheide G (2010) Improved phylogenomic taxon sampling noticeably affects non-bilaterian relationships. Molecular biology and evolution *in press*

Roark EB, Guilderson TP, Dunbar RB, Fallon SJ, Mucciarone DA (2009) Extreme longevity in proteinaceous deep-sea corals. PNAS 106:5204-5208

Roberts S, Hirshfield M (2004) Deep-sea corals: out of sight, but no longer out of mind. Front Ecol Environ 2:123-130

Sarikaya M, Fong H, Sunderland N, Flinn BD, Mayer G, Mescher A, Gaino E (2001) Biomimetic model of a sponge-spicular optical fiber – mechanical properties and structure. J Mater Res 16:1420-1428

Sperling EA, Peterson KJ, Pisani D (2009) Phylogenetic-signal dissection of nuclear housekeeping genes supports the paraphyly of sponges and the monophyly of Eumetazoa. Mol Biol Evol 26:2261-2274

Tabachnick, KR (1994) Distribution of recent Hexactinellida. In: van Soest RWM, van Kempen B, Braekman G (eds) Sponges in time and space. Balkema Rotterdam p 225-232

Thrush S, Dayton PK (2002) Disturbance to marine benthic habitats by trawling and dredging: Implications for marine biodiversity. Ann Rev Ecol Syst 33:449–473.

Tompkins-MacDonald GJ, Leys, SP (2008) Glass sponges arrest pumping in response to sediment: implications for the physiology of the hexactinellid conduction system. Mar Biol 154: 973-984

Tunnicliffe V (1982) The effects of wave-induced flow on a reef coral. J Exp Mar Biol Ecol 64:1-10

Vogel S (1981) Life in moving fluids. Princeton University press, Princeton.

Vogel S (2003) Comparative biomechanics life's physical world. Princeton University Press, Princeton.

Wainwright SA, Biggs WD, Currey JD, Gosline JM (1976) Mechanical design in organisms. Princeton University Press, Princeton.

Warburton FE (1960) Influence of currents on form of sponges. Science 132:89

Watling L, Norse EA (1998) Disturbance of the seabed by mobile fishing gear: A comparison to forest clearcutting. Conserv Biol 12:1180-1197

Woesz A, Weaver JC, Kazanci M, Dauphin Y, Aizenberg J, Morse DE, Fratzl P (2006) Micromechanical properties of biological silica in skeletons of deep-sea sponges. J Mat Res 21: 2068-2078

Table 5-1. Stiffness (Young's modulus) of naturally occurring substances in nature. Data are compiled from Wainwright et al. (1976) and Vogel (2003) and references therein.

Material in nature	Young's Modulus ($N\ m^{-2}$)
Slimes	
Sea anemone mesoglea	1.0×10^{3}
Rubbers	
Resilin	1.8×10^{6}
Abductin	4.0×10^{6}
Kelp Stipe	2.0×10^{7}
Fibers	
Collagen	1.0×10^{9}
Wood (Cellulose-oak)	6.4×10^{9}
Arthropod carapace (chitin)	1.2×10^{10}
Crystalline composites	
Bone (human femur)	1.7×10^{10}
Mollusc shell ($CaCO_3$)	5.0×10^{10}
Coral skeleton ($CaCO_3$)	6.0×10^{10}

Figure 5-1. Conceptional foodweb of all known direct species interactions in a glass sponge reef community. The base of the glass sponge foodweb is detrital with stable isotope analysis indicating carbon input from both marine and terrestrial sources. The first order consumers include two levels within the living component of the POM consists of heterotrophic bacteria and protists. Direct consumers of POM in the glass sponge food web are *A. vastus* and *H. calyx*. I consider the epizootic growth of *D. austini* on *H. calyx* as a direct effect, but as *H. calyx* is not eaten, I have indicated this interaction with a dashed arrow. *P. lentiginosa* is the top carnivore in this foodweb as a predator on *A. vastus, H. calyx* and *D. austinni*.

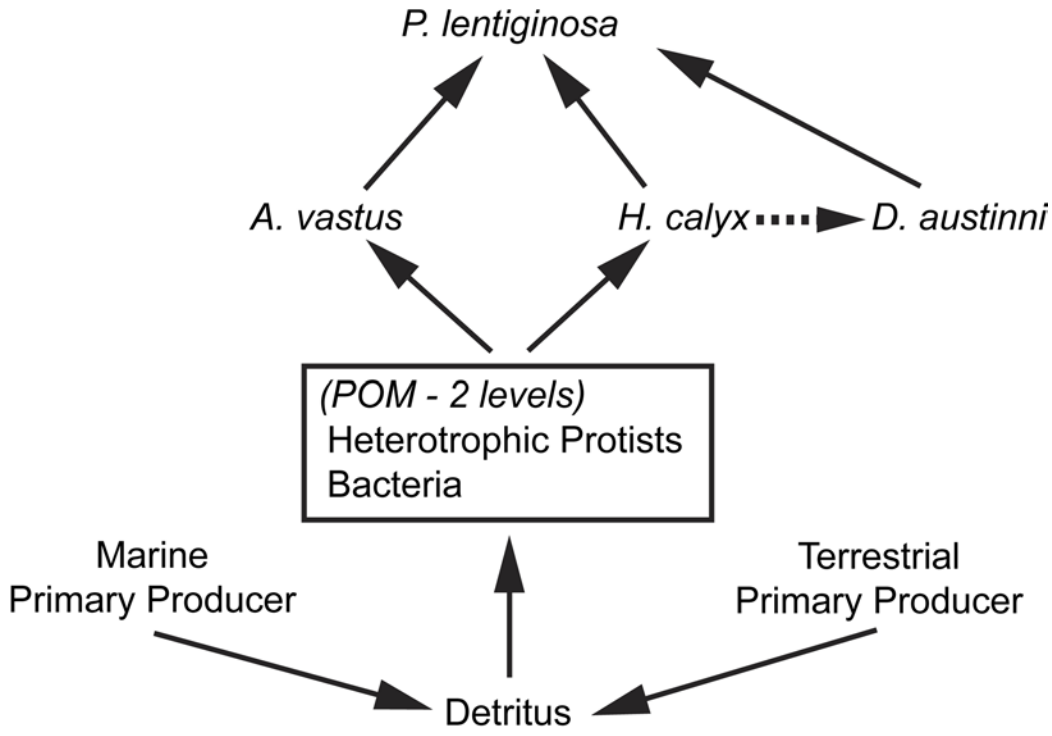
P. lentiginosa
A. vastus
H. calyx
D. austinni
(POM - 2 levels)
Heterotrophic Protists
Bacteria
Marine
Primary Producer
Terrestrial
Primary Producer
Detritus

Figure 5-1

Figure 5-2. The encrusting demosponge *Desmacella austini*. *D. austini* is found in glass sponge reefs as a thin epizoic growth on *Heterochone calyx* (Lehnert et al. 2005) and may also be growing on *Aphrocallistes vastus*. (A) *D. austini* (white colored regions areas) encrusts over the dictyonine skeletons of glass sponges (cream colored regions) (B) A sampled glass sponge encrusted by *D. austini* has the thin coating of spicules from *D. austini* thinly coating the dermal surface of the dictyonine skeleton.

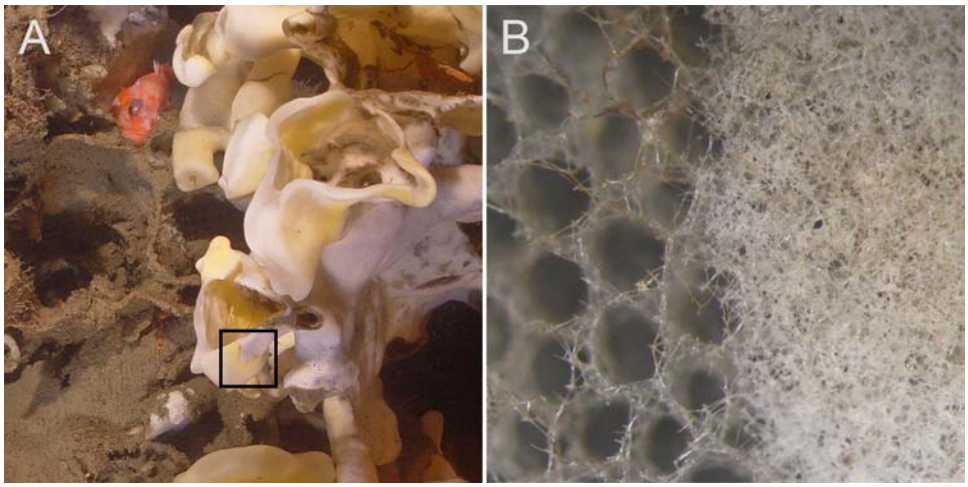

Figure 5-2

Figure 5-3. Mechanically broken glass sponges observed at Howe reef in 2009. Fresh (cream colored) and older (black) fragments of *Aphrocallistes vastus* and *Heterochone calyx* were scattered across the sediment. Although there is no emperical evidence that correlates the broken sponges with fishing activity, the active shrimp fishery in the Strait of Georgia drags otter trawls across the bottom of the Strait of Georgia which may damage glass sponge reefs.

Figure 5-3

Figure 5-4. Surveys of Learmonth Bank, Dixon Entrance. Learmonth Bank is a large underwater mound found in Dixon Entrance, 10.5 km north of Langara Island in the Queen Charlotte Islands (Haida Gwaii). This region was glaciated during the Pleistocene (1.8 million to 10,000 ya). When deglaciation occurred over the Haida Gwaii, isostatic rebound pushed the islands up as well as Learmonth Bank causing the shallowest regions to be subaerially exposed (Barrie & Conway 1999). At present, Learmonth Bank is over 30 km long, 10 km wide and completely submerged with a base depth of 470 m and shallow portions reaching 40 m. Areas shallower than 160 m remain as exposed bedrock with glacial drift covering the deeper depths. Five areas were surveyed around the periphery of Learmonth Bank with ROPOS. Thirty-four 1-km transect lines were surveyed accumulating 91 hrs of high definition video (1080i) and digital still photographs.

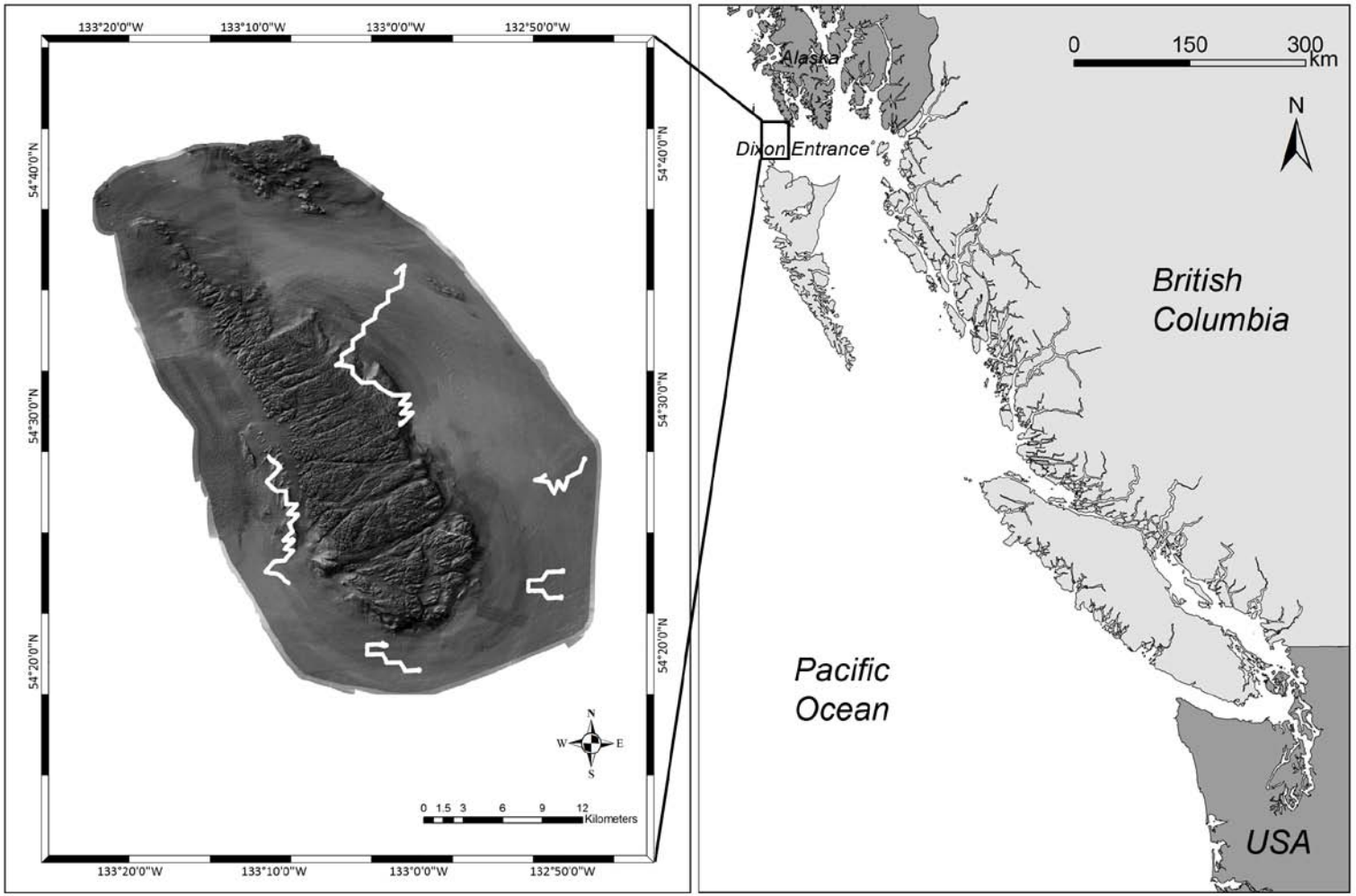
133°20'0"W
133°10'0"W
133°0'0"W
132°50'0"W
54°40'0"N
54°30'0"N
54°20'0"N
N
W
E
S
0 1.5 3 6 9 12
Kilometers
Alaska
Dixon Entrance
0 150 300
km
N
British Columbia
Pacific Ocean
USA

Figure 5-4

Figure 5-5. Glass sponges at Learmonth Bank. (A) Dense populations of lyssacine and dictyonine glass sponges were found in the shallowest depths explored (~150 m) on the eastern flank of Learmonth Bank at. (A) A large number of lyssacine sponges were discovered to be budding forming double oscula morphologies (arrows). (B, C) Dictyonine sponges (*Heterochone calyx*) were observed to have extensions of tissue branching off at their base and form new oscula.

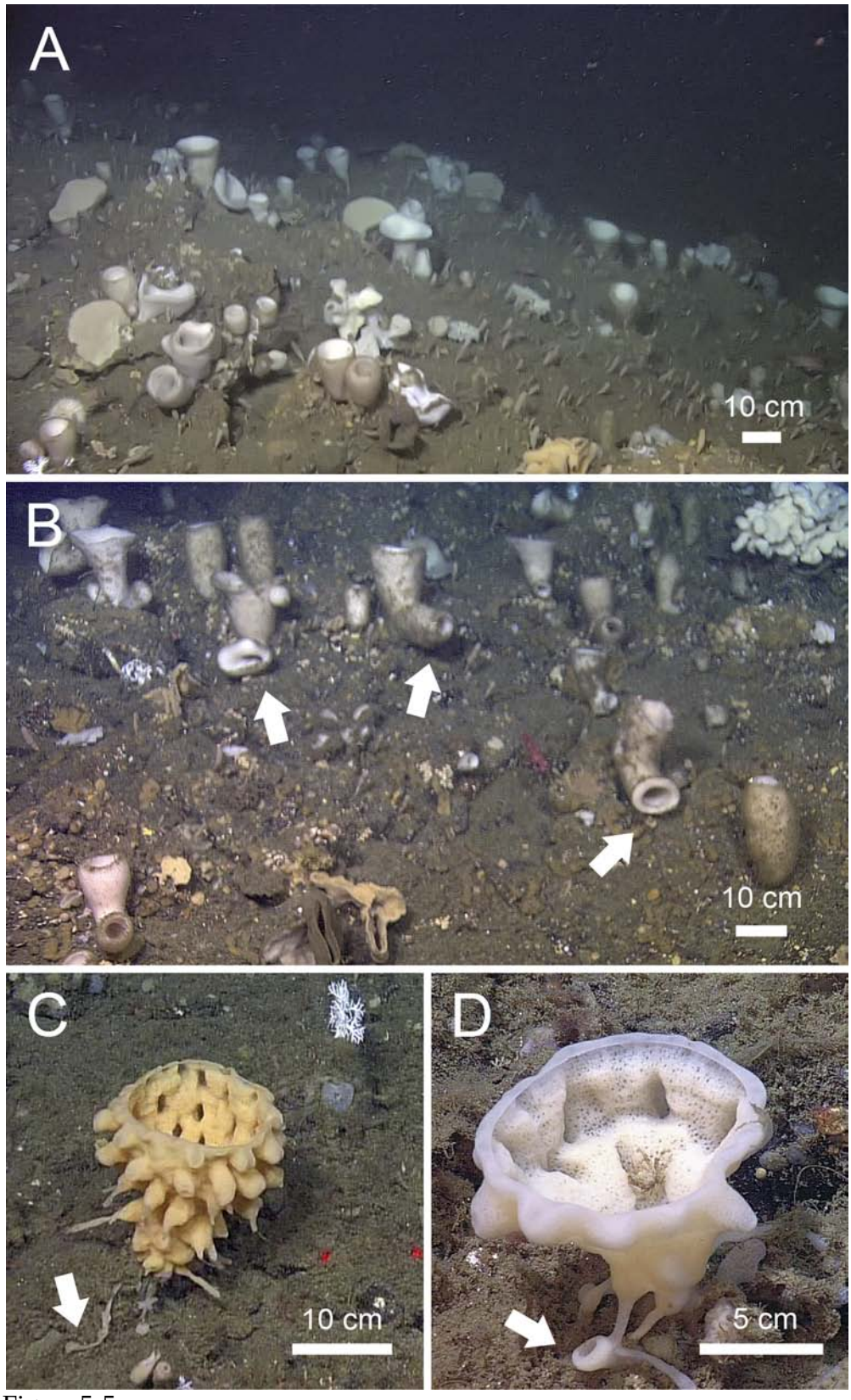

Figure 5-5

Figure 5-6. The Sponge Graveyard. (A) At the base of the eastern flank of Learmonth Bank (~344 m) a large pile of dead glass sponges was discovered. (B) Sponge debris accumulated to create a ~7 m high ridge with the freshest material (white) on top of the pile.

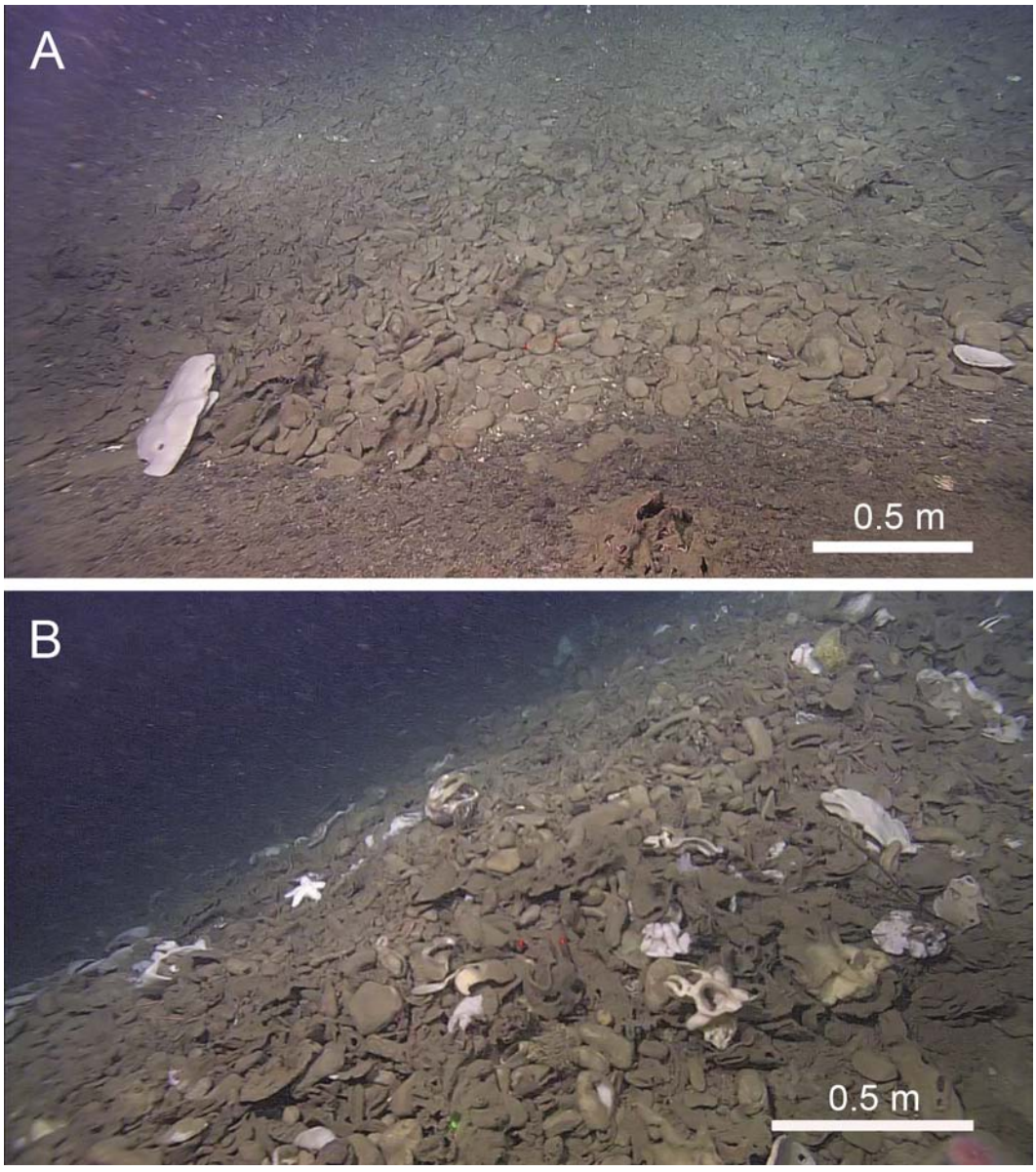

Figure 5-6

Appendices

Appendix 1- The discovery of the dorid nudibranch *Peltodoris lentiginosa* as a predator of glass sponges

A1.0 Material and Methods

Four sampled specimens of *P. lentiginosa* came from Galiano reef and the end of the final ROV dive in 2009. Three individuals were retrieved without damage using a low force suction sampler and placed in a collection box with sealing lid. One individual, sampled with a manipulator arm did not survive and was fixed in 4% formaldehyde. Live individuals were kept in flowing sea water onboard the ship before being immediately transported in sealed buckets filled with fresh sea water to the Bamfield Marine Sciences Centre in Bamfield, British Columbia. The three individuals were kept alive, separated, and unfed in flowing sea water tables pumped from a depth of 25 m from Bamfield Inlet and returned to the Strait of Georgia after the study.

Daily sampling of fecal matter from each individual nudibranch was observed under a microscope for identifying microsclere sponge spicules. Upon finding spicules, the samples were cleaned in a small volume of hot nitric acid (95°C for 5 mins), diluted with distilled water and filtered through 0.22 µm millipore membrane filter papers. Spicules were then lightly rinsed onto petri dishes with distilled water, mounted wet on glass slides and digitally photographed. Gut contents analysis was performed on the nudibranch fixed in formaldehyde. Spicules found in the gut contents were processed as above. The high definition video footage and digital still photographs, both with 10 cm laser dot scales, were analyzed for nudibranch distributions in the field. Distribution and depths were extracted from the navigation cruise files corresponding to the timestamp on the video and photographs. Nudibranch sizes were measured from video screen captures and still photos with Adobe Photoshop CS3.

Table A1-1. Video observations and summary statistics of *Peltodoris lentiginosa* at each glass sponge reef. No nudibranchs were observed at Fraser reef in the survey video. Area units are given in m^2 and depth is given in m.

			Depth Distributions			
Reef	Area surveyed	N	Mean	SD	Maximum	Minimum
Howe	166,500	9	77.4	11.7	102	66
Fraser	142,775	0	-	-	-	-
Galiano	25,966	17	91.1	2.0	94	89

N, number; SD, standard deviation.

Appendix 2 - Stiffness of the spicules of *Aphrocallistes vastus* as measured by cantilever beam bending theory

A2.1 Materials and Methods

A2.1.1 Field sampling of sponges

Field sampling of *Aphrocallistes vastus* was done from populations found along vertical fjord walls of San Josie Islets and Hosie Islands in Barkley Sound, British Columbia in June 2008. Whole *A. vastus* (n=10) as well as fragments from multiple live individuals (n=10-20) were randomly sampled with the remotely operated vehicle ROPOS at 120 to 160 m depths. The populations of *A. vastus* in Barkley Sound are geographically located in close proximity to the Bamfield Marine Sciences Centre (BMSC), making this area ideally situated for field and lab research on live glass sponges. The live sponges were brought back to BMSC and kept in darkened tanks with flow through water pumped from 25 m depth in Bamfield Inlet providing particulates for the sponges to suspension feed. However, sponge health deteriorated after 2 months and were then removed from the tanks and air dried.

A2.1.2 Biomechanics of glass sponges

To examine the mechanical properties of the spicules and dictyonine skeleton of *A. vastus*, I used static beam theory. I used the assumptions of cantilever beam bending (Denny 1988) to determine the second moment of area (*I*) and Young's Modulus (*E*) of the dictyonine skeleton. The second moment of area relates the cross sectional area of the beam to the applied force bending the beam (Boller et al. 2002). Young's modulus describes the relation of stress to strain in the material of interest and indicates the degree of deformation in tension and compression forces (Vogel 1988). Thus, by using basic engineering principles to calculate these mechanical property values, the design of a glass sponge body can be empirically defined and related back to the natural history and ecology of the animal.

A2.1.3 Measurements of the Young's modulus of individual spicules

Details of the microscopic manipulations are outlined in Emlet (1982) which were modified to use on hexactinellid spicules. Individual diactine spicules were cleaned with bleach and oven dried at 60°C. Calibrated glass needles (Young's modulus = 62.75 x 10^9 N m^{-2}) were created with a Flaming/Brown micropipette puller (Sutter Instrument Co. Model P-87 Settings: Heat = 604, Pull= 60, Velocity = 70, Time = 80, Pressure = 200). Spicules and calibrated needles were fixed perpendicular onto the edge of glass cover slips (Fig. A2-1). The spicule and needle were both aligned horizontally and focused under 400x magnification of a compound microscope. The cover slips were then slid in opposite directions creating a slight deflection in the spicule. Digital images were taken before (Fig. A2-2A) and after the deflection (Fig. A2-2B). The relative displacements from bending of the needle and spicule were ameasured in Adobe Photoshop CS3. The force required for the vertical deflection in the spicule is equal to the force required in the needle and thus the Young's modulus can be calculated following the formula:

$$F_n = 3(E_n I_n Y_{nmax})/L_n^3 = F_s = 3(E_s I_s Y_{smax})/L_s^3$$

Where,

F_n = Force exerted by needle on the spicule (N)

F_s = Force exerted by the spicule on the needle (N)

E_n = Young's modulus of the glass capillary needle (N m^{-2})

E_s = Young's modulus of the spicule (N m^{-2})

I_n = Second moment of area of the needle (m^4), calculated as $I = \pi/4(R^4 - R_i^4)$ for a hollow circular cross section where R is the larger diameter and R_i is the radius of the hollow cavity (see Denny 1988)

I_s = Second moment of area of the spicule (m^4), calculated as $I = \pi R^4/4$ for a circular cross-section where R is the radius (see Denny 1988).

Y_{nmax} = Deflection of the needle where it contacts of the spicule (m)

Y_{smax} = Deflection of the spicule where it contacts the spicule (m)

L_s = Length of the spicule to point of contact with needle (m)

A2.1.4 Measurements of the Young's modulus of the dictyonine skeleton

Fragments of *A. vastus* were randomly selected to determine mechanical properties and cut into rectangular beams of ~4 cm length. Beams were fixed with cyanoacrylate to a raised aluminum platform that was firmly held to a desk bench edge with two C clamps. Weights of known mass (20, 50, 100 g) were hung from each sponge beam from a piece of monofilament wire. Cross sectional area (width * height), vertical deflection caused by the hanging weight, and length of deflected beam was measured with digital callipers (±0.03 mm) (Fig. A2-3). A plexiglass beam of similar dimensions was used as a control standard to compare for accuracy.

A. vastus spicules and pieces of dictyonine skeleton were selected from sampled fragments. Pieces were either: (1) oven dried skeleton with tissue (24h at 60 ºC) (2) dried skeleton without tissue, removed by cleaning with 10% sodium hypochlorite (24 hrs and then oven dried at 60 ºC) (3) rehydrated skeleton with tissue, rehydrated with a soak in seawater and then blotted dry to remove excess water (4) rehydrated skeleton without tissue.

The second moment of area (I) and Young's modulus (E) was calculated assuming a rectangular beam using the formulas (see Vogel 2003):

$$I = (\text{width} * \text{height})^3 / 12$$

and,

$$E = (m*g*L^3) / (3*\delta y*I)$$

where,

M = mass of hanging calibrated weight (kg)

g = gravity (9.81 m s^{-2})

L = length of cantilever beam (m)

Δy = vertical deflection caused by hanging weight (m)

A2.2 Literature Cited

Boller ML, Swain TD, Lasker HR (2002) Skeletal morphology and material properties of a fragmenting gorgonian coral. Mar Ecol Prog Ser 228:131-141

Denny MW (1988) Biology and the Mechanics of the Wave-Swept Enviornment. Princeton University Press, Princeton

Emlet RB (1982) Echinoderm calcite: a mechanical analysis from larval spicules. Biol Bull 163:264-275

Vogel S (2003) Comparative biomechanics life's physical world. Princeton University Press, Princeton.

Table A2-1. Young's modulus summary statistics of the dictyonine skeleton of *A. vastus* measured from using applied static beam bending theory.

	Young's modulus (*E*) Units are in MN m^{-2} (10^6)				
Skeleton Type	Mean*	SD	Minimum	Maximum	N
With tissue	2.76 (a)	0.82	1.55	4.19	10
Without tissue	2.65 (a)	0.94	1.33	4.33	10
Rehydrated, with tissue	9.97 (b)	2.75	6.80	14.65	10
Rehydrated, without tissue	10.04 (b)	3.19	5.32	14.49	10

*Significantly different means between treatment types are indicated by the letters in parentheses (Tukey-Kramer post hoc comparisons, $p < 0.0001$)

Figure A2-1. Spicule bending assay for measuring Young's modulus of individual hexactinellid spicules. Both a calibrated needle and spicule were superglued onto glass cover slips and aligned in parallel (not to scale) under the magnification of a compound microscope.

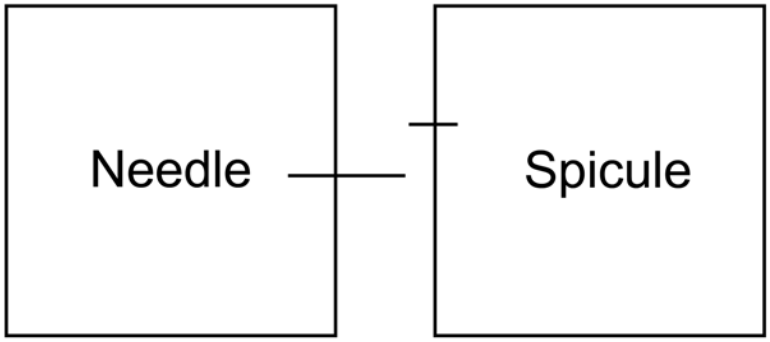

Figure A2-1

Figure A2-2. Application of engineering theory to microscopic glass sponge spicules. (A) A calibrated glass needle and an *A. vastus* spicule were fixed onto glass cover slips and aligned parallel underneath a compound microscope under 40x magnification. (B) Tips of the needle and spicule were touched and then manually deflected by sliding cover slips in opposite directions. Stiffness (Young's modulus) of the spicule wase derived following calculations outlined by Emlet (1982).

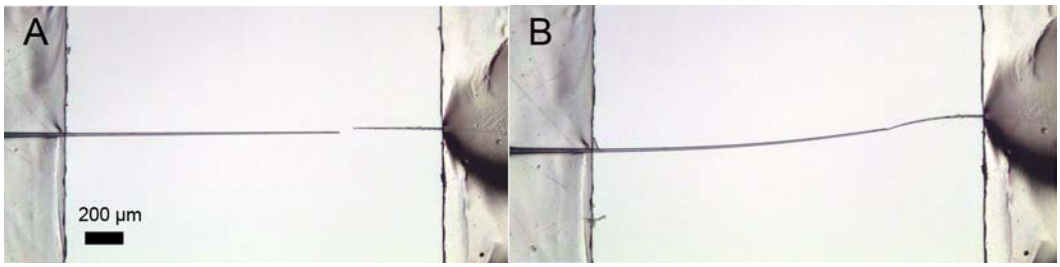

Figure A2-2

Figure A2-3. Application of static beam bending theory to dictyonine skeleton. A cantilever was created by fixing one end of the beam of dictyonine skeleton and bearing a load on the opposite end. The Young's modulus was determined from measurements of the cross sectional area (width * height), length of the beam (L) and vertical deflection (Δy), from the force (m = mass, g = gravity).

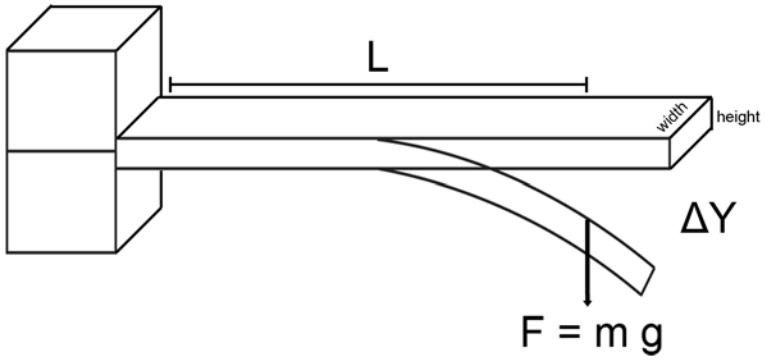

Figure A2-3

Appendix 3 – ROV Cruise participation

Table A3-1. ROV Cruises and dive numbers. The dates, locations and dive numbers of all ROV cruise participation from this thesis.

Dates	ROV Platform	Location	Dive Numbers
2007, Oct. 20-27	ROPOS	Strait of Georgia: Glass Sponge Reefs	R1110-R1118
2008, May 19-25	Phantom	Strait of Georgia: Galiano Reef	PAC-044
2008, June 30-July 1	ROPOS	Barkley Sound: Hosie San Jose Islets	R1144-R1151
2008. July 1-7	ROPOS	Learmonth Bank, Dixon Entrance	R1152-R1156
2008, July7-14	ROPOS	Olympic Coast National Marine Sanctuary	R1157-R1165
2008, Sept. 22-27	ROPOS	Strait of Georgia	R1166-R1180
2009, Sept. 30-Oct. 2	ROPOS	Strait of Georgia: Glass Sponge Reefs	R1278-R1283